Synthetic Lethal Interactions With Oncogenic KRAS

Abstract

KRAS is one of the most frequently mutated genes across human cancers, including 96% of pancreatic cancers, 40% of colorectal cancers, and 35% of lung cancers. The majority of human cancer cell lines and tumors from genetically engineered mouse models harboring an oncogenic mutant *KRAS* allele demonstrate a strong dependence on KRAS for proliferation and survival. This KRAS dependency is a type of 'oncogene addiction,' a state in which cancer cells depend on signaling from a single oncogene for survival. Unfortunately, the development of clinically effective KRAS-directed cancer therapies has been unsuccessful, and KRAS-mutant cancers are refractory to standard and targeted therapies. Alternative approaches to combatting *KRAS*-mutant cancers are clearly needed. We postulate that oncogenic KRAS signaling induces changes in cell signaling networks that cause cells to become dependent on certain genes, termed a 'synthetic lethal' interaction. Identifying these selective vulnerabilities would lend insight to the pathways altered in *KRAS*-mutant cancers and may inform novel strategies to target KRAS-addicted cancers. In this thesis, we systematically identify candidate co-dependencies of oncogenic KRAS by analyzing genetic dependencies revealed by genome-scale RNAi screens across a large panel of cell lines. We highlight methods to facilitate candidate selection/validation and integrate analyses of gene-expression data and genome-scale CRISPR/Cas9 screens to nominate candidate co-dependencies for further study. In addition, we examine CRISPR-Cas9 screens to identify genes that modify sensitivity to small molecule MAPK pathway inhibition (MAPKi) in *RAS*-mutant cancers. We propose that suppression of the DOCK5-RAC1 pathway demonstrates a drug-conditional lethal interaction with small molecule MAPK pathway inhibitors in *RAS*-mutant cancers. We believe that these data provide a foundation for further examination of genetic co-dependencies of oncogenic *KRAS* and the potential synthetic lethal interaction between DOCK5-RAC1 pathway suppression and MAPKi in *RAS* mutant cancers.

Table of Contents

Abstract i

Table of Contents ii

Acknowledgments iii

Abbreviations iv

Introduction 1

Overview 1

The RAS pathway 2

RAS regulators and effectors 2

RAS mutations in cancer 3

Oncogene addiction 4

Strategies to target mutant RAS for cancer therapy 4

Inhibiting upstream RAS activators 4

Direct RAS inhibition 5

Targeting RAS post-translational modifications 5

Inhibiting RAS effector pathways 6

Synthetic lethality 8

Synthetic lethal interactions for cancer therapy 8

Screening approaches to identify synthetic lethal interactions 9

Challenges in screening for synthetic lethal interactions 11

Genotype-selective synthetic lethal interactions with oncogenic RAS 12

Drug-conditional synthetic lethal interactions 14

Results 16

Candidate synthetic lethal interactions with oncogenic KRAS 16

Off-target effects complicate the interpretation of RNAi screens 17

Prioritized candidate co-dependencies of oncogenic KRAS 20

Potential dependency of *KRAS*-mutant cancer cells on DOCK5 22

DOCK5 modifies sensitivity to MAPKi in *RAS*-mutant cancers 23

Discussion 26

Candidate synthetic lethal interactions with oncogenic KRAS 26

DOCK5-RAC1 pathway in *RAS*-mutant cells 29

Further exploration is warranted to determine if DOCK5 suppression is synthetic lethal to oncogenic KRAS 29

DOCK5-RAC1 pathway modulates sensitivity to MAPKi in *RAS*-mutant cells 31

Conclusion 33

Materials and methods 34

Tables 41

Figures 46

References 67

Acknowledgments

I have received invaluable support and guidance from many people. I would like to thank my advisor, Bill Hahn, who has been an exceptional role model. He has been unfailingly supportive of diverse endeavors, granting me the freedom and resources to explore different projects while offering constructive criticism and clear feedback; his positive attitude and reassuring presence has been indispensible to making me a more confident, creative, and resilient scientist. Being a member of the Hahn lab has been a wonderful experience, and I feel lucky to have interacted with and befriended such inspiring, talented, and kind people. In particular, I would like to thank Andy Aguirre, who spent an immense amount of time and energy teaching me experimental techniques and, more importantly, how to think like a scientist. In addition, I would like to thank Elsa Beyer Krall, my partner in screening, for helping me become a more thoughtful and rigorous scientist. I am grateful for the support of all members of the Hahn lab - especially Eejung Kim, David Takeda, William Kim, Mik Rinne, Yaara Zwang, Andy Hong, Sri Raghavan, Francesca Izzo, and Barbara Weir – for always having time to troubleshoot and for innumerable fascinating and enjoyable conversations.

I learned much from members of the Genetic Perturbation Platform, including Glenn Cowley, John Doench, Federica Piccioni, and David Root, whose work and feedback was critical for several of the screens and analyses presented here. I would also like to thank the members of the Broad Cancer Program for their camaraderie, company, and insights.

I would also like to thank the HST and MD/PhD faculty and staff - particularly Matt Frosch, Rick Mitchell, Loren Walensky, Amy Cohen, and Patty Cunningham - for their tireless support and guidance. Last but not least, I must thank my HMS/HST/BBS colleagues, friends, and family for innumerable enriching conversations and lots of fun!

Abbreviations

ATARiS	Analysis Technique for Assessment of RNAi by Similarity
BRAFi	BRAF inhibition
Cas9	CRISPR associated protein 9
cDNA	Complementary DNA
CRISPR	Clustered regularly interspaced short palindromic repeats
DOCK5	Dedicator of cytokinesis 5
FTase	Farnesyltransferase
FTI	Farnesyltransferase inhibitor
GAP	GTPase activating protein
GeCKO	Genome scale CRISPR knockout
GEF	Guanine nucleotide exchange factor
GEMM	Genetically engineered mouse model
GGTase	Geranylgeranyltransferase
GOF	Gain-of-function
HRAS	Harvey rat sarcoma viral oncogene homolog
ICGC	International Cancer Genome Consortium
KO	Knockout
KRAS	Kirsten rat sarcoma viral oncogene homolog
LOF	Loss-of-function
MAPK	Mitogen activated protein kinase
MAPKi	MAPK pathway inhibition
MEKi	MEK1/2 inhibition
NRAS	neuroblastoma RAS viral oncogene homolog
NSCLC	Non-small cell lung cancer
ORF	Open reading frame
p-ERK	Phospho-ERK1/2
PI3K	Phosphatidylinositol 3-kinase
PIP2	Phosphatidylinositol-4,5-bisphosphate
PIP3	Phosphatidylinositol-3,4,5-triphosphate
RAC1	Ras related botulinum toxin substrate 1
RAL	RAS-like GTPase
RALGDS	RAL guanine nucleotide dissociation stimulator
RNAi	RNA interference
RTK	Receptor tyrosine kinase
gRNA	Short guide RNA
SH3	Src homology 3
shRNA	Short hairpin RNA
siRNA	Small interfering RNA
TCGA	The Cancer Genome Atlas
WT	Wildtype

Introduction

Overview

The *RAS* family of genes (*KRAS, NRAS,* and *HRAS*) are frequently mutated in human cancers, including nearly all pancreatic cancers, ~50% of colorectal cancers, ~30% of lung cancers, and ~30% of melanomas. *RAS* mutations are associated with poor prognosis, and are used to exclude patients from treatment with some targeted therapies. Most *RAS*-mutant cancers require RAS signaling for continued proliferation and survival. This phenomenon, termed “RAS addiction,” makes RAS an appealing target for therapeutic intervention. Unfortunately, pharmacologic approaches to directly target RAS proteins have not yet succeeded in clinic.

An alternative strategy of targeted drug development for *RAS*-mutant cancers is to identify signaling pathways that become essential for cancer cell survival in the context of oncogenic RAS signaling. These ‘synthetic lethal’ interactions provide opportunities for rational drug development to treat *RAS*-mutant malignancies. Our laboratory and others have performed RNAi screens as an unbiased approach to identify synthetic lethal interactions with oncogenic KRAS[1,2]. These screens have led to several potential targets - including *TBK1*, *PLK1*, and *WT1* - which are the focus of ongoing investigation[3-8]. Notably, *TBK1* shows promise as a novel therapeutic target for *KRAS*-driven malignancies. Preclinical studies using a small molecule inhibitor of TBK1 achieved therapeutic responses in *Kras*-mutant GEMMs[9]. Additionally, studying TBK1 has led to the discovery of a novel effector pathway of oncogenic KRAS, in which TBK1 promotes KRAS-driven tumorigenesis by regulating an autocrine cytokine circuit. Such data support the idea that synthetic lethal genetic interactions can identify valuable therapeutic targets and broaden our understanding of critical mediators of oncogenic KRAS, motivating our interest in identifying further novel candidates.

Prior RNAi screens for synthetic lethal interactions with oncogenic KRAS harbor several limitations: these screens were performed in a limited number of cell lines and lineages, and most were not performed at genetic saturation. We hypothesize that many synthetic lethal partners of oncogenic KRAS remain unidentified. Recent technological

advances have provided the means to perform comprehensive loss-of-function screens in mammalian cells using RNAi[10-12] or clustered regularly interspaced short palindromic repeats (CRISPR)-Cas9[13-15] libraries. Our laboratory has performed genome-scale lentivirally-delivered short hairpin RNA (shRNA) screens across ~216 independent cancer cell lines[12]. This effort, termed Project Achilles, is among the most comprehensive genome-scale shRNA screens performed on human cancer cell lines, and provides an opportunity to identify novel pathways essential to the survival of *KRAS*-mutant cancer cells. Prior studies demonstrated that this data has sufficient power to identify co-dependent genetic interactions in a genotype or lineage-specific manner[10,16,17].

The RAS pathway

The three *RAS* proto-oncogenes (*HRAS, KRAS,* and *NRAS)* encode four distinct but highly homologous ~21 kDa RAS proteins: HRAS, NRAS, KRAS4A and KRAS4B, where KRAS4A and KRAS4B are alternative splice variants of the *KRAS* gene[18]. Here, 'RAS' will be used to refer generally to all isoforms. RAS are guanine nucleotide-binding proteins[19,20] that cycle between active and inactive conformations conferred by GTP and GDP binding, respectively[21,22].

RAS regulators and effectors

RAS proteins function as transducers of mitogenic signaling that link cell surface receptors to intracellular effector pathways (**Figure 1**). External growth factors induce cell proliferation by binding to receptor tyrosine kinases (RTKs) at the cell surface. Signal transduction between RTKs and RAS is mediated by cytosolic adaptor proteins, such as GRB2, CRKL, and IRS1. This RTK-adaptor protein-GEF interaction promotes RAS activation by recruiting the normally cytosolic guanine exchange factors (GEFs) to the plasma membrane where RAS is located[18,23,24].

Under physiologic conditions, the transition between RAS GTP- and GDP-bound states is regulated by GEFs and GTPase-activating proteins (GAPs). GEFs accelerate the release of GDP from RAS, enabling the more abundant GTP to bind in its place. On the other hand, GAPs accelerate RAS GTPase activity over 200-fold[18]. The most common oncogenic RAS mutations abrogate its interaction with GAPs[25,26] and reduce

intrinsic RAS GTPase activity ~10-fold, leading to the accumulation of active GTP-bound RAS.

Active, GTP-bound RAS interacts with numerous downstream effectors to activate signaling pathways important for cell growth and survival[18,23,24]. The three major effectors of oncogenic RAS signaling are RAF, PI3K, and RALGDS (**Figure 1**). Several other RAS effectors, such as the RAC-GEF TIAM1, PLCε, and pro-apoptotic RASSF family members have been identified, but their functions are not as well studied.

The relative contribution of different RAS effector arms to RAS signaling is still unclear. Genetic suppression of individual effector pathways was shown to be sufficient to prevent RAS-mediated transformation in different model systems[27-31]. In certain contexts, signaling through a specific effector pathway is sufficient to induce cell transformation. For example, in a mouse model of pancreatic cancer, active BRAF, but not PIK3CA, was sufficient to induce tumorigenesis[29]. Contrastingly, in immortalized mouse cells, RAF activation induced transformation whereas RALGDS and PI3K activation did not[32]. Yet, in immortalized human cells, activation of RALGDS, but not RAF or PI3K, induced cell transformation[32]. Together, these findings demonstrate that the relative importance of each RAS effector arm is context-specific.

RAS mutations in cancer

RAS is the most frequently mutated oncogene in human cancers[22,33]. *RAS* mutations occur in nearly all pancreatic cancers, ~50% of colorectal cancers, and ~30% of lung cancers[33] (**Table 1**). The involvement of RAS signaling in cancer is evident not only by the high incidence of *RAS* mutations, but also by the high frequency of mutations in RAS regulators (such as RTKs and NF1) and RAS effectors (such as members of the MAPK and PI3K pathways)[34,35].

Over 95% of oncogenic *RAS* mutations involve point mutations in codons 12, 13, or 61 (analysis of the Catalog of Somatic Mutations in Cancer (COSMIC) database[36]). These G12, G13, or Q61 mutations decrease RAS intrinsic GTPase activity, reduce GAP binding affinity, and abrogate the ability of GAPs to stimulate RAS GTPase activity[37]. This causes RAS to accumulate in the active GTP-bound state, constitutively activating downstream effectors even in the absence of extracellular stimuli.

Oncogene addiction

Cancer cells harboring mutationally activated oncogenes are frequently dependent on continued signaling from the activated signaling pathways. This phenomenon, termed "oncogene addiction," provides a therapeutic opportunity because it renders cancer cells sensitive to drugs targeting these pathways. Of note, there is often a greater dependency on the oncogenic gene in cancer cells than in normal cells, conferring a large therapeutic window[38,39]. Targeting oncogene addiction has been successful in chronic myelogenous leukemia with the *BCR-ABL* fusion oncogene treated with ABL kinase inhibitors, in *EGFR*-mutant lung cancer with EGFR inhibitors, and in *BRAF*-mutant melanoma with BRAF inhibitors[40,41].

RAS-mutant cells are dependent on continued RAS signaling for sustained survival/proliferation. An analysis of *KRAS*-mutant cell lines suggested that there is a spectrum of dependency[42]. However, the majority of human cancer cell lines[3,42-44] and tumors from genetically engineered mouse models (GEMMs) harboring a mutant *RAS* allele demonstrate RAS addiction[45-51]. Indeed, removing KRAS from established tumors in mouse models results in dramatic tumor regression[46,48,50]. As the majority of *RAS*-mutant cancers are addicted to RAS, there has been much interest in inhibiting RAS for cancer therapy.

Strategies to target mutant RAS for cancer therapy

Several approaches have been taken to therapeutically target *RAS*-mutant cancers, including: **(1)** inhibiting upstream RAS activators, **(2)** directly inhibiting RAS, **(3)** preventing RAS from associating with the plasma membrane, **(4)** inhibiting RAS effector pathways, and **(5)** inhibiting tumor-specific vulnerabilities that are induced by the oncogenic state (non-oncogene addictions or synthetic lethal interactions)[52] (**Figure 2**).

Inhibiting upstream RAS activators

Inhibiting upstream RTKs could be effective in treating *RAS*-mutant cancers because these cells produce autocrine growth factors, such as EGF[53]. Indeed, an *in vivo* study demonstrated that autocrine EGFR activation is important for tumorigenesis in cancers driven by active SOS, which activates RAS[54]. However, subsequent clinical studies indicated that *KRAS* mutations predict insensitivity to EGFR inhibitor therapy, and *RAS*

mutation is currently an exclusionary criterion for EGFR inhibitor treatment for colorectal cancer[55,56]. Similarly, patients with *RAS*-mutant NSCLC are likely insensitive to EGFR inhibitor therapy[57-61].

Direct RAS inhibition

As the majority of *RAS*-mutant cancers are addicted to RAS, there has been much interest in developing RAS inhibitors. Unfortunately RAS has proven difficult to target. RAS has a picomolar affinity for GTP/GDP, and the millimolar concentration of guanine nucleotides in the cytosol makes it unlikely that a competitive inhibitory nucleotide analogue will be developed[62]. Additionally, RAS activation and signaling is mediated by transient protein-protein interactions which are difficult to target via small molecules[63]. Despite these challenges, several groups have identified compounds that bind to RAS noncovalently and either abrogate RAS-RAF interaction[64-69] or inhibit nucleotide exchange[70-75]. However, these early-stage compounds have low RAS-binding affinity and potency, and will have to be improved before clinical application. More recently, covalent inhibitors targeting $KRAS^{G12C}$ have been developed[76,77]. These mutation-specific electrophilic compounds irreversibly bind to the reactive cysteine in $KRAS^{G12C}$, blocking KRAS nucleotide exchange[76,77]. While $KRAS^{G12C}$ mutations arise in ~15% of lung adenocarcinomas[78], it occurs infrequently in other cancer types. It is possible that other compounds could be identified that specifically target RAS^{G12D} and RAS^{G13D}, but it will likely be difficult to selectively target other common RAS mutations due to their less reactive side chains. While the advances in efforts to directly target oncogenic RAS are encouraging, these approaches have yet to produce clinically usable agents.

Targeting RAS post-translational modifications

Another approach to inhibiting RAS is to target its post-translational modifications, which are necessary for RAS membrane association and biological activity[79]. RAS farnesylation by farnesyltransferase (FTase) is the first, irreversible, and rate-limiting step of the RAS post-translational modifications that increase RAS hydrophobicity and enable membrane association. Unfortunately, these FTIs did not demonstrate significant clinical benefit in patients, likely because KRAS4B and NRAS can be alternatively prenylated by geranylgeranyltransferase (GGTase) in the context of FTI treatment[80-83];

this addition of a geranylgeranyl modification in place of farnesyl enables KRAS4B and NRAS to remain fully functional.

Inhibiting RAS effector pathways

Given that targeting RAS proteins or RAS modifier proteins directly has proven difficult, efforts have shifted towards alternative ways of selectively targeting *RAS*-mutant cells, such as inhibiting RAS effector pathways. While many RAS effector families have been identified, the RAF serine/threonine kinases (ARAF, BRAF, and CRAF) are thought to play a key role in *RAS*-mediated oncogenesis[28,29]. RAF activates the MEK1/MEK2 kinases, for which the only known substrates are the ERK1/ERK2 kinases. However, because the MAPK signaling pathway involves multiple feed-forward and feedback mechanisms that dynamically modulate ERK activity, pharmacological inhibition of the MAPK pathway at the level of RAF and MEK have not demonstrated equivalent outcomes[33,84,85].

The ATP-competitive RAF inhibitors vemurafenib and dabrafenib have been approved for treatment of *BRAF*-mutant melanoma[86,87]. However, in *NRAS*-mutant melanoma, treatment with these first-generation BRAF inhibitors paradoxically activates the MAPK pathway through induction of RAF dimerization and consequent CRAF activation[88-91]. A second generation of 'paradox-breaking' BRAF inhibitors that do not promote RAF dimerizaton[92] or pan-RAF inhibitors that inhibit all three RAF proteins[93] have been generated and may have improved efficacy in treating *RAS*-mutant cancers.

Several MEK inhibitors are currently being tested in clinical trials for *RAS*-mutant pancreatic cancer, colorectal cancer, lung cancer, and melanoma. While MEKi has been successful in treating *BRAF*-mutant melanoma[87,94], success has been limited in *RAS*-mutant NSCLC[95-97], pancreatic cancer[96], and melanoma[98]. A major mode of intrinsic or acquired resistance to MEK inhibitor monotherapy in *RAS*-mutant cancers is the reactivation of the RTK-RAS-MAPK pathway[84]. It was thought that ERK inhibition would overcome this mode of resistance. Unexpectedly, ERK inhibition was found to alleviate feedback inhibition of RAF, resulting in enhanced MEK activation[99]. Combined inhibition of RAF, MEK, and ERK may be necessary for more effective MAPKi, though overlapping toxicities could be limiting in patients.

The p110 catalytic subunits (α- γ- and δ-subunits) of class I PI3Ks are also important effectors of oncogenic RAS[27,100,101]. A *Kras*-driven mouse model of lung cancer suggested that PI3K signaling was essential for tumorigenesis and tumor maintenance[102]. However, small molecule inhibition of the PI3K pathway in a mouse model of lung cancer had little effect on *Kras*-driven tumor growth[103], and subsequent *in vitro* studies suggested that oncogenic *RAS* confers resistance to PI3K inhibition[104]. It is unclear whether *RAS*-mutant cancers demonstrate greater dependence on PI3K signaling than cells driven by other oncogenes[105], and several inhibitors of the PI3K-AKT-mTOR signaling pathway are currently under clinical evaluation in *RAS*-mutant cancers.

Oncogenic RAS signals through multiple signaling pathways, and it is possible that inhibition of a single effector arm will not be sufficient to induce tumor regression. In pre-clinical studies, combined MAPK and PI3K inhibition effectively induced regression of *KRAS*-mutant tumors[103]. There are several clinical trials assessing the efficacy of combined MAPK (MEK or ERK) and PI3K pathway (PI3K, AKT, or mTOR) inhibition in *RAS*-mutant cancers. The results of most of these trials are not yet available. However, while this dual-targeting strategy has the potential of being more effective than inhibition of either pathway alone, there may not be a wide enough therapeutic window to effectively suppress both pathways in human cancers[106]. In a recent trial that combined MK-2206 (AKT inhibitor) with selumetinib (MEK inhibitor), no patient achieved over 70% inhibition of both targets at the maximum tolerated drug dose[107].

In summary, while RAS effector inhibition is a promising strategy to target oncogenic RAS, several challenges endure. Inhibition of effector pathways are complicated by compensatory feedback mechanisms, which necessitate inhibition at multiple levels of the pathway. In addition, as several effectors pathways are important in oncogenic RAS signaling, concurrent inhibition of multiple pathways may be important. However, while combination inhibition of more than one effector pathway (such as RAF and PI3K) may be more effective in inducing tumor regression, the resulting increase in toxicity to normal cells may reduce the therapeutic window. Nevertheless, it remains possible that combined inhibition of different nodes of these

effector pathways (RAF, MEK, or ERK and PI3K, AKT, or mTOR) will yield different toxicities, with greater therapeutic windows in specific combination strategies.

Synthetic lethality

Synthetic lethal interactions for cancer therapy

A synthetic lethal interaction (also known as induced essentiality, non-oncogene addiction, or co-dependency) refers to a genetic principle in which the combination of two genetic perturbations is lethal, whereas each individually is not[38,39,108] (**Figure 3**). The concept of synthetic lethality emerged from genetic studies in model organisms[109,110]. Genotype-selective synthetic lethality is based on the concept that genetic alterations in cancer cells confer vulnerabilities that can be therapeutically targeted. Such vulnerabilities may be secondary to the inability to respond appropriately to a specific signal (such as DNA damage or cell cycle arrest) or the inability to maintain cellular homeostasis. It was first proposed over 20 years ago that synthetic lethal interactions could be used to identify new anticancer drug targets[111].

There are several theoretical benefits to a therapeutic strategy based on synthetic lethal interactions. If the targeted synthetic lethal interaction is selective for a cancer-specific mutation, this mutation could be used as a biomarker to stratify patients for treatment. In addition, targeting a synthetic lethal interaction should provide a large therapeutic window, as only tumor cells that harbor the mutation should be sensitive. Lastly, the synthetic lethal strategy enables indirect targeting of “undruggable” mutations (such as loss of tumor suppressors and RAS) through the identification of an alternative synthetic lethal target.

Exploiting synthetic lethal interactions may provide opportunities for rational drug development to treat *RAS* mutant malignancies. Breast and ovarian cancers with mutations in the tumor suppressor genes *BRCA1* or *BRCA2* are a paradigm for exploiting genotype-selective synthetic lethal interactions in targeted cancer therapy[112,113]. These tumors are dependent on the DNA repair enzyme PARP1 and respond to treatment with PARP inhibitors[114]. An attractive strategy for targeted drug development for *RAS*-mutant cancers involves identifying signaling pathways that become essential for cancer cell survival in the context of oncogenic RAS signaling.

Screening approaches to identify synthetic lethal interactions

Screening approaches to identify clinically relevant synthetic lethal interactions face several hurdles[115,116]: **(1)** systematic identification of synthetic lethal interactions requires interrogation of large numbers of gene-pair combinations; **(2)** synthetic lethal interactions result in lethality, making mutant recovery and identification challenging; and **(3)** many synthetic lethal interactions are context-dependent, and may not be observed in all genetic backgrounds or cellular conditions. These challenges can be partly addressed through the use of high-throughput screening approaches.

Two commonly used tools for genetic interrogation in human cells are RNA interference (RNAi) and CRISPR/Cas9. RNAi takes advantage of a conserved endogenous pathway that regulates gene expression via small RNAs[117,118]. Endogenous RNAi machinery can be appropriated by introducing synthetic small RNAs into cells. The introduced short interfering RNA (siRNA) or short hairpin RNA (shRNA) is loaded into the RNA-induced silencing complex (RISC), which in turn promotes the degradation of complementary target mRNA[118,119].

The CRISPR/Cas9 genome editing technique uses a guide RNA (gRNA) that targets the Cas9 endonuclease to specific sequences in the genome, and Cas9 introduces a blunt-ended double-strand break (DSB). Repair can occur through the homologous recombination repair pathway or end-joining pathways such as non-homologous end-joining (NHEJ) and alternative end-joining (AltEJ). The end-joining pathways are error-prone, and typically result in small insertions and/or deletions (indels). Indels are selected for in CRISPR screens, as error-free repair re-establishes the wildtype sequence, which is targeted again by the gRNA-guided Cas9. Indels in the gene can result in either a frameshift mutation that generates knockout through protein truncation or mRNA nonsense-mediated decay, or an in-frame mutation that may have a phenotypic effect depending on the structural or functional importance of the altered region[120,121].

Recent advances in RNAi and CRISPR technology have enabled massively parallel screens for synthetic lethal interactions in human cells. These screens are typically performed on either pairs of isogenic cell lines that differ only on the status of the gene of interest (**Figure 4Ai**), or a panel of genetically diverse cell lines that are split

into two groups depending on the status of the gene of interest (**Figure 4Aii**). Large-scale perturbation of the expression of individual genes can be achieved using libraries of siRNAs, shRNAs, or gRNAs for CRISPR/Cas9 genome editing[115,122]. These reagents can be applied in an arrayed format (**Figure 4B)**, in which the effect of each siRNA or shRNA is analyzed in individual wells, or in a pooled format, in which shRNA or gRNA vectors are combined in a pool and the change in relative abundance of individual shRNAs or gRNAs in the population is quantified (**Figure 4C**). A major advantage of the pooled screening approach is that large collections of shRNAs or gRNAs can be efficiently interrogated.

RNAi-based targeted gene suppression provided the first opportunity to perform scalable genetic screens in human cells[10,123-125]. These systematic synthetic lethality screens have contributed much knowledge to human functional genomics. However, the lack of overlap in findings among independent RNAi screens have raised concern regarding RNAi reagent specificity[116]. More recently, large scale CRISPR/Cas9 screens have proven to be a powerful method to identify gene dependencies[14].

RNAi and CRISPR/Cas9 based screens have different technical and methodical advantages[126]. The major differences between the two technologies are in kinetics, penetrance, nature of phenotype, and specificity. **(1)** RNAi-mediated attenuation of gene expression is rapid, typically achieved in a matter of 1-2 days. Conversely, the CRISPR/Cas9 system usually requires at least a week to achieve maximum gene knockout[120]. **(2)** RNAi-mediated gene depletion is highly penetrant, with fairly uniform effects across individual cells. Contrastingly, to achieve complete gene knockout with the CRISPR/Cas9 system, every functional copy of the target gene must be disrupted; however, editing efficiencies of Cas9-expressing cells vary and can be below 50%[120,121,127,128], suggesting that many cells have incomplete gene knockout. Moreover, approximately 1/3 of indels are expected to be in-frame, and may not disrupt the ORF. Individual cells within a population may express the same gRNA, but acquire different mutations in the targeted gene, leading to phenotypic heterogeneity that contribute noise to large-scale screens[126,129]. **(3)** RNAi approaches typically result in incomplete knockdown phenotypes; for applications such as drug target discovery, phenotypic hypomorphs achieved by RNAi may better mimic the effect of chemical inhibition during

therapeutic application. CRISPR/Cas9 can achieve full genetic knockout, which may demonstrate a stronger phenotype and unveil additional genetic interactions. **(4)** Lastly, a major disadvantage of RNAi based approached is lack of specificity due to off-target effects, in which siRNAs can silence non-target mRNAs with limited sequence complementarity, often through interactions with the 3'-UTR[130-132]. The minimal overlap reported among independent RNAi screens have raised concern over the ability of RNAi to annotate gene function[133]. The CRISPR/Cas9 system is thought to be highly specific[129], though off-target effects of the CRISPR/Cas9 system are likely not yet fully appreciated. Notably, genome editing by the CRISPR/Cas9 system has toxic effects, and in the setting of genome-scale screens in aneuploid cancer cells may result in the identification of false positive gene dependencies[15,134].

Challenges in screening for synthetic lethal interactions

For large scale RNAI and CRISPR/Cas9 screens for synthetic lethal interactions, the two greatest remaining challenges are in reagent specificity and context dependence. For both RNAi and CRISPR/Cas9 screens, the efficiency of gene inactivation varies among individual shRNAs or gRNAs targeting the same gene. In addition, off-target effects associated with specific sequences contribute to false positive and false negative findings. Extensive efforts have been made to improve the specificity of RNAi libraries. RNAi design principles have emerged to increase on-target robustness and reduce off-target effects[130,132,135,136], and library generation has improved through the incorporation of bioinformatics algorithms[135,137,138]. In addition, the analysis of large-scale RNAi screens have emphasized the importance of reducing false positives by observing consistent phenotypes in multiple RNAi reagents that target the same gene[3,11,125,139]. The CRISPR/Cas9 system was more recently discovered, and efforts are ongoing to improve on-target robustness and to define off-target effects[129]. However, early discoveries have been incorporated into the design of new gRNA libraries[140-143]. Loss-of-function screens for essential genes using these improved gRNA libraries have uncovered many common as well as cell line-specific fitness genes[14,15,127,134] Ultimately, using the orthogonal RNAi and CRISPR/Cas9 systems in parallel will facilitate the identification of high-confidence synthetic lethal interactions.

An enduring challenge to identifying reproducible synthetic lethal interactions is context-dependence. Cell intrinsic (such as genetic background) and cell extrinsic (such as microenvironment) factors can modify synthetic lethal interactions. In yeast, it has been shown that certain genetic interactions are revealed only with the disruption of three or more genes[144]. This suggests that the genetic background of a cell line (such as loss of a tumor suppressor gene and nearby genes, oncogene activation, or even passenger mutations) could uncover or suppress synthetic lethal interactions. A major complication in screening for synthetic lethal interactions in isogenic cell lines is that the interactions identified may be context-dependent, occurring only in combination with other mutations or in a specific cell type or lineage (**Figure 4Ai**). Hence, a synthetic lethal interaction identified in any given cell pair may not be broadly valid. Issues of context dependency can be overcome by performing genetic screens in panels of diverse cell lines that are split during analysis based on the status of the gene of interest (**Figure 4Aii,C**). This thorough approach enables the identification of genes that are universally lethal in cells of diverse genotypes and lineages that harbor a specific mutation, circumventing the problem of context-dependence. However, this approach requires screening large numbers of cell lines, and could preclude the identification of strong synthetic lethal interactions that would be of clinical interest, but are conditional on specific genetic contexts.

Genotype-selective synthetic lethal interactions with oncogenic RAS

Several systematic genetic screens have been performed in human cancer cell lines to identify synthetic lethal interactions with mutant RAS. These studies have employed different screening modalities (cell line selection, time frame, pooled versus arrayed screening) and reagents (siRNA, shRNA, or CRISPR/Cas9)[14,116,122,145]. Screens were typically performed with pairs of isogenic cell lines, or with a panel of cancer cell lines that differ in *RAS* mutation status. These screens have confirmed that many *KRAS*-mutant cell lines are addicted to RAS, and identified many genes that may be synthetic lethal with oncogenic RAS (**Table 2**). These genes are involved in diverse processes, including cell cycle (*BIRK5, PLK1,* and *APC/C*), cell survival (*BCL2L1* and *WT1*), transcription (*GATA2* and *SNAIL1*), and parallel pro-proliferative pathways (*TAK1* and *TBK1*) (**Table 2**).

Thus far, none of the proposed synthetic lethal interactors have been able to discriminate between *RAS*-mutant and *RAS*-wildtype cells as well as KRAS itself[145]. In addition, there has been a striking lack of overlap in RAS synthetic lethal genes identified from different screens. The only genes to score across multiple screens have been proteasome complex members[3,4,146,147]. Oncogenic *RAS* has been reported to increase rates of protein synthesis, which may render cells more dependent on the proteasomal degradation of mutated or misfolded proteins[148]. However, it remains unclear whether *RAS* mutation status predicts response to proteasome inhibitor therapy in the clinic[149].

The first generation of *RAS* synthetic lethal screens have uncovered interesting biology in *RAS*-mutant cancers. However, the lack of overlap in identified synthetic lethal interactors with oncogenic *RAS* have raised concerns about the applicability of these findings[116]. There are multiple possible explanations for the low overlap across different screens. Studies have employed different reagents (siRNA or shRNA), screening modalities (time frame, pooled versus arrayed, and *in vitro* versus *in vivo* screening), and contexts (cell lineage, isogenic cell lines versus cell line panel)[33,145]. Each of these factors has unique limitations and likely contributes to false-negative and false-positive rates. It is likely that many synthetic lethal partners of oncogenic KRAS remain unidentified.

While the first-generation RAS synthetic lethal screens have numerous limitations, they have led to several interesting targets, including *TBK1* and *WT1*, which continue to be the focus of ongoing investigation[3,5]. Notably, *TBK1* shows promise as a novel therapeutic target for *KRAS*-driven malignancies. Preclinical studies using a small molecule inhibitor of TBK1 achieved clear therapeutic responses in *Kras*-mutant GEMMs[9]. Additionally, studying TBK1 has led to the discovery of a novel effector pathway of oncogenic RAS, in which TBK1 promotes RAS-driven tumorigenesis by regulating an autocrine cytokine circuit. Such data support the idea that synthetic lethal genetic interactions can identify valuable therapeutic targets and broaden our understanding of critical mediators of oncogenic RAS, motivating our interest in identifying further novel candidates. Improvements in genome-scale screening technology, such as improved RNAi libraries and CRISPR/Cas9 knockout libraries, and

the use of expanded collections of cancer cell lines are promising for the discovery of novel synthetic lethal targets.

Drug-conditional synthetic lethal interactions

Single-agent targeted therapies have achieved impressive clinical responses in a variety of oncogene-addicted cancers[87,150-154]. However, the rapid development of drug resistance limits therapeutic efficacy, and single-agent targeted therapies are rarely curative[155,156]. The highly interconnected nature of signaling pathways limits the benefits of inhibiting a single signaling pathway[156-158]. Feedback mechanisms among signaling pathways enable cells to maintain pathway activity despite the presence of a small molecule inhibitor. A better understanding of the alternative pathways that become essential to maintain viability when a major signaling pathway is pharmacologically inhibited (termed 'drug-conditional synthetic lethal interactions') would facilitate the design of rational combination therapeutic regimens (**Figure 5**). For example, a drug-conditional synthetic lethal interaction was recently identified in *BRAF*-mutant colon cancers: shRNA screens demonstrated that depletion of EGFR is synthetic lethal with small molecule BRAF inhibition, suggesting a that combined BRAF and EGFR inhibition could be of clinical utility[159,160]. Several clinical trials assessing the clinical utility of this combination of inhibitors are currently ongoing, and early phase clinical trials have reported promising results[161]. This suggests that pharmacologically targeting drug-conditional synthetic lethal interactions may increase the efficacy of existing therapeutic agents.

Given that RAS has proven difficult to target directly, therapeutic efforts in *RAS*-mutant cancers have focused on inhibiting downstream RAS effector pathways, such as the MAPK and PI3K pathways. As discussed previously, the strategy of inhibiting downstream RAS effectors (such as the MAPK and PI3K pathways) has had limited therapeutic efficacy. There has been much interest in conducting drug-conditional synthetic lethality screens to identify enhancers of MEK inhibition in *KRAS*-mutant tumors. shRNA screens have identified BCL-XL[162] and HER3[163] as synthetic lethal interactors with MEKi in *KRAS*-mutant cancers . Clinical trials combining MEK inhibitors with pan-HER inhibitors or BCL-XL inhibitors are currently in progress. Such data support the idea that drug-specific synthetic lethal interactions can be leveraged to

increase the cytotoxicity of existing therapies and deepen our understanding of oncogenic RAS signaling.

Results

Candidate synthetic lethal interactions with oncogenic KRAS

We analyzed the data from Project Achilles v2.4, which consists of 216 cell lines screened with a genome scale shRNA library[12], to identify synthetic lethal target genes with specific essentiality in *KRAS*-mutant cells (**Figure 2-1**). To reduce the likelihood of identifying lineage-specific rather than *KRAS*-mutant-specific essential genes, we focused our analyses on carcinoma cell lines (133 of 216 cell lines).

To address potential off-target effects, we used a computational method developed in our laboratory, ATARiS (Analytic Technique for Assessment of RNAi by Similarity) to generate a gene-level essentiality score based on RNAi reagents whose phenotypic effects are most likely related to suppression of their intended targets[139]. The underlying assumption is that shRNAs designed to interrogate the same gene should have similar on-target effects in addition to individual off-target effects from perturbation of unintended transcripts. Hence, the on-target effects of shRNAs targeting the same gene can be estimated by quantifying the similarity in the pattern of phenotypic effect across multiple cell lines.

A two-class comparison was performed by classifying cell lines as *KRAS*-mutant (37 cell lines) or *KRAS*-WT (96 cell lines) using *KRAS* mutation status reported in the Broad-Novartis Cancer Cell Line Encyclopedia (CCLE) database[164] and using a mutual information based metric[12] to rank dependency data (shRNA- or gene- level) based on the degree of correlation with *KRAS* mutation status. In this analysis, *KRAS* itself was identified as the top candidate whose expression is selectively essential for the survival/proliferation of *KRAS*-mutant cells (**Table 3**). As KRAS depletion is known to induce cell death in *KRAS*-mutant cells (KRAS addiction), the identification of *KRAS* as a genetic dependency of *KRAS*-mutant cell lines serves as a positive control for this analysis. Aside from *KRAS*, 8 genes scored as significantly essential (FDR < 0.25) for the proliferation/survival of *KRAS*-mutant cells (**Table 3**).

Prior studies indicate that a subset of *KRAS*-mutant cell lines are insensitive to KRAS depletion[3,42]. Conversely, while the majority of *KRAS*-WT cell lines are KRAS-independent, some are sensitive to KRAS depletion. Indeed, we found that *KRAS*

mutation status did not always predict KRAS dependency (**Figure 7**). To identify genes whose expression is essential in cell lines that are both *KRAS*-mutant and KRAS dependent, two-class comparisons were performed in which cell lines were classified by **(1)** KRAS mutation status and sensitivity to KRAS depletion as measured by the KRAS ATARiS score[139], a value that reflects the aggregate effects of 10 KRAS shRNAs screened in Project Achilles; or **(2)** KRAS mutation and sensitivity to KRAS depletion by shKRAS-1, a KRAS-targeting shRNA that effectively depletes KRAS expression at a protein level[3] (**Figure 8, Table 4)**. Two-class comparisons were performed on shRNA level and ATARiS (gene) level data (**Figure 6**). In all two-class comparisons, KRAS was identified as the most statistically significant candidate. In total, 59 candidate oncogenic KRAS co-dependencies were identified for further study (**Table 5**).

There is little overlap between the previously identified co-dependencies of oncogenic KRAS (**Table 2**) and candidates from this analysis (**Table 5**, highlighted in gray**)**. Of the previously identified co-dependencies, only TAK1[42], WT1[5], CDK2 and CDK6[165] score in any of the analyses. This could be attributable to a variety of factors: some of the previously identified genes may be cell line or lineage specific dependencies. Several candidates identified in these analyses were not screened in prior studies. Additionally, some of the previously identified candidates that were not identified as significant co-dependencies in these analyses (GATA2 and STK33) may have been false positives secondary to shRNA off-target effects[11]. Lastly, genes involved in autocrine pro-survival cytokine signaling pathways, such as TBK1[3], are unlikely to be identified from pooled screens such as Project Achilles due to compensatory cytokine signaling from neighboring cells.

Off-target effects complicate the interpretation of RNAi screens

In the two-class-comparison analysis in which cell lines were classified by *KRAS* mutation status, COG2 was the most statistically significant gene, and its depletion had the greatest magnitude of differential effect between *KRAS*-mutant and *KRAS*-WT cell lines, with the exception of KRAS itself. COG2 remained a significant candidate gene in the analyses in which cell lines were classified by KRAS mutation status and dependency (**Table 5).** Moreover, when the analogous analyses were performed on an

independently derived dataset[166], in which genome-scale pooled shRNA screens were performed across 72 cancer cell lines (59 with known KRAS mutation status, including 26 *KRAS*-mutant and 33 *KRAS*-WT), COG2 was again identified as a co-dependency of *KRAS*-mutant cell lines (**Table 3** and **5)**. Hence, COG2 was prioritized for validation as a selective dependency of *KRAS*-mutant cells.

All five COG2-targeting shRNAs screened in Project Achilles deplete COG2 expression at the mRNA and protein level (**Figure 9**). The two shRNAs (shCOG2-4 and shCOG2-5) that best distinguished between *KRAS*-mutant and *KRAS*-WT cell lines in Project Achilles were selected to be assessed in a cell proliferation assay. One *KRAS*-WT cell line (BXPC3) and three *KRAS*-mutant cell lines (HPAC, HPAFII, and YAPC) were infected with two shCOG2, two shKRAS, and two control shRNAs. In this initial assay, both *KRAS*-WT and *KRAS*-mutant cell lines appear sensitive to COG2 depletion (**10A**).

The possible off-target effects of shCOG2 shRNAs were assessed in four ways: 1) performing a rescue experiment; 2) assessing the effect of three additional COG2-targeting shRNAs on cell viability; 3) evaluating sh911 seed-control shRNAs[167] for individual shCOG2 shRNAs; and 4) using the CRISPR/Cas9 system to evaluate the effect of COG2 knockout. In the rescue experiment, a *KRAS*-mutant cell line (HPAC) was infected with either LacZ (control) or COG2 cDNA. Subsequently, COG2 expression was suppressed using two shRNAs, one (shCOG2-6) of which targets the 3'-untranslated region (UTR) of *COG2* (**Figure 11A**). Overexpressing COG2 did not restore cell viability/proliferation (**Figure 11B**). However, it is possible that the exogenously expressed COG2 was not functionally active, as it contains a N-terminal V5 tag.

COG2 was evaluated as a putative co-dependency of oncogenic KRAS by testing additional shCOG2 shRNAs tested in a cell proliferation assay. Three shCOG2 shRNAs, which were not screened in Project Achilles and which effectively reduce COG2 expression were selected (**Figure 12A**). In two *KRAS*-mutant and two *KRAS*-WT cell lines, the effect of the two shCOG2 shRNAs that were screened in Project Achilles (shCOG2-5 and shCOG2-6) mirror the effects of the two shKRAS shRNAs (**Figure 12B**). However, the effects of the three novel shCOG2 shRNAs (shCOG2-7, shCOG2-8,

and shCOG2-9) did not correlate with KRAS mutation or KRAS dependency (**Figure 12B**). This suggested that COG2 might not be a true co-dependency of *KRAS*-mutant cells.

C911 seed-control shRNAs[167], in which bases 9 through 11 of the shRNA targeting sequence are replaced with their complement (**Figure 13A)**, were used to assess off-target effects of two shKRAS shRNAs and the two shCOG2 shRNAs that were found to correlate with KRAS dependency. These shRNAs were evaluated in a cell proliferation assay in one *KRAS*-WT cell line (NCIH1437) and two *KRAS*-mutant cell lines (PANC0203 and YAPC) (**Figure 13B**). Results indicate that one of the shRNAs targeting KRAS, shKRAS-2, has off-target effects that decrease cell viability (**Figure 13B**, both C911 shKRAS-2 and shKRAS-2 decrease the viability of *KRAS*-WT NCIH1437). shKRAS-1, on the other hand, does not demonstrate such off-target effects (**Figure 13B**, neither C911 shKRAS-1 nor shKRAS-1 decrease the viability of *KRAS*-WT NCIH1437). shCOG2-4 and shCOG2-5 do not appear to have strong off-target effects that decrease cell viability (cell viability is decreased by both shCOG2 shRNAs but not the C911 seed-control shRNAs, **Figure 13B**). As COG2 depletion decreased viability of all cell lines assessed, one of which was *KRAS*-WT and KRAS-independent (NCIH1437), COG2 is not a selective co-dependency of *KRAS*-mutant or KRAS-dependent cell lines.

The CRISPR/Cas9 gene knockout system[120] provides an orthogonal method to assess the effect of COG2 loss. We assessed the effect of COG2 (gCOG2) or KRAS (gKRAS) knockout in a *KRAS*-WT cell line (NCIH1437) and a *KRAS*-mutant cell line (YAPC) in a crystal violet cell proliferation assay. We found that KRAS knockout reduced viability in *KRAS*-mutant cells, but had no effect in NCIH1437. COG2 knockout did not affect viability in *KRAS*-WT or *KRAS*-mutant cells (**Figure 14**).

In summary, our experiments demonstrate that COG2 suppression result in no differences in viability between *KRAS*-WT and *KRAS*-mutant cells, indicating that COG2 is not a co-dependency of *KRAS*-mutant cells. Off-target effects can be a significant source of false-positives in shRNA-based experiments. Additionally, the *KRAS*-mutant cell lines screened in Project Achilles are predominantly of pancreatic, lung, and colon lineages; the candidate genes identified from the two-class comparisons described

above (**Table 5**) could be confounded by lineage-specific (rather than *KRAS*-mutant-specific) dependencies. The fact that COG2, the highest priority candidate from the analyses described above, failed to validate as a co-dependency of *KRAS*-mutant cells highlights the importance of incorporating additional filters to prioritize candidate genes and the use of efficient and unambiguous assays to validate candidate co-dependencies of oncogenic KRAS.

Prioritized candidate co-dependencies of oncogenic KRAS

We have considered three approaches to refining the list of candidate synthetic lethal interactors with oncogenic KRAS identified through analyzing Project Achilles shRNA screens (**Table 5**): **(1)** prioritize genes that are more highly expressed in *KRAS*-mutant cells; **(2)** analyze genome scale CRISPR/Cas9 knockout screens and prioritize genes that are confirmed to be selectively essential in *KRAS*-mutant cells using this orthogonal approach to genetic perturbation; and **(3)** exclude candidate genes that likely score secondary to off-target effects by computationally estimating the seed effects of the shRNAs used in the Project Achilles screens.

The list of the candidate genes (**Table 5**) can be refined by prioritizing genes that are more highly expressed in *KRAS*-mutant cells. This selection criterion assumes that genes that promote cell proliferation/survival selectively in the context of oncogenic KRAS are likely to be overexpressed in *KRAS*-mutant cells than in *KRAS*-WT cells. We analyzed RNA-sequencing data of cell lines in the Cancer Cell Line Encyclopedia (CCLE)[164] to identify genes that were significantly upregulated in 130 *KRAS*-mutant carcinoma cell lines compared to 769 *KRAS*-WT carcinoma cell lines (t-test, FDR < 0.05). Of the 59 candidate genes, 6 were overexpressed in *KRAS*-mutant cell lines (ABP1, BCL2L1, CXCL6, DOCK5, FERMT1, and NCOR2) (**Figure 15A**). Of note, not all genes that are selectively essential in *KRAS*-mutant cell lines are expected to be upregulated – indeed, KRAS itself is not significantly overexpressed in *KRAS*-mutant cells.

As an orthogonal approach to identify KRAS synthetic lethal interactions, our laboratory has performed genome-scale CRISPR/Cas9 loss-of-function genetic screens. The screens have performed in 53 cancer cell lines (32 *KRAS*-mutant and 21

KRAS-WT). In this screen, candidate genes are knocked out through genome editing by the CRISPR/Cas9 system using the genome-scale CRISPR/Cas9 knockout version 2 (GeCKOv2)[168] or Avana[141] library. Conceptually, this screen is analogous to the shRNA-mediated Project Achilles screen described above (**Figure 6**). However, there are several advantages to a knockout (versus knockdown) approach. The CRISPR/Cas9 system is a highly specific and efficient tool for genetic ablation, with greater consistency of effect among gRNAs targeting the same gene than is typically observed with shRNAs. This specificity likely improves the signal-to-noise ratio and decreases the false-positive rate of the screen. Additionally, CRISPR-mediated genome editing completely eliminates target gene expression, and may induce stronger phenotypes than shRNA-mediated gene suppression, which only partially depletes target genes. Lastly, shRNAs and gRNAs presumably have non-overlapping off-target effects, making data from the CRISPR/Cas9 screen useful for prioritizing the candidate co-dependencies of oncogenic KRAS identified from the shRNA screens.

We performed a two class comparison on the Project Achilles CRISPR/Cas9 knockout v3.6.2 dataset to identify genes that were selectively essential in *KRAS*-mutant carcinoma cell lines. We identified 360 significant (FDR < 0.25) candidate genes, but only 4 (ATP2B4, DOCK5, KRAS, and RAF1) overlapped with the 59 candidates nominated from analyses of the Project Achilles shRNA dataset (**Figure 15B**). KRAS and RAF1 (CRAF) were anticipated co-dependencies of *KRAS*-mutant cells. However, DOCK5 and ATP2B4 have not been implicated in RAS signaling, and are high-priority candidates for follow-up studies.

Lastly, DEMETER is an algorithm that models the effects produced by individual shRNA as a linear combination of gene-related effects and seed-related effects[11]. In the shRNA library used in project Achilles, each gene is targeted by ~6 shRNAs. Each of these shRNAs have “seedalogs,” which are shRNAs that share the same seed sequence (residues 1-8 at the 5’ end of the guide strand) but that are designed target different genes. Similar to ATARiS, DEMETER estimates the on-target effect of shRNAs targeting the same gene by quantifying the similarity in their phenotypic effects across multiple samples. DEMETER also quantifies the off-target “seed” effect of individual shRNAs by quantifying the similarity in its phenotypic effect across multiple samples to

the effect of its seedalogs. If the effect of a given shRNA across multiple cell lines appears to be more similar to its seedalogs than to other shRNAs targeting the same gene, the primary effect of this shRNA is likely off-target. We used DEMETER on the Project Achilles v2.4 dataset to quantify the on- and off-target effects of individual shRNAs. We found that only 14 of the 59 candidate genes were identified by at least 2 shRNAs that had an estimated on-target effect of >50% (**Figure 15C**). These candidate genes are less likely to have been identified as a candidate co-dependency of *KRAS*-mutant cells due to off-target shRNA effects.

Potential dependency of *KRAS*-mutant cancer cells on DOCK5

DOCK5 is a guanine exchange factor (GEF) that is known to activate RAC1, a member of the Rho GTPase family[169]. We selected DOCK5 for further study because it was more highly expressed in *KRAS*-mutant than *KRAS*-WT cell lines (**Figures 15A** and **16**). Moreover, analyses of both Project Achilles shRNA and CRISPR/Cas9 screens identified DOCK5 as being specifically essential in *KRAS*-mutant cells (**Figure 15B**).

We assessed the effect of DOCK5 depletion in a *KRAS*-WT cell line (NCIH1437) and a *KRAS*-mutant cell line (PATU8902). We found that DOCK5 depletion reduced viability of *KRAS*-mutant cells, but had no effect on *KRAS*-WT cells (**Figure 7A**). Interestingly, we noticed that shRNAs targeting DOCK5 not only reduced DOCK5 expression, but also reduced *KRAS* expression (**Figure 7B**). We generated C911 seed-control shRNAs[167] to assess the potential off-target effects of the DOCK5-targeting shRNAs. We found that both C911 shDOCK5-2 and shDOCK5-2 reduce *KRAS* expression, though only shDOCK5-2 reduces *DOCK5* expression (**Figure 18A-C**). Notably, both C911 shDOCK5-2 and shDOCK5-2 reduce viability of *KRAS*-mutant cells, suggesting that shDOCK5-2 reduces viability of *KRAS*-mutant cells due to off-target suppression of *KRAS* expression rather than its suppression of DOCK5 expression (**Figure 18D**). In line with this hypothesis, a different DOCK5-targeting shRNA (shDOCK5-3) and its seed control (C911 DOCK5-3) do not reduce *KRAS* expression have no effect on cell viability (**Figure 18**).

To further assess the effect of DOCK5 loss on KRAS expression and cell viability, we reduced DOCK5 expression using two tools: siRNAs and CRISPR/Cas9.

We assessed the effect of siRNA-mediated DOCK5 depletion in two *KRAS*-mutant cell lines (HCT116 and PATU8902). We utilized a pool of four siRNA duplexes designed to target distinct sites within DOCK5 (Dharmacon SMARTpool). We found that siRNAs targeting DOCK5 effectively reduced DOCK5 expression without decreasing KRAS expression at the mRNA or protein level (**Figure 19A-C**). However, DOCK5 depletion had no effect on cell viability (**Figure 19D**).

Subsequently, we used the CRISPR/Cas9 system to knockout DOCK5 in the *KRAS*-mutant cell line PATU8902. We tested 4 gRNAs targeting DOCK5, and found 3 that effectively knocked out DOCK5 as indicated by reduced DOCK5 mRNA expression (**Figure 20A**). We found that DOCK5 deletion had no effect on KRAS expression or on downstream MAPK or PI3K pathway activity (**Figure 20B,C**). In addition, we found that DOCK5 deletion had no effect on cell viability **(Figure 20D,E**). Overall, our findings suggest that DOCK5 does not regulate KRAS expression, and that DOCK5 depletion does not affect viability in *KRAS*-mutant cells.

DOCK5 modifies sensitivity to MAPKi in *RAS*-mutant cancers

Drug-conditional synthetic lethal interactions may be leveraged to increase the efficacy of existing therapeutic agents. As discussed above, one of the most promising methods of targeting *RAS*-mutant cancers is to inhibit downstream effector pathways, such as the MAPK pathway. Unfortunately, many *RAS*-mutant cancers demonstrate intrinsic or acquired resistance to MAPKi[96,97]. The development of genome-scale RNAi[170] and CRISPR/Cas9[141,168,171] libraries enable the systematic identification of loss-or-function events that increase drug sensitivity. These drug-conditional synthetic lethal interactions could inform the rational design of combined chemotherapy regimens.

Our laboratory has previously performed 6 genome-scale CRISPR/Cas9 screens to identify modifiers of sensitivity to MAPKi in 5 cancer cell lines harboring *KRAS*, *NRAS*, or *BRAF* mutations[172,173] (**Figure 21A**). In PATU8902 (*KRAS*-mutant, pancreas) cells treated with the MEK inhibitor trametinib, 4 of the 6 gRNAs targeting DOCK5 became strongly enriched; strikingly, out of ~200,000 screened gRNAs, there were 3 gRNAs targeting DOCK5 among the 15 most enriched gRNAs (**Figure 21B**). This suggests that DOCK5 knockout might confer resistance to MAPKi. The major known

function of DOCK5 is to activate the small GTPase RAC1[174,175]. However, the majority of gRNAs targeting RAC1 were depleted in this screen, suggesting that RAC1 knockout sensitizes cells to MAPKi (**Figure 21Bi**).

When we examined the sequences of the gDOCK5 gRNAs, we found that the 4 DOCK5-targeting gRNAs that were enriched in the PATU8902 screen clustered around amino acids 31-56, which maps to the middle of the SH3 domain of DOCK5 (**Figure 21C**). DOCK5 activity is thought to be autoinhibited through interactions between its N-terminal SH3 domain and the C-terminal DHR2 domain[176]. In the process of gene editing, the CRISPR/Cas9 system may generate in-frame insertion/deletions or point mutations[177], a property that has been capitalized on to rapidly generate diverse variants for gain-of-function screens[178,179] Notably, an I32K point mutation in the SH3 domain of the closely related protein DOCK1 abrogates autoinhibition and results in constitutively active DOCK1[176]. It is possible that the enriched *DOCK5*-targeting gRNAs introduced gain-of-function mutations in the SH3 domain of DOCK5 that abrogate its autoinhibition. Consistent with this vein of thought, a gRNA targeting *MAP2K1* (MEK1) was the fourth most enriched gRNA in this screen (**Figure 21Bii**); as trametinib is a MEK1 inhibitor, this particular gRNA likely induced a gain-of-function mutation in MEK1.

We analyzed screening data[172,173] from 4 other cell lines (*RAS*- *or BRAF*-mutant lung or pancreatic cancer cells) treated with MAPK pathway inhibitors (MEK inhibitor trametinib or BRAF inhibitor vemurafenib) to assess how gRNAs targeting *DOCK5* and *RAC1* modulated sensitivity. We found that in most cell lines, gRNAs targeting *DOCK5* and *RAC1* were significantly depleted, suggesting that reduction in DOCK5-RAC1 pathway activity increases sensitivity to MAPKi in *RAS*- and *BRAF*-mutant cells.

To determine whether *DOCK5* knockout altered sensitivity to MEKi in PATU8902 cells, we performed a competition assay to determine whether *DOCK5* knockout altered sensitivity to MEKi. PATU8902 cells that were *DOCK5*-WT (gGFP) were mixed with PATU8902 cells that were *DOCK5*-KO (gDOCK5) in a 1:1 ratio, and the change in proportion of *DOCK5*-WT vs. *DOCK5*-KO cells was monitored over time. We found that DOCK5 deletion reduced cell proliferation/viability only when cells were exposed to the MEK inhibitor trametinib (**Figure 22B**). This suggests that loss of DOCK5 increases sensitivity to MEKi in *RAS*-mutant cells.

Given our observation that *DOCK5* deletion increases sensitivity to MAPKi in *RAS*- and *BRAF*-mutant cells, we hypothesized that *DOCK5* deletion might perturb *RAS* effector pathways such as the MAPK or PI3K pathways. We found that *DOCK5* deletion reduces PI3K pathway activity but has no effect on MAPK pathway activity (**Figures 23, 24**).

Discussion

Candidate synthetic lethal interactions with oncogenic KRAS

Targeting genes that are selectively essential in the context of oncogenic *RAS* signaling is an attractive approach to targeted therapy for *RAS*-mutant cancers. We analyzed data from Project Achilles v2.4, in which a comprehensive genome-scale shRNA screen was performed across 216 human cancer cell lines, and identified 59 candidate genes that may be selectively essential in *KRAS*-mutant cancer cells. We found that the most statistically significant candidate gene, COG2, failed to validate and was likely identified as a consequence of shRNA off-target effects. Our experience with COG2 highlights the need to unambiguously determine whether a putative co-dependency identified from shRNA screening data scored due to on- or off-target shRNA effects. This can be achieved in a variety of ways, including **(1)** testing additional RNAi reagents, **(2)** using C911 seed-control shRNAs to evaluate off-target effects[167], **(3)** performing a rescue experiment, and **(4)** utilizing the orthogonal CRISPR/Cas9 system to knockout[120] or inhibit[180] gene expression.

We propose three ways to filter candidate genes in order to enrich for *bona fide* *KRAS*-mutant co-dependencies: **(1)** prioritize genes that are overexpressed in *KRAS*-mutant cells (6 genes), **(2)** exclude genes that likely scored due to off-target seed effects as estimated using the recently developed bioinformatics algorithm DEMETER[11] (14 genes), and **(3)** prioritize genes that also scored in our analyses of Project Achilles v3.6.2, in which 53 cancer cell lines were screened using a genome scale CRISPR/Cas9 library (4 genes).

It is increasingly appreciated that shRNA off-target effects confound the interpretation of RNAi-based screens. For the majority of this work, we endeavor to minimize the identification of false positive candidates through using multiple shRNA constructs to target each gene and inferring on-target reagents by using the algorithm ATARiS[139] to identify the shRNA constructs that have strongly concordant effects across cell lines. However, residual RNAi off-target effects persisted, and the most statistically significant gene (COG2) failed to validate experimentally.

Analysis of shRNA screening data across a panel of >500 cancer cell lines demonstrated that the viability phenotype across cell lines for pairs of shRNAs that share 7-mer seed sequences (which are responsible for the miRNA-like off-target effects) were significantly more correlated than that of shRNAs targeting the same gene[11], highlighting the prevalence and robustness of miRNA-like seed effects. DEMETER[11] is a recently developed analytical approach that takes advantage of the fact that both the on-target and seed-based effects of RNAi are sequence specific[130,167]. DEMETER deconvolutes the effects of each shRNA into a linear combination of the effects due to target gene depletion and the effects associated with the seed sequences, outperforming algorithms that are based solely on correlation (such as ATARiS, which was used to identify genes in this work) in identifying on-target biologically meaningful genetic dependencies[11]. Using DEMETER, we found that 14 of the 59 proposed candidate genes have at least 2 shRNAs with an estimated on-target effect >50%. These 14 genes are likely enriched for genuine co-dependencies of oncogenic KRAS, and are of high priority for further investigation.

An alternative approach to address shRNA off-target effects is to use an orthogonal system, such as CRISPR-Cas9, and investigating genes that are identified from both screening approaches. Analysis of the Project Achilles shRNA and CRISPR/Cas9 screens identified 59 and 360 candidate synthetic lethal interactions with mutant *KRAS,* respectively, with only 4 genes identified in both. The low overlap between *KRAS*-mutant synthetic lethal candidate genes nominated from analyses of Project Achilles shRNA and CRISPR/Cas9 data is likely attributable to a combination of technical artifacts and biologic factors.

As discussed previously, RNAi reagents are associated with off-target miRNA-like seed effects. While the CRISPR/Cas9 system demonstrates high specificity in gene targeting[129,177], off-target effects are likely not yet fully appreciated. Indeed, our laboratory and others have recently identified target gene-independent induction of cell-cycle arrest mediated by Cas9 endonuclease activity, likely secondary to DNA damage[15,134]. shRNA or CRISPR/Cas9 off-target effects may result in the identification of false-positive candidates or the exclusion of *bona fide* candidates due to false-

negative results, contributing to the low overlap in candidate genes nominated from analysis of the shRNA and CRISPR/Cas9 screens.

Technical artifacts, such as reagent off-target effects or incomplete penetrance of CRISPR/Cas9-mediated gene knockout, limit the degree of saturation achieved in the shRNA and CRISPR/Cas9 screens. If a particular pathway or complex is essential in the context of a genetic alteration, genes encoding all the important components of that pathway or complex should be identified in a saturated synthetic lethal screen. In large-scale screens for synthetic lethal genetic interactions in *Saccharomyces cerevisiae*, a microorganism in which high fidelity gene disruption is readily achieved[181], the set of synthetic lethal interactions associated with a particular gene is typically enriched for all of the genes encoding the components of a functionally related pathway or complex[182-185]. The paucity of relationships (such as pathway or complex membership) observed among the candidate synthetic lethal interactors with oncogenic KRAS nominated here suggests that our screens have not reached genetic saturation.

In addition, several biologic factors contribute to the low overlap in candidate genes nominated from the shRNA and CRISPR/Cas9 screens. Certain candidates (such as cell essential genes) may only have a differential effect as hypomorphs, and would score only in the shRNA screen[186]. Conversely, genes with large functional reserve that are not effectively depleted in the shRNA-based screen may only score in the CRISPR-mediated screen. Moreover, the cell line panels used in the shRNA versus CRISPR/Cas9 screens differed in number (216 versus 53 cell lines) and proportion of particular cell lineages (such as lung, pancreas, or colorectal). As synthetic lethal interactions are highly context dependent, the differences in composition of cell line panels likely reduced the overlap in candidate genes identified from the shRNA and CRISPR/Cas9 screens.

In both RNAi and CRISPR/Cas9 screens, KRAS depletion appears to be the most robust and consistent mode of reducing proliferation/viability of *KRAS*-mutant cancer cells. There may be no universal synthetic lethal interaction with mutant *KRAS* that has equivalent potency to targeting *KRAS* itself across the spectrum of *KRAS*-mutant cancers. Nevertheless, while *KRAS* itself appears to be the strongest genetic dependency in *KRAS*-mutant cells, the identification of weaker but consistent co-

dependencies across *KRAS*-mutant cancers could provide valuable insight into oncogenic KRAS signaling and function. It is likely that strong synthetic lethal interactions with mutant *KRAS* exist within specific combinations of tissue type and mutational background; these context-specific synthetic lethal interactors are attractive candidates for targeted therapy[3,9].

Overall, our findings suggest that screening large numbers of cell lines will be necessary for sufficient power to overcome the genetic heterogeneity of cancer cell lines to identify co-dependencies of *KRAS*-mutant cells that are widely applicable, and which may enhance our understanding of oncogenic *KRAS* signaling. Focusing screening efforts on specific cell lineages would reduce the number of cell lines required, and may unveil robust context-specific dependencies that are clinically valuable. The information derived from shRNA and CRISPR/Cas9 screens are complementary, and may identify non-overlapping co-dependencies for a variety of technical and biologic reasons. Secondary screens (such as an arrayed shRNA screen with appropriate C911 control shRNAs or a candidate mini-pool CRISPR/Cas9 screen) that enable head-to-head comparison of the union of candidate genes nominated by analyses of shRNA and CRISPR/Cas9 screens across large panels of cell lines could be an effective method of initial candidate gene validation and prioritization.

DOCK5-RAC1 pathway in *RAS*-mutant cells

Further exploration is warranted to determine if DOCK5 suppression is synthetic lethal to oncogenic KRAS

We initially identified DOCK5, which is overexpressed in *KRAS*-mutant cells and scores in both Project Achilles shRNA and CRISPR/Cas9 screens, as a candidate co-dependency of oncogenic KRAS. Our validation experiments suggested that DOCK5 depletion is not synthetic lethal in the context of mutant *RAS*. However, this could be definitively concluded as there were weaknesses in our validation experiments: **(1)** the shDOCK5 shRNA that best distinguishes between *KRAS*-mutant and *KRAS*-wildtype cells has an off target effect in which it reduces *KRAS* expression. However, the seed effects of other shDOCK5 shRNAs that selectively reduced viability of *KRAS*-mutant were not evaluated. **(2)** We used pooled siRNAs to deplete DOCK5 in *KRAS*-mutant

cells, and found no effect on cell viability despite ~50% reduction in *DOCK5* mRNA expression. Given the transient effect of siRNA-mediated mRNA depletion, we assessed for differences in viability 4 days after siRNA transfection. The screens in Project Achilles are conducted over the course of 16 cell doublings (typically >20 days); this allows time for protein turnover and amplification of differences in proliferation rate. Although we reduced *DOCK5* mRNA expression (protein level could not be assessed due to lack of DOCK5-specific antibody), residual DOCK5 protein may have compensated in the short term. Additionally, we used CellTiter-Glo, a luminescence based cell viability assay, to quantify cell number; in our experience, this reagent is not sufficiently sensitive to detect modest differences in cell number. **(3)** We found that CRISPR/Cas9-mediated *DOCK5* knockout did not affect viability of *KRAS*-mutant cells. There are major limitations to our CRISPR/Cas9 experimental approach. In a population of cells expressing the same gRNA, there are some that achieve true knockout, others that express truncation or missense proteins, and yet others that suppress Cas9 or gRNA expression and evade genome editing. This heterogeneity may result in a mixture of individual phenotypes that cannot be detected at the population level. Additionally, we passage cells for at least 7 days after gRNA infection to allow time for gene editing[120]. However, if DOCK5 is required for viability, cells that achieve DOCK5 knockout will drop out, and over time we would select for a subpopulation of cells that have maintained DOCK5 expression or which acquired additional genetic alternations that rendered them resistant to DOCK5 deletion. An approach to definitively assess whether DOCK5 depletion is synthetic lethal in the context of oncogenic *RAS* would be to use the CRISPR/Cas9 system to stably knockout *DOCK5* in cells expressing exogenous DOCK5 (such as with a dox-inducible expression construct), and subsequently assess the effect of removing exogenous DOCK5.

DOCK5 is an GEF that activates the small GTPase RAC1 by promoting the dissociation of GDP from RAC1, thereby facilitating GTP binding[187,188]. At least 20 GEFs are implicated in directly activating RAC1. These GEFs are subdivided into the Dbl or DOCK families, which differ in the domain mediating their GEF activity[189]. Intriguingly, since the experiments performed here (*c.* 2012-2014), a second generation CRISPR/Cas9 screen in a panel of acute myelogenous leukemia cells identified the

deletion of *PREX1*, a Dbl RAC1-GEF, to be synthetic lethal with mutant *RAS*[14]. Mechanistically, PREX1 expression was necessary to maintain MAPK pathway activity in *RAS*-mutant cells. Intriguingly, Wang et al. found that that *PREX1* expression is restricted mainly to myeloid cells, and that in *RAS*-mutant non-myeloid hematopoietic cancers, a different Dbl-RAC-GEF, TIAM1*,* was selectively essential[14]. It is possible that RAC1 activity is essential in all *RAS*-mutant cells, and that RAC1 is activated by different RAC1-GEFs in different cell lineages (PREX1 in myeloid cells, TIAM1 in non-myeloid hematopoietic cells, and DOCK5 in epithelial cells). Definitively determining whether DOCK5 expression is selectively essential in *KRAS*-mutant carcinomas will be critical to explore this hypothesis.

DOCK5-RAC1 pathway modulates sensitivity to MAPKi in *RAS*-mutant cells

Identifying genes whose suppression enhances drug sensitivity can enable rational design of combined therapy. We analyzed 6 genome-scale CRISPR/Cas9 screens to identify modifiers of sensitivity to MAPKi in *RAS*-mutant cells. We found that in 4 of the screens, gRNAs targeting DOCK5 were depleted, suggesting that DOCK5 deletion enhances sensitivity to small molecule MEK or BRAF inhibitors. The major known function of DOCK5 is to activate RAC1[174,175]. Notably, gRNAs targeting RAC1 were depleted in all 6 screens, suggesting that suppression of RAC1 signaling increases sensitivity to MAPKi.

Interestingly, one of the screens (PATU8902 cells treated with the MEK inhibitor trametinib) showed strong enrichment of gRNAs targeting DOCK5. However, subsequent examination of the enriched gDOCK5 gRNAs showed that they target the autoinhibitory SH3 domain of DOCK5, where mutations might result in constitutively active DOCK5. We hypothesize that these gRNAs induced gain-of-function DOCK5 mutations, and that this increase in DOCK5 activity conferred resistance to MEKi. Sequencing the DOCK5 locus from the genomic DNA of the end population of cells from this screen would allow us to profile the gRNA-induced mutations.

We confirmed that in *KRAS*-mutant PATU8902 cells, *DOCK5* deletion increases sensitivity to MEKi. An initial experiment suggested that deletion of DOCK5 reduces PI3K signaling as measured by p-AKT. The RAC1 and PI3K pathways are known to have significant crosstalk. For example, PI3K is thought to be directly activated by

RAC1. In turn, PIP3 (the lipid product of active PI3K), recruits and activates RAC1-GEFs, further upregulating RAC1 activity[190,191]. This feed-forward circuitry between RAC1 and PI3K is necessary for the generation of a leading edge in migrating cells[190], and may contribute to proliferation and survival of *RAS*-mutant cancer cells. In addition, prior studies suggest that RAC1 is able to is able to indirectly activate the MAPK pathway through PAK[172,192]. The next steps in determining if and how the DOCK5-RAC1 pathway modulates sensitivity to MAPKi in *RAS*-mutant cells include: **(1)** suppress and overexpress DOCK5 and RAC1 in a panel of cell lines and evaluate the effect on cell viability, and **(2)** evaluate the effect of DOCK5 overexpression and suppression on levels of active (GTP-bound) RAC1 as well as MAPK and PI3K pathway activity.

Oncogenic RAS activates several effector pathways, and concurrent inhibition of multiple pathways may be important. In pre-clinical studies, combined MAPK and PI3K inhibition effectively induced regression of *KRAS*-mutant tumors[193]. However, while this dual-targeting strategy has the potential of being more effective than inhibition of either pathway alone, there may not be a wide enough therapeutic window to effectively suppress both pathways in human cancers[106]. In a recent trial that combined MK-2206 (AKT inhibitor) with selumetinib (MEK inhibitor), no patient achieved over 70% inhibition of both targets at the maximum tolerated drug dose[107]. Dock5-knockout mice demonstrate minor phenotypes, including high bone mass[194], cataracts[195], and reduced myoblast fusion[196], suggesting that DOCK5 inhibition may have low toxicity. It will be interesting to evaluate whether C21[194], a chemical inhibitor of DOCK, or small molecule inhibitors of the RAC1 pathway[197] synergize with small molecule MAPK inhibitors to treat *RAS*-mutant cancers.

Conclusion

In summary, we analyzed shRNA and CRISPR-Cas9 screening data across a large panel of cancer cell lines to nominate genes that are selectively essential in cells with mutant *KRAS,* highlighted experimental methods to unambiguously validate candidate genes, and identified DOCK5 as a modifier of sensitivity to MAPKi in *RAS*- or *BRAF*-mutant cancers.

A major factor that has limited progress in RNAi screens for co-dependencies of oncogenic *KRAS* is the abundant off-target effects of RNAi technology. We highlight approaches to address this at the analysis stage (using algorithms to account for miRNA-like off-target seed effects, filtering by gene expression, and integrating RNAi and CRISPR/Cas9 screening data) and at the validation stage (using seed-control shRNAs, orthogonal modes of genetic perturbation, and ORF rescue).

Aside from genotype-specific synthetic lethal interactions, drug-conditional synthetic lethal interactions hold much promise for the identification of rational combination therapy regimens. Our analysis of genome-scale CRISPR-Cas9 screens for genetic modulators of sensitivity to MAPKi indicates that suppression of the DOCK5-RAC1 pathway may enhance sensitivity to MAPKi in *RAS*-mutant cancers. Notably, recent CRISPR-Cas9 screens in hematopoietic cells identified the RAC1 pathway to be selectively essential in *RAS*-mutant hematopoietic cancers[14]. Further evaluation of the effect of perturbing DOCK5-RAC1 pathway activity in combination with MAPKi may unveil a tractable therapeutic target.

Synthetic lethality is a simple genetic concept that continues to have a major impact on cancer research. Direct screening of human cancer cell lines have identified synthetic lethal interactions with oncogenic KRAS that have enhanced our understanding of oncogenic KRAS signaling and informed novel therapeutic strategies[3,161,198-200]. The small number of cell lines screened and the experimental artifacts associated with RNAi off-target effects have limited the power of prior studies. It is likely that the use of expanded RNAi libraries with improved analysis techniques to estimate off-target effects as well as orthogonal CRISPR/Cas9 knockout libraries in an expanded collection of cell lines will enable the discovery of novel synthetic lethal interactions that are relevant across broad contexts.

Materials and methods

Analysis of Project Achilles v2.4 (shRNA)

The generation of the Project Achilles v2.4 dataset has been previously described[12], and was analyzed at the shRNA level and gene level. Gene level data was generated using ATARiS (Analytic Technique for Assessment of RNAi by Similarity)[139]. Data was analyzed by two-class comparison using PARIS[12], an algorithm that uses a mutual information based metric to rank sample data (shRNA/gene dependency) based on the degree of correlation to a classification scheme (*KRAS* mutation status). Analyses were performed in which carcinoma cell lines were classified by 1) KRAS mutation status; 2) *KRAS* mutation status and KRAS dependency as determined by KRAS ATARiS score (cell lines with KRAS ATARiS score < -0.875 were considered to be KRAS dependent); 3) *KRAS* mutation status and KRAS dependency as determined by the shKRAS-3 shRNA that was previously shown to effectively deplete KRAS[3](cell lines with shKRAS-3 ZMAD score < -0.77 were considered to be KRAS dependent). shRNAs or genes with an FDR < 0.25 were considered to be statistically significant. shRNA on-target effects were determined using DEMETER[11], an recently developed algorithm that models the effects produced by individual shRNAs as a linear combination of gene-related effects and seed-related effects. We used DEMETER on the Project Achilles v2.4 dataset to quantify the on- and off-target effects of individual shRNAs. High priority candidate genes were those which had at least 2 shRNAs with an estimated on-target effect of >50%.

Analysis of Project Achilles v3.6.2 (CRISPR/Cas9)

The Project Achilles v3 (CRISPR/Cas9) dataset was recently published[15]. Here, we analyzed a preliminary dataset (Project Achilles v3.6.2). Briefly, Cas9-expressing cells were infected with the genome scale Avana pooled CRISPR library[141], in which each gene is targeted by 4 different gRNA constructs. After puromycin selection, cells are passaged for 14 days. At this time, genomic DNA is harvested, and the change in gRNA representation compared to the original gRNA plasmid pool is determined. Gene-level data was generated using ATARiS[139], and data was analyzed by two-class comparison

using PARIS. Carcinoma cell lines were classified by KRAS mutation status, and genes with an FDR < 0.25 were considered to be statistically significant.

Analysis of CCLE RNA-sequencing expression data

Cell line RNA-sequencing data was obtained from the Cancer Cell Line Encyclopedia [164]and analyzed using GENE-E, a matrix visualization and analysis platform developed by Joshua Gould (http://www.broadinstitute.org/cancer/software/GENE-E/). The 889 carcinoma cell lines were classified by KRAS mutation status (130 *KRAS*-mutant and 759 *KRAS*-WT), and differentially regulated genes were identified using the "Signal to Noise" metric; genes with a FDR < 0.05 were considered statistically significant.

CRISPR/Cas9 + MAPKi drug modifier screen data

The CRISPR/Cas9 drug modifier screens were recently published[172,173]. Briefly, for each screen, two infection replicates were performed with 30-40% infection efficiency and an average of 500 cells per gRNA after selection. 24 hours after infection, cells were selected in 2 µg/mL puromycin for 6 days and expanded in puromycin-free media for 4 days (PATU8988T) or 7 days (PATU8902, CALU1, HCC364, and NCIH1299). After puromycin selection, for CALU1, HCC364, and H1299, 60 x 10^6 cells were harvested for the Day 0 time point, and 60 x 10^6 cells were treated with drug. HCC364 cells were treated with 25 nM trametinib or 6.25 µM vemurafenib; H1299 cells were treated with 1.5 µM trametinib; and CALU1 cells were treated with 50 nM trametinib. For PATU8902, 75 x 10^6 cells were seeded in T225 flasks in media without drug on Day -1. Cells were allowed to adhere for 24 hours, and 100 nM trametinib was added to the cells on Day 0. For PATU8988T, 40 x 10^6 cells were seeded in T225 flasks with 10 nM trametinib on Day 0. Cells were passaged in drug or fresh media containing trametinib was added every 3-4 days. Drug-treated cells were harvested 14 days (all cell lines) and 21 days (CALU1, HCC364, H1299, and PATU8902) after initiation of trametinib treatment. Genomic DNA was extracted using the Qiagen Blood and Cell Culture DNA Maxi Kit according to the manufacturer's protocol. PCR of gDNA and pDNA (gRNA plasmid pool used to generate virus) was performed as previously described[141]. Sequencing and analysis of genome scale CRISPR-Cas9 knockout screens was performed as

previously described[141]. The $\log_2$(fold-change) in gRNA representation between cells treated with trametinib for 14 or 21 days and baseline sample (Day -3 sample for PATU8988T, Day -1 sample for PATU8902, and Day 0 sample for CALU1, HCC364, and NCIH1299) was calculated.

Cell lines and reagents

Cells were maintained in DMEM (BXPC3, HPAC, HPAFII, PATU8902, PATU8988T, RKO, YAPC; Corning) or RPMI-1640 (NCIH1437, PANC0327; Corning) supplemented with 2 mM glutamine, 50 U/mL penicillin, 50 U/mL of streptomycin (Gibco), and 10% fetal bovine serum (Sigma), and incubated at 37°C in 5% CO_2.

Virus production

293T cells were seeded in 6 cm dishes. 24 hours later, cells were transfected with 100 ng VSVG, 900 ng delta8.9, and 1 µg ORF, shRNA or gRNA plasmid using OptiMEM and Mirus TransIT. Culture supernatants containing lentivirus was harvested 48 – 72 hours after transfection. Virus was pooled and stored at -80 °C.

Generation of isogenic cell lines

To generate cell lines stably expressing Cas9, cells were infected with the Cas9 expression vector pXPR_BRD111 and selected with 10 µg/mL blasticidin for 4-7 days. Cas9-expressing cells were maintained in 2-5 µg/mL blasticidin. To generate isogenic cell lines using the CRISPR/Cas9 system, 200,000 Cas9-expressing cells per well were seeded in 6-well plates in 2 mL media with 8 µg/mL polybrene. 100-200 µL virus (gControl, gGFP, gCOG2, or gDOCK5) was added per well and plates were spun for 30 minutes at 2250 rpm at 30°C. 24 hours later, cells were selected with 2 µg/mL puromycin for 2-3 days. Cells were passaged for a minimum of 7 days after infection before use in subsequent experiments. To generate cells that constitutively express a particular shRNA, parental cells were infected as described and selected with 2ug/mL puromycin for 2-3 days; shRNA-expressing cells were used in subsequent experiments 4 days after infection. Lysates were collected 4 days after shRNA expression to assess gene suppression. To generate cells expressing exogenous COG2 or LacZ, 300,000

cells per well were seeded in 6-well plates in 2 mL media with 8 µg/mL polybrene. 1mL virus (COG2-V5 or LacZ-V5) was added per well and plates were spun for 30 minutes at 2250 rpm at 30°C. 24 hours later, cells were selected with 10 µg/mL blasticidin for 4 days. COG2 and LacZ expression was confirmed by immunoblot >7 days after infection.

Crystal violet proliferation assay

Cells were infected with the indicated shRNAs and selected in puromycin for 4 days. Subsequently, cells were seeded in 24-well plates at a density of 10,000-20,000 cells per well. Media was changed every 3 days. 6 hours after seeding (Day 0) and 5-8 days after seeding, cells were fixed with 10% formalin and stained with 0.5% crystal violet in 10% ethanol for 20 minutes. After acquiring images, crystal violet uptake was extracted with 10% acetic acid and quantified by measuring absorbance at 565 nm using a SpectraMax M5 microplate reader (Molecular Devices).

Cell counting assay

Cells were seeded in 10 cm (1 – 2 x 10^6 cells) or 15 cm (1 – 3 x 10^6 cells) plates and treated with drug or DMSO as indicated. Cells were propagated or media was refreshed every 3 – 4 days. Cells were counted at each passage, and number of cell doublings was calculated.

siRNA viability assay

Negative control (D-001810) and DOCK5-targeting (L-018931) SMARTpool siRNA reagent was obtained from Dharmacon. Transfection was performed according to manufacturer's protocol by combining siRNA (final concentration of 50nM siRNA), Dharmafect, and with 4000 cells (293T, HCT116, or PATU8902) per well in white, opaque-bottom 96-well plates (Costar, for viability assay) or 6-well plates (for qRTPCR and immunoblot analysis). Cells were harvested 2 and days after transfection for qRTPCR and immunoblot analysis, respectively. 2, 4, and 6 days after transfection, cell viability was assessed using CellTiter-Glo (Promega) according to manufacturer's protocol

GFP competition assay

50,000 PATU8902-Cas9 cells were seeded in 48 well plates in 25uL media with 4 µg/mL polybrene. 25uL virus (pRosetta-GFP, gGFP, or gDOCK5) was added per well and plates were spun for 2 hours at 2,000 rpm at 30°C. after 6 hours, cells were split into a 10cm dish. 24 hours after infection, cells were selected with 2µg/mL puromycin for 8 days, passaging when necessary. 10 days after infection, GFP-expressing cells were mixed with gRNA-expressing cells in a 1:1 ratio. This cell mixture was analyzed by FACS to determine the baseline proportion of GFP-positive cells. Cells were seeded in 15cm plates (3E6 cells for DMSO-treated plates, 8E6 cells for trametinib-treated plates) in duplicate. Cells were treated with 50nM trametinib or DMSO. DMSO cells were passaged every 3 days. The media of trametinib-treated cells was refreshed after 3 days and passaged after 6 days. Percent GFP-positive cells was assessed via FACS on day 6 and day 12 after seeding.

Quantitative PCR

RNA was isolated using an RNeasy kit (Qiagen). cDNA was synthesized using Superscript III First-Strand Synthesis Supermix for qRT-PCR (Invitrogen), and analyzed by quantitative PCR (q-PCR) using Power Sybr Green PCR Master Mix (Invitrogen) on a QuantStudio 6 Flex PCR system (Applied Biosystems) according to the manufacturer's recommendations. Target gene expression was normalized to GAPDH expression, and shown relative to control samples. Primer sequences used for q-PCR:

qRTPCR primer sequences

Gene	*Forward Primer*	*Reverse Primer*
COG2	AAACCTCTGCACTAGAAGCAAG	GCTATACGCGGTCTTACTTTGTC
DOCK5	CCCTCGTACATCTCCAGGAT	ACCAAGAGGCAGAAGTACGG
GAPDH	CCTGTTCGACAGTCAGCCG	CGACCAAATCCGTTGACTCC
KRAS	CAGTACAGTGCAATGAGGGAC	CCTGAGCCTGTTTTGTGTCTAC

Immunoblots and antibodies

COG2, KRAS, ERK, AKT, β-Actin, and GAPDH immunoblots were performed by separating 10 – 40 µg cell lysate per sample on a 4%-12% Bis-Tris gel (Invitrogen

NuPage) and transferring to nitrocellulose membrane using the iBlot system (Life Technologies). Primary antibodies were obtained from Abcam (COG2 ab167416), Cell Signaling (GAPDH #2118, total ERK #9102, phospho-ERK #4370, total AKT #9272, phosphor-AKT #4060), Proteintech (KRAS 12063-1-AP), Santa Cruz Biotechnology (β-Actin sc-47778), and Sigma Aldrich (KRAS WH0003845M1). Immunoblots were visualized by infrared imaging (LI-COR). Protein quantification was performed according to manufacturer's recommendation (LI-COR), and expression was normalized to a control gene (GAPDH or β-Actin).

Vectors

LacZ and COG2 in the pLX304 backbone and Cas9 in the pLX311 backbone (pXPR_BRD111) were obtained from the Genetic Perturbation Platform at the Broad Institute. shRNAs in the pLKO.1 backbone and gRNAs in the pXPR_BRD003 backbone were cloned as recommended by the Genetic Perturbation Platform at the Broad Institute. shRNA gRNA sequences are listed below.

shRNA sequences

Vector Name	Sequence
shControl	ACACTCGAGCACTTTTTGAAT
pLKO1_shKRAS-1	CCTATGGTCCTAGTAGGAAAT
pLKO1_shKRAS-2	GAGGGCTTTCTTTGTGTATTT
pLKO1_shKRAS-3	CCTCGTTTCTACACAGAGAAA
pLKO1_shKRAS-4	CAGTTGAGACCTTCTAATTGG
pLKO1_shCOG2-1	CGAACTCATCAACAAGGATTA
pLKO1_shCOG2-2	CCATACATAGACGAGGTGATT
pLKO1_shCOG2-3	CCTGCCTATCACAGCTTCAAT
pLKO1_shCOG2-4	CGGAAACAAAGCCTGTGGTTT
pLKO1_shCOG2-5	GCACTCATAAGTACTATGAAA
pLKO1_shCOG2-6	GCGTCTTCTCTCAGCGTATTT
pLKO1_shCOG2-7	GACCTGGAGCTCTACTATAAA
pLKO1_shCOG2-8	ATTGAGGCTTATACAAGTTAT
pLKO1_shCOG2-9	AGACGTCTGACGTCGATATAA
pLKO1_shCOG2-10	TGGATCACAGGCTAGTGTAAA
pLKO1_shDOCK5-1	GCGACTAATAGCATTACAGAT
pLKO1_shDOCK5-2	AGTACCTTCCTAGCATAATTA
pLKO1_shDOCK5-3	GCCACTCACTTCAGTCTTGAA
pLKO1_C911-shKRAS-1	CCTATGGTAGGAGTAGGAAAT
pLKO1_C911-shKRAS-2	GAGGGCTTAGATTGTGTATTT

pLKO1_C911-shKRAS-3	CCTCGTTTTAGCACAGAGAAA
pLKO1_C911-shKRAS-4	CAGTTGAGGGTTTCTAATTGG
pLKO1_C911_shCOG2-1	CGAACTCATGAACAAGGATTA
pLKO1_C911_shCOG2-2	CCATACATTCTCGAGGTGATT
pLKO1_C911_shCOG2-3	CCTGCCTATGACAGCTTCAAT
pLKO1_C911_shCOG2-4	CGGAAACACTTCCTGTGGTTT
pLKO1_C911_shCOG2-5	GCACTCATCTTTACTATGAAA
pLKO1_C911_shCOG2-6	GCGTCTTCAGACAGCGTATTT
pLKO1_C911_shDOCK5-1	GCGACTAACTACATTACAGAT
pLKO1_C911_shDOCK5-2	AGTACCTTAGGAGCATAATTA
pLKO1_C911_shDOCK5-3	GCCACTCAAAGCAGTCTTGAA

gRNA sequences

Vector Name	Sequence
gControl	ACACTCGAGCACTTTTTGAAT
gGFP A02	GGCGAGGGCGATGCCACCTA
gGFP B09	GGTGCCCATCCTGGTCGAGC
gKRAS-1	AACATCAGCAAAGACAAGAC
gKRAS-2	CAATGAGGGACCAGTACATG
gKRAS-3	TTTGCTGATGTTTCAATAAA
gDOCK5-1	ACTTACCCTCGTACATCTCC
gDOCK5-2	CCTCCAAAATAAATCTAAAA
gDOCK5-3	CGGTGACACAGTTCACATCC
gDOCK5-4	GCTCTGACAGGTTGGTACAG
gDOCK5-5	AACATATATCCATTTGAAAG
gDOCK5-6	CCACAGTTGCCTCTTTCAAA

Tables

Table 1. Frequency of *RAS* mutations in human cancers.

Cancer	% *KRAS*	% *NRAS*	% *HRAS*	% *RAS*
Pancreatic ductal adenocarcinoma	97.7	0	0	97.7
Colorectal adenocarcinoma	44.7	7.5	0	52.2
Multiple myeloma	22.8	19.9	0	42.6
Lung adenocarcinoma	30.9	0.9	0.3	32.2
Skin cutaneous melanoma	0.8	27.6	1	29.1
Uterine corpus endometrioid carcinoma	21.4	3.6	0.4	24.6
Uterine caricinosarcoma	12.3	1.8	0	14.3
Thyroid carcinoma	1	8.5	3.5	12.5
Acute myeloid leukemia	3.1	6.7	1.6	11.4
Bladder urothelial carcinoma	3.1	1.4	5.9	10.6
Gastric adenocarcinoma	11.4	0.9	0	10
Cervical adenocarcinoma	8.3	0	0	8.3
Head and neck squamous cell carcinoma	0.5	0.3	4.7	5.5
Diffuse large B cell lymphoma	5.2	0	0	5.2

Adapted from Cox et al. (2014)[33], where data were compiled from a variety of sources, including but not limited to The Cancer Genome Atlas, the International Cancer Genome Consortium, and cBioPortal[201,202].

Table 2. RAS synthetic lethal genes.

Synthetic lethal genes or pathways	Library (assay and format)	Cells in primary screen	Drug inhibition	References
RAN, TPX2, SCD1	~3,700 druggable genes, siRNA, arrayed cell death	NCIH1299 (*NRAS*^{Q61K} NSCLC)	Not tested	Morgan Lappe et al. 2007[203]
BIRC5 (survivinn), *CDK1, RBCK1*	~4,000 genes, siRNA, arrayed cell death	Isogenic DLD1 (CRC, *KRAS*^{G13D})	Not tested	Sarthy et al. 2007[204]
PLK1, APC/C, proteosome	Genome scale, shRNA, pooled proliferation screen with microarray readout	Isogenic DLD1 (CRC, *KRAS*^{G13D})	BI-2536	Luo et al. 2009[4]
STK33, AKT3, CPNE1, CAMPK1, MLKL, FLT3LG, and *DGKZ*	~1,000 druggable genes, shRNA, arrayed proliferation	Pan-cancer cell line panel (4 *KRAS*-mutant, 4 *KRAS*-wildtype) and 2 immortalized cell lines	STK33 kinase inhibitor, failed to suppress proliferation in *KRAS*-mutant cells [205-207]	Scholl et al. 2009[8]
TBK1, PSKH2, PTCH2, CPNE1, MAP3K8,	~1,000 druggable genes, shRNA, arrayed proliferation	Pan-cancer cell line panel (7 *KRAS*-mutant, 10 *KRAS*-wildtype) and 2 immortalized cell	CYT387 (TBK1 and JAK inhibitor), assessed in [9]	Barbie et al. 2009[3]

proteasome		lines		
WT1, RAC1, PHB2	162 KRAS related genes, shRNA, *in vitro* and *in vivo* pooled proliferation screens with bead array readout	LKR10 and LKR13 (*Kras;Trp53* mutant mouse lung tumor derived cell lines)	Not tested	Vicent et al. 2010[5]
SNAI2 (SNAIL2)	~2,500 druggable genes, shRNA, pooled proliferation with microarray readout	Isogenic HCT116 (CRC, *KRAS*^{G13D})	Not tested	Wang et al. 2010[6]
GATA2, CDC6, proteasome	~8,000 druggable genes, siRNA, arrayed apoptosis and cell proliferation	Isogenic HCT116 (*KRAS*^{G13D}) and pan-cancer cell line panel (14 *KRAS*-mutant, 12 *KRAS*-wildtype)	Bortezomib with fasudil (GATA2)	Kumar et al. 2012[146] Steckel et al. 2012[147]
MAP3K7 (TAK1)	17 kinases highly expressed in *KRAS*-dependent CRC, shRNA, arrayed proliferation	KRAS-dependent SW620 and KRAS-independent SW837 (CRC, *KRAS*-mutant)	5Z-7-oxozeaenol	Singh et al. 2012[208]
Cttnb1 (β-catenin)*, Mllt6*	Genome scale, shRNA, pooled *in vivo* proliferation with NGS readout	Mouse keratinocytes (*Hras*^{G12V})	Not tested	Beronja et al. 2013[209]
COP1 coatomer	Genome scale, siRNA, arrayed proliferation	17 *KRAS*- and *LKB1*-mutant lung cancer cell lines, matched tumor (*KRAS*-mutant) and normal NSCLC cell line pair	Saliphenylhalamide A	Kim et al. 2013[210]
ARHGEF2 (GEFH1)	Genome scale, shRNA, pooled proliferation with NGS readout	Pan-cancer panel (72 cell lines).	Not tested	Marcotte et al. 2012[166] Cullis et al. 2014[211]
BCL2L1 (BCLXL)	~1,200 druggable genes in presence of MEK inhibitor (selumetinib), shRNA, pooled proliferation with NGS readout, synergistic death with MEK inhibitor	HCT116 and SW620 (CRC, *KRAS*-mutant)	Selumetinib and navitoclax	Corcoran et al. 2013[162]
CDK1	784 genes, siRNA (Dharmacon SMARTPool), arrayed proliferation	Isogenic LIM1215 (CRC, KRAS-WT)	RO-3306 (CDK1 inhibitor), AZD5438 (CDK1/2 and 9 inhibitor)	Costa-Cabra; et al. 2016[212]
RCE, ICMT, RAF1, SHOC2, PREX1	Genome scale, gRNA, pooled proliferation with NGS readout	12 human AML cell lines (6 *RAS*-mutant, 6 *RAS*-WT), BaF3 cells (mouse, NRAS-WT)	FRAX-597 (PAK inhibitor)	Wang et al. 2017[14]

Abbreviations: NSCLC (non-small cell lung cancer), CRC (colorectal cancer), NGS (next-generation sequencing). Table from Wang 2016[213].

Table 3. *KRAS*-mutant co-dependencies.

Gene	FDR	DM	Marcotte et al.
KRAS	< 0.0001	-1.0379	Yes
COG2	< 0.0001	-0.7876	Yes
MEST	0.02222	-0.5692	No
TXNDC8	0.06667	-0.4931	No
RHOV	0.09333	-0.4898	No
ABP1	0.1333	-0.4983	No
RGS2	0.1333	-0.6031	No
ZBTB48	0.1926	-0.487	No
FERMT1	0.1926	-0.5555	Yes

FDR- ranked list of genes essential for proliferation/survival of *KRAS*-mutant cells. Column guide: FDR (false discovery rate q-value); DM (difference in mean gene dependency score between *KRAS*-mutant and *KRAS*-WT cell lines, where a negative score reflects preferentially negative effect on proliferation/viability for *KRAS*-mutant cell lines); Marcotte et al. (identification as a significant candidate in analysis of the independent Marcotte et al. 2012 dataset of 72 cancer cell lines[166]).

Table 4. KRAS classification schemes.

Classification criterion	KRAS WT (KRAS-independent)	KRAS mutant (KRAS-dependent)
KRAS mutation status and KRAS dependency (shRNA)	48	23
KRAS mutation status and KRAS dependency (ATARiS)	28	35
KRAS mutation status	96	37

Carcinoma cell lines screened in Project Achilles v2.4 were classified by KRAS mutation status and KRAS dependency status (assessed by shKRAS 509 or KRAS ATARiS score). Numbers refer to the number of cell lines in each classification.

Table 5. Candidate co-dependencies in *KRAS*-mutant cells

Gene	Mutation	Mut + shKRAS	Mut + ATARiS	On-target
KRAS	X	X	X	X
COG2	X	X	X	
MEST	X	X	X	
TXNDC8	X	X	X	
RHOV	X	X	X	
ABP1	X	X	X	
RGS2	X	X	X	
ZBTB48	X	X	X	
FERMT1	X	X	X	
ALDH9A1	X	X	X	
DOCK5	X	X	X	
GPR182	X	X	X	
CELF6	X	X	X	
TMX3	X	X	X	
KIRREL3	X	X	X	
HBG1	X	X	X	
NOTCH2	X	X	X	
NCOR2	X	X	X	
RGL1	X	X	X	
FLT3	X	X	X	
IFI16	X	X	X	
API5	X	X	X	
GTF3A	X	X	X	X
SCN5A	X	X	X	
CD58	X	X	X	
ATP2B4	X	X	X	
DHPS	X	X	X	
BCL2L1	X	X	X	X
TASP1	X		X	
APOE	X		X	X
PNO1	X		X	
CDK6		X	X	
JUNB		X	X	
HIATL1		X	X	X
MED30		X	X	X
RAF1 (CRAF)		X	X	
CDA		X		
RPS15A		X		X
CTNNB1		X	X	
SCAP			X	X
EPRS			X	X
PRKAG3			X	
ZPLD1			X	
HDAC3			X	
CXCL6			X	
VPS28			X	X
NOG			X	

PIK3CA			X	X
MTOR			X	X
MAPK1			X	
MAP2K1			X	
PLK1			X	
MAP3K7 (TAK1)			X	
WT1			X	
CDK2			X	X
BCL2			X	
MYC			X	X
RPS6			X	
MCL1			X	

Genes that are selectively essential in *KRAS*-mutant cell lines as determined by two class comparisons in which cell lines were classified by KRAS mutation status ("Mutation"), by KRAS mutation status and KRAS dependency as measured by the shKRAS 509 shRNA ("Mut + shKRAS"), or by KRAS mutation status and KRAS dependency as measured by KRAS ATARiS score ("Mut + ATARiS"). Significant genes (FDR < 0.25) are marked by an 'X.' "On-target" indicates that the gene had at least 2 shRNAs that were estimated to have an on-target effect of > 50% by DEMETER[11]. Genes that have been previously identified as co-dependencies in *KRAS*-mutant cells are shaded in gray.

Figures

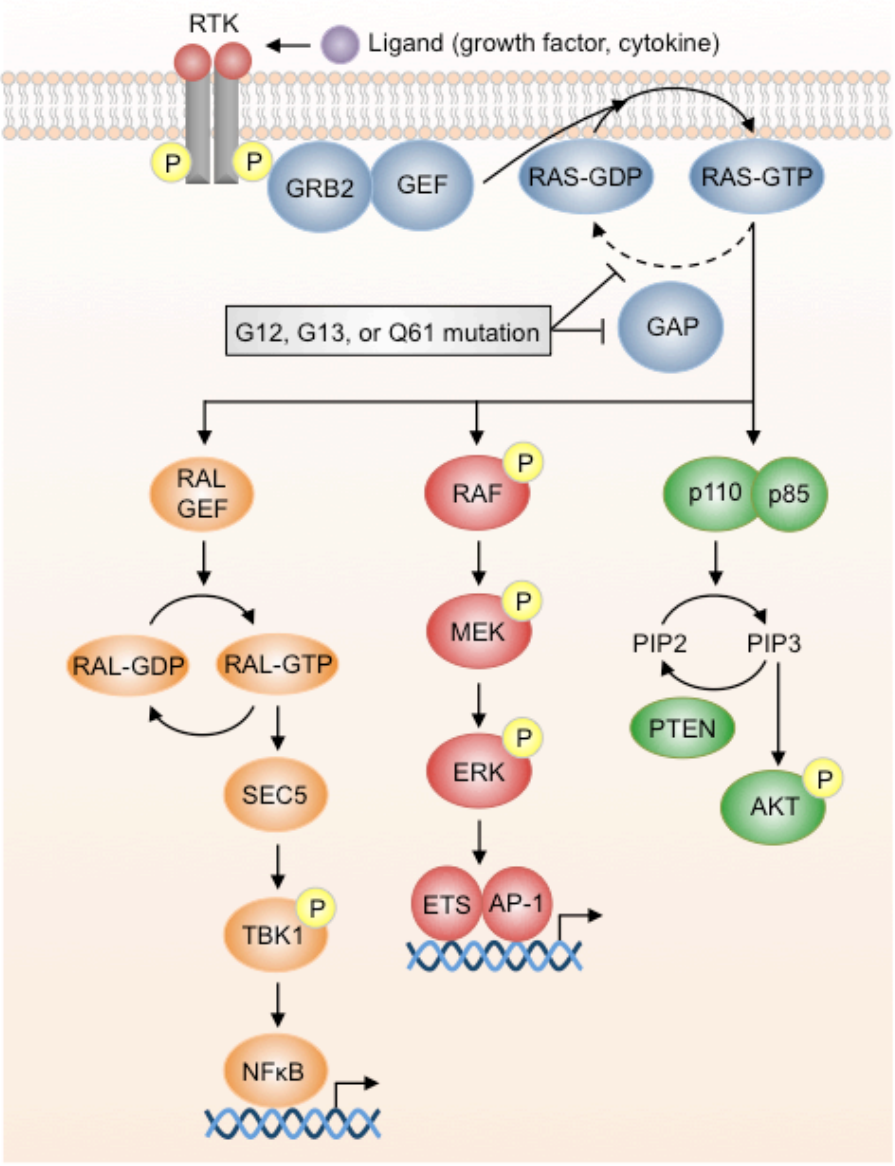

Figure 1. The RAS pathway. RTKs are activated by extracellular ligand binding, which induces dimerization and trans-phosphorylation of intracellular tyrosine residues. The adaptor protein GRB2 binds to the phospho-tyrosine site on RTKs and to cytosolic GEFs. RAS proteins are activated by GEFs and inactivated by GAPs. RAS missense mutations, which primarily arise in resides G12, G13, and Q61, impair intrinsic and/or GAP-stimulated GTPase activity. Key RAS effectors include the MAPK , PI3K, and RAL-GEF pathways. Abbreviations: RTK (receptor tyrosine kinase), GEF (guanine nucleotide exchange factor), GAP (GTPase activating protein), PIP3 (phosphatidylinositol 3,4,5-bisphosphate), PIP2 (phosphatidylinositol 4,5-bisphosphate). Figure from Wang (2016)[213].

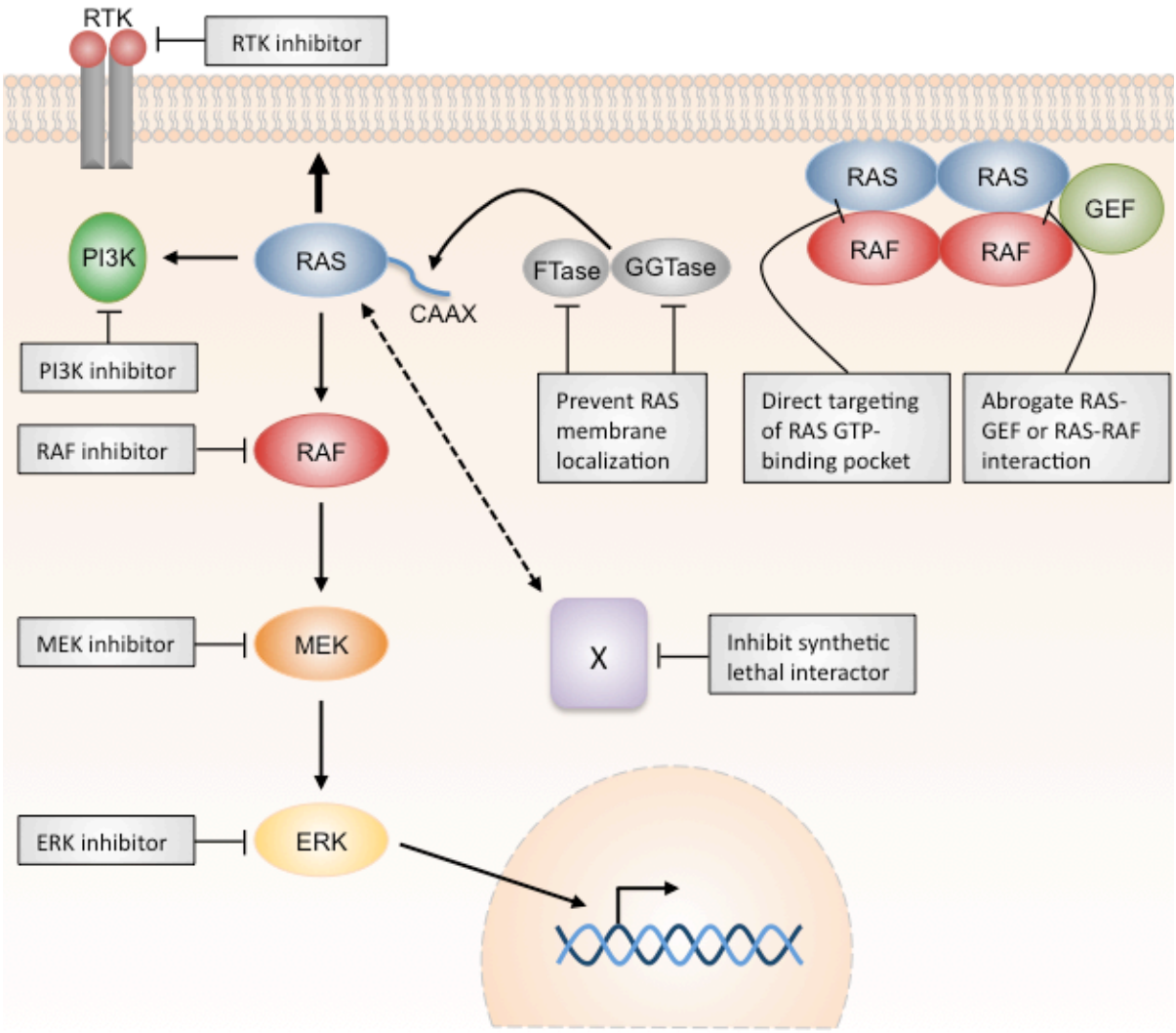

Figure 2. Strategies to target mutant RAS. Major pharmacologic approaches to inhibit oncogenic RAS include inhibiting upstream RAS activators, such as RTKs; directly targeting RAS at its GTP-binding pocket or interfering with the RAS–SOS or RAS–RAF interaction; preventing RAS membrane localization of by inhibiting RAS prenylation with FTIs (farnesyltransferase inhibitors) or GGTIs (geranyl geranyltransferase inhibitors), or by inhibiting PDEδ (phosphodiesterase δ); inhibiting downstream RAS effectors using RAF, MEK, ERK, or PI3K pathway inhibitors; and inhibiting RAS synthetic lethal interactors. Figure from Wang (2016)[213].

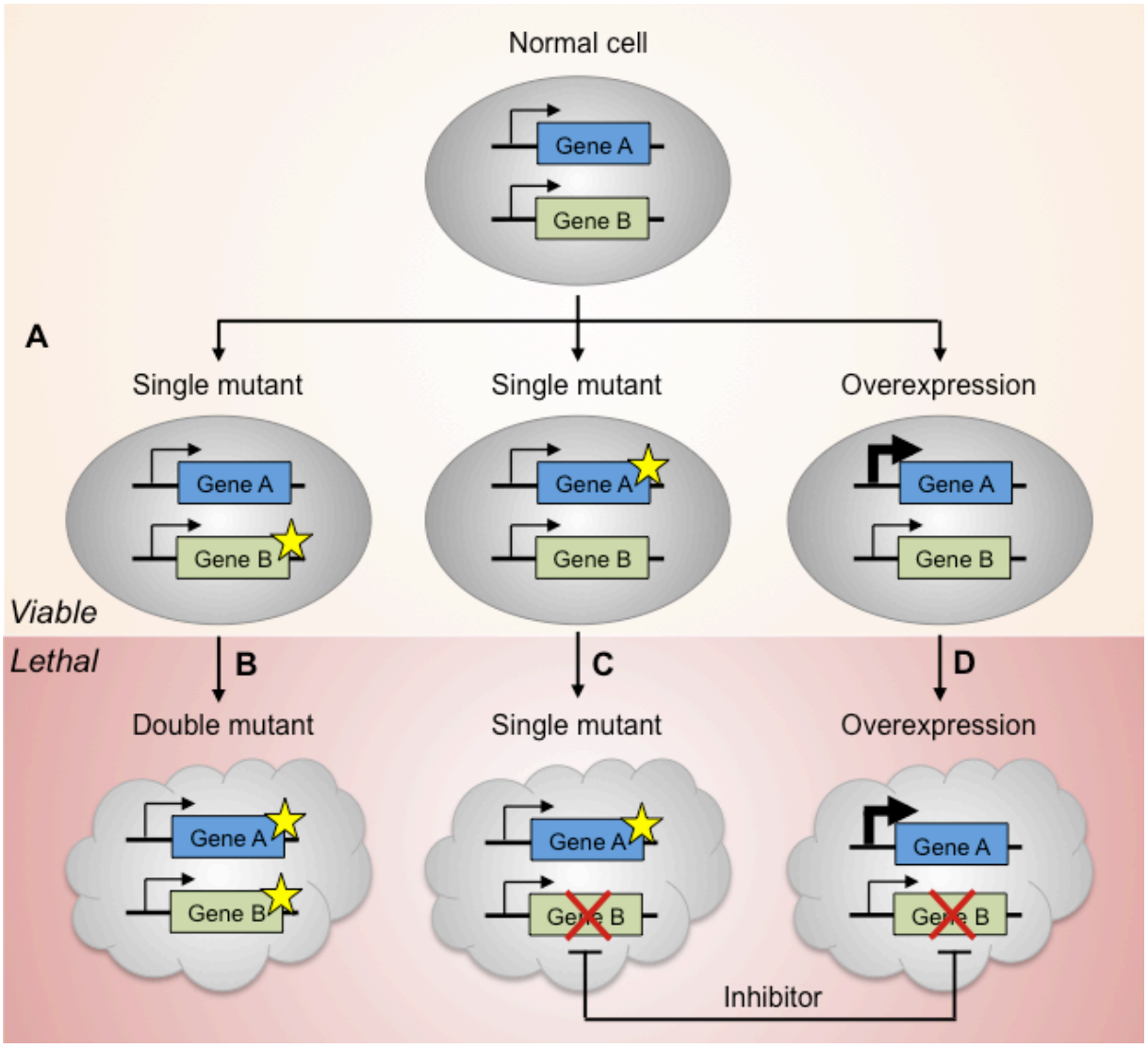

Figure 3. Synthetic lethality in cancer. (A) The loss or inhibition of gene A or gene B alone or the overexpression of gene A have no effect on viability. However, mutation **(B)** or pharmacologic inhibition of the protein product of gene B in cells that harbor a mutation **(B, C)** or overexpressioon **(D)** of gene A results in synthetic lethality. Star indicates mutation, red cross indicates pharmacologic inhibition, and thick arrow indicates overexpression. Figure adapted from O'Neil et al. (2017)[115].

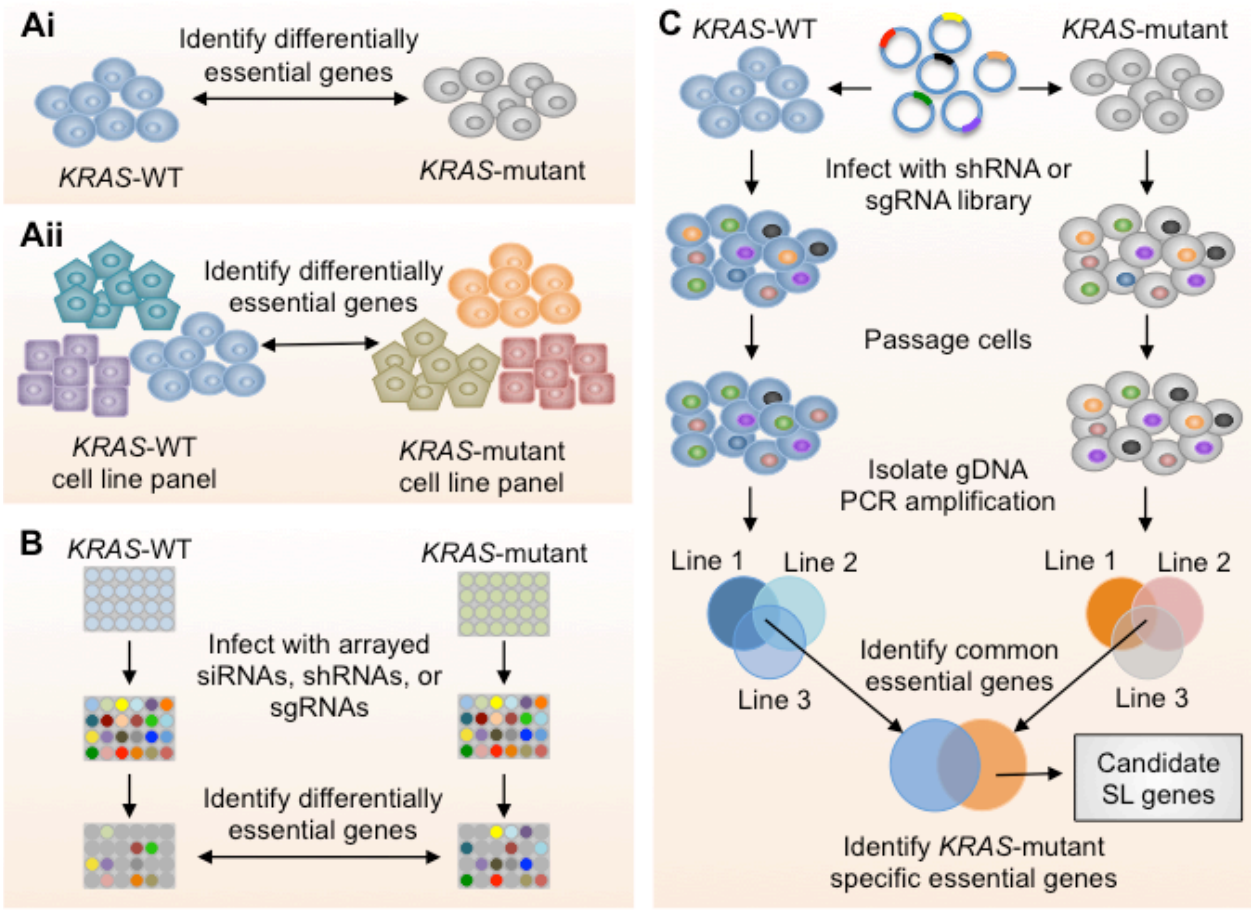

Figure 4. Experimental approaches to synthetic lethality screens in cancer cell lines. (A) Human synthetic lethality screens most commonly use either pairs of matched isogenic cell lines derived from the same parental cell line which differ only in the gene of interest **(Ai)** or a panel of genetically diverse cell lines that are split into two groups depending o the mutation status of the gene of interest **(Aii). (B**) In arrayed format screens, cells are seeded in 96-, 384-, or 1536-well plates. Each well is transfected with an individual siRNA or infected with an individual shRNA or gRNA. After a period of time, the number of cell in each well is quantified, and genes that are specifically essential in *KRAS*-mutant cells can be identified. **(C)** In pooled format screens, cells are infected with a pooled lentivirus shRNA or gRNA library, and a baseline sample of gDNA is obtained. Cells populations are grown and next-generation sequencing technologies are used to identify sequences that are underrepresented specifically in the cell lines that harbor the mutant gene of interest. Genes targeted by multiple shRNAs or gRNAs in this subset are candidate synthetic lethal (SL) interactions for the mutant gene of interest. Figure adapted from O'Neil et al. (2017)[115].

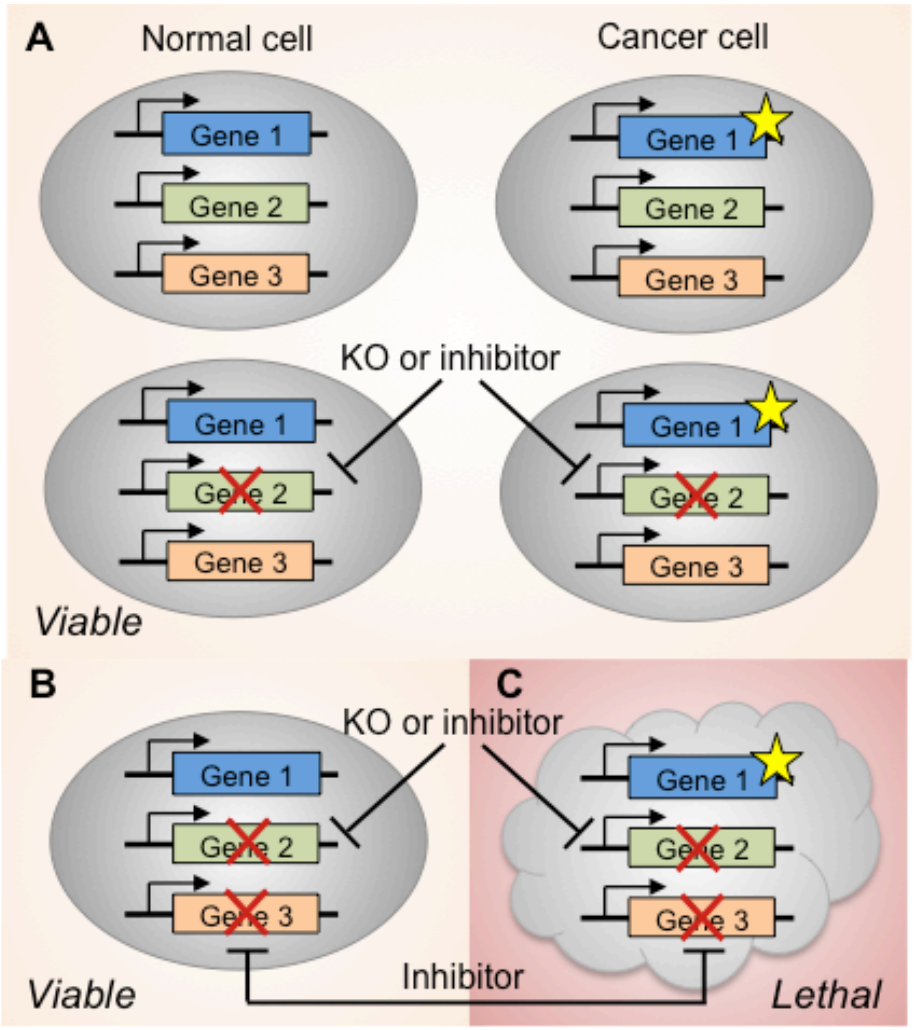

Figure 5. Drug-conditional synthetic lethal interactions. Synthetic lethal interactions may be dependent on specific conditions such as the presence of a chemical inhibitor. **(A)** In normal cells or cancer cells with a mutation in gene 1, the loss of gene 2 or pharmacologic inhibition gene 2 has no effect on viability. However, when gene 3 is inhibited pharmacologically, mutation or pharmacologic inhibition of gene 2 does not affect viability in normal cells **(B)**, but is synthetic lethal to cells with mutant gene 1 **(C)**. Star indicates mutation, red cross indicates pharmacologic inhibition of protein product or genetic knockout.

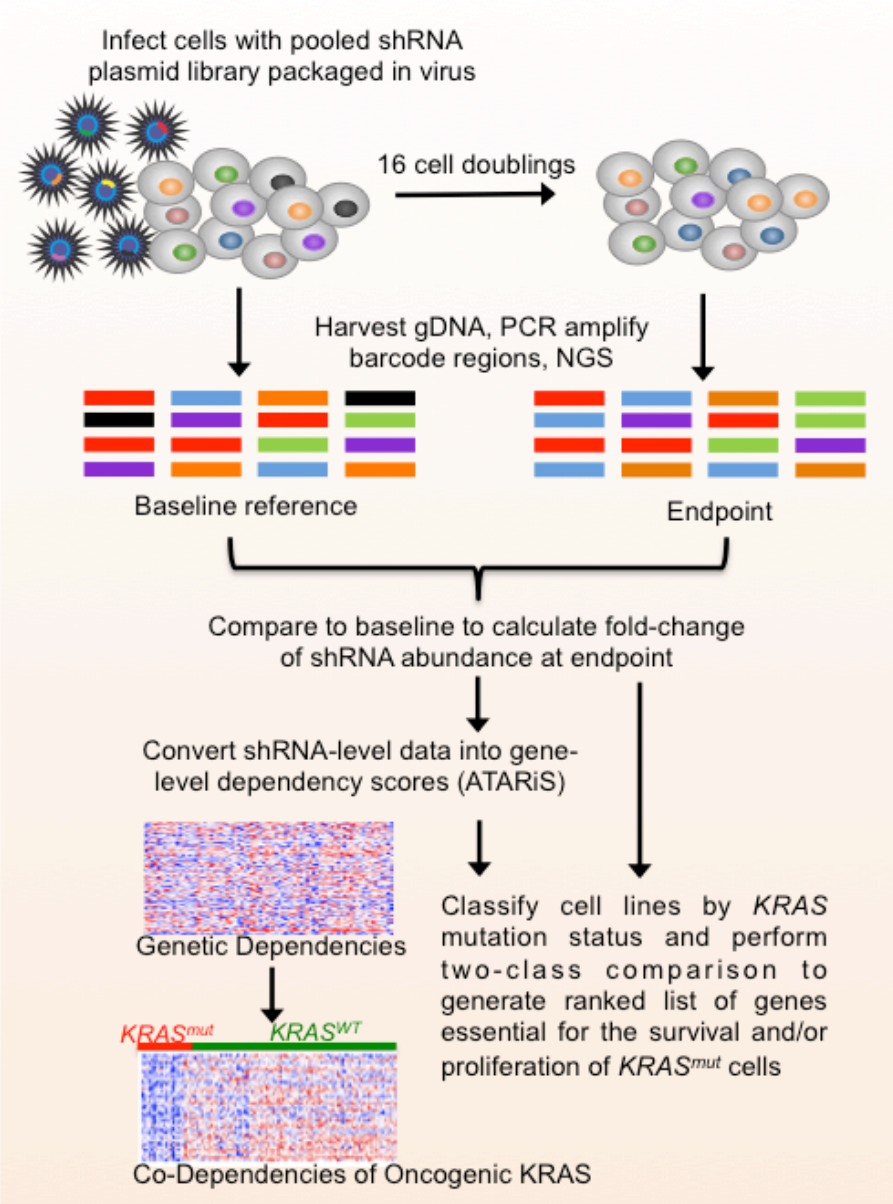

Figure 6. Project Achilles overview and analysis. Genome scale negative selection screens to identify synthetic lethal interactions with oncogenic KRAS. In Project Achilles, cells are infected with a pooled genome-scale shRNA library, selected, and propagated for 16 doublings. shRNA abundance at the endpoint relative to the baseline reference is assessed by massively parallel sequencing. Depleted shRNAs target genes whose suppression impairs cell proliferation/survival. For Project Achilles, shRNA-level data can be analyzed directly or converted to gene-level dependency scores using the ATARiS method[139]. Cell lines are classified by *KRAS* mutation status or KRAS dependency, and a two-class comparison is performed using PARIS (Probability Analysis by Ranked Information Score), a mutual information-based algorithm[12], to identify genes that are selectively essential for the survival of *KRAS*-mutant cells. Significance (FDR q-value) is determined by permuting class labels.

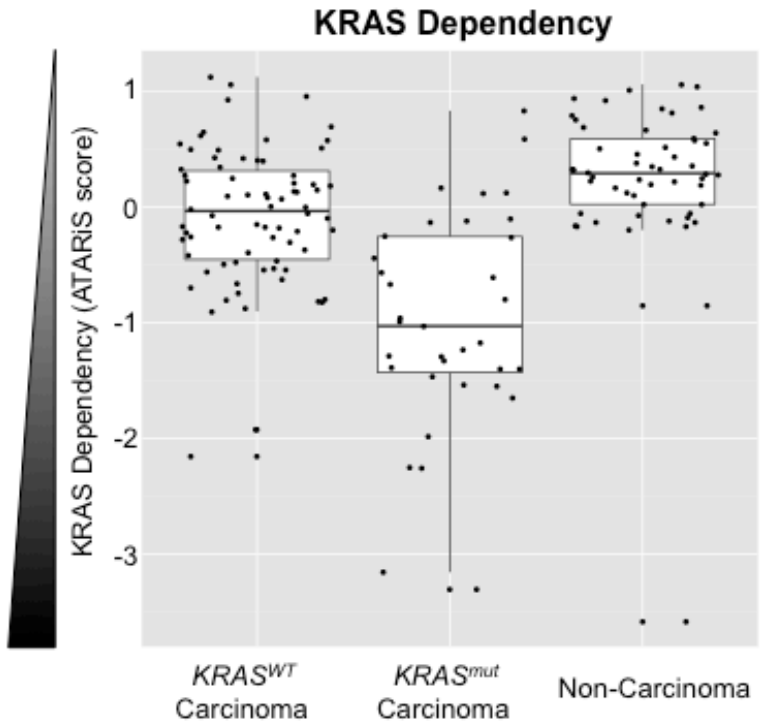

Figure 7. *KRAS* mutation status does not always predict KRAS dependency. The KRAS dependency of the cell lines screened in Project Achilles v2.4 was quantified by their KRAS ATARiS score[139], a value that reflects the aggregate effects of the 10 KRAS shRNAs in the screening library. Negative ATARiS scores indicate greater gene dependency.

Figure 8. KRAS classifications for two-class comparisons. KRAS mutation status and KRAS dependency do not correlate perfectly. Hence, cell lines were classified by using 3 separate metrics: **(1)** *KRAS* mutation status and sensitivity to KRAS-depletion as measured by the KRAS ATARiS score[139], a value that reflects the aggregate effects of 10 KRAS shRNAs screened in Project Achilles; (**2**) *KRAS* mutation and sensitivity to KRAS-depletion by shKRAS 509, a KRAS-targeting shRNA that effectively depletes KRAS expression at a protein level[3]; or **(3)** only *KRAS* mutation status. Each bar represents an individual cell line screened in Project Achilles v2.4.

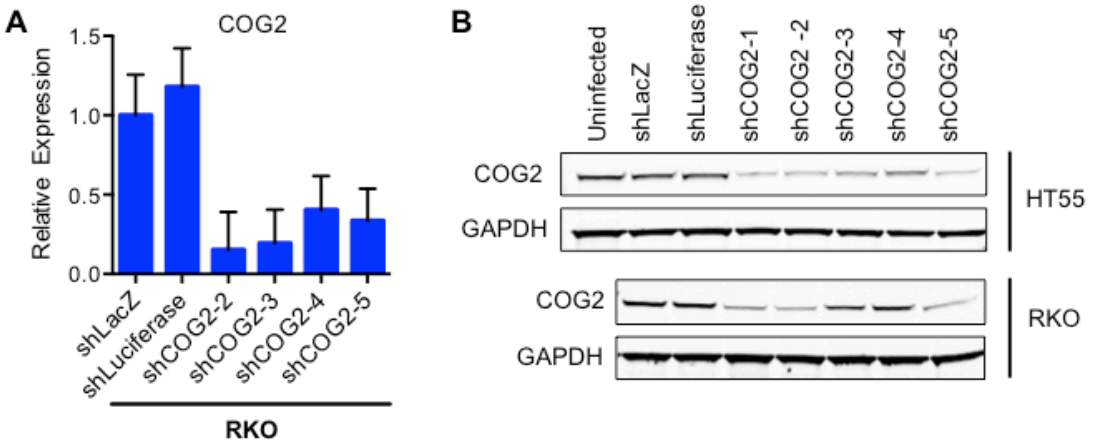

Figure 9. COG2 shRNAs reduce COG2 expression. RKO (*KRAS*-WT, colon) cells were infected with the indicated shRNAs and selected. COG2 expression was assessed by qRT-PCR **(A)** and immunoblot **(B)** 6 days post infection. 4 technical replicates representative of 2 independent experiments, data represented as mean ± SEM.

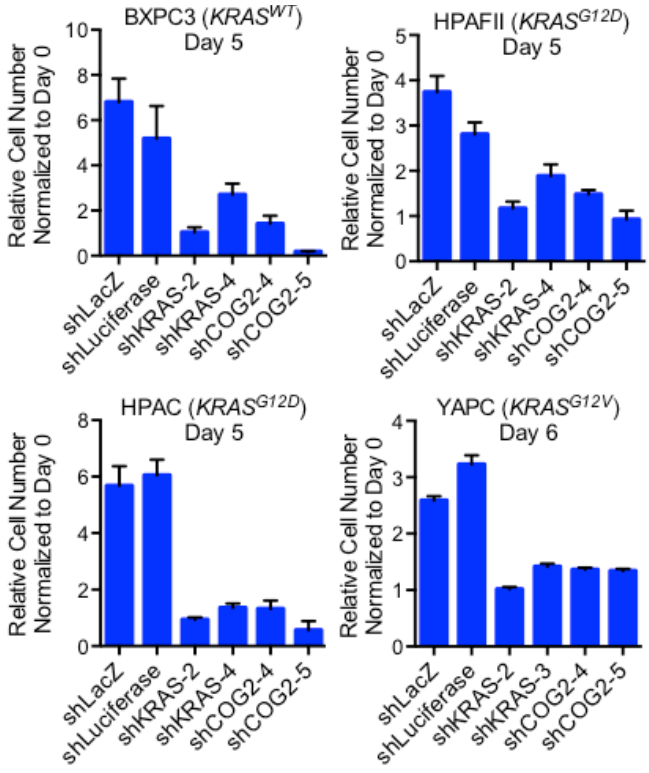

Figure 10. COG2 shRNAs decrease proliferation viability in both *KRAS*-WT and *KRAS*-mutant cells. Crystal violet cell proliferation assay to determine the effect of COG2 depletion on cell proliferation/viability. 4 technical replicates, data represented as mean ± SEM.

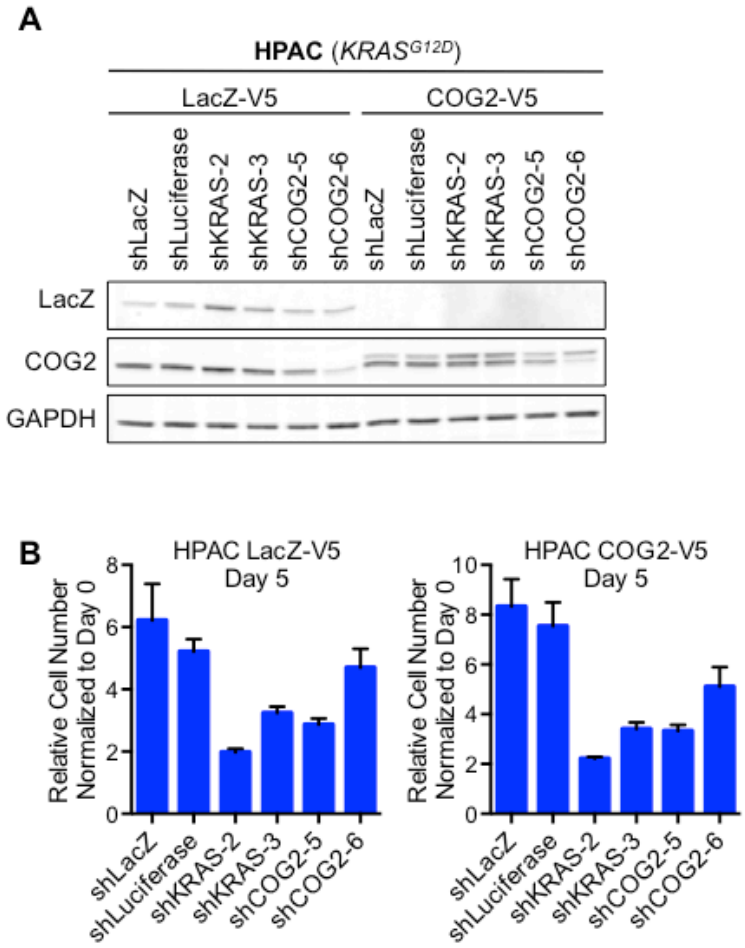

Figure 11. Exogenous COG2 expression does not rescue shRNA-mediated COG2 depletion. (A) Immunoblot analysis of COG2 expression in cell lines expressing COG2-specific shRNAs and/or exogenous COG2-V5 cDNA. **(B)** Cell proliferation assay to whether exogenous COG2-V5 overexpression could rescue viability upon shCOG2-mediated suppression of endogenous COG2 expression in HPAC (*KRAS*^{G12D}) cells. 4 technical replicates representative of 2 independent experiments, data represented as mean ± SEM.

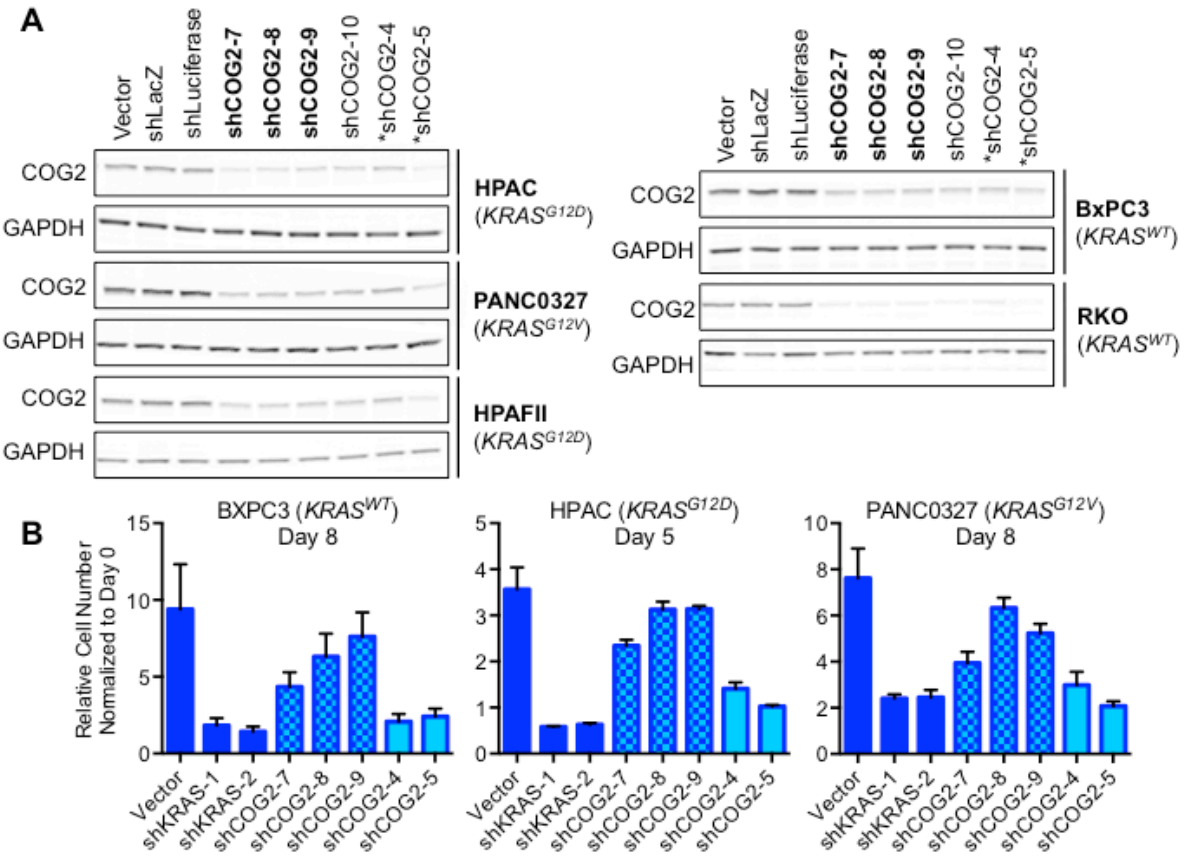

Figure 12. Additional COG2-targeting shRNAs do not selectively decrease proliferation/viability in *KRAS*-mutant cells. (A) Immunoblot analysis of COG2 expression. Bold: COG2-targeting shRNAs that were not included in the Project Achilles shRNA screen. *COG2-targeting shRNAs that distinguished between *KRAS*-WT and *KRAS*-mutant cell lines in the Project Achilles screens. **(B)** Cell proliferation assay to determine effect of COG2 depletion on cell proliferation/viability. Checkered bars: COG2-targeting shRNAs that were not included in the Project Achilles shRNA screen. Light blue bars: COG2-targeting shRNAs that distinguished between *KRAS*-WT and *KRAS*- mutant cell lines in the Project Achilles screens. 4 technical replicates, data represented as mean ± SEM.

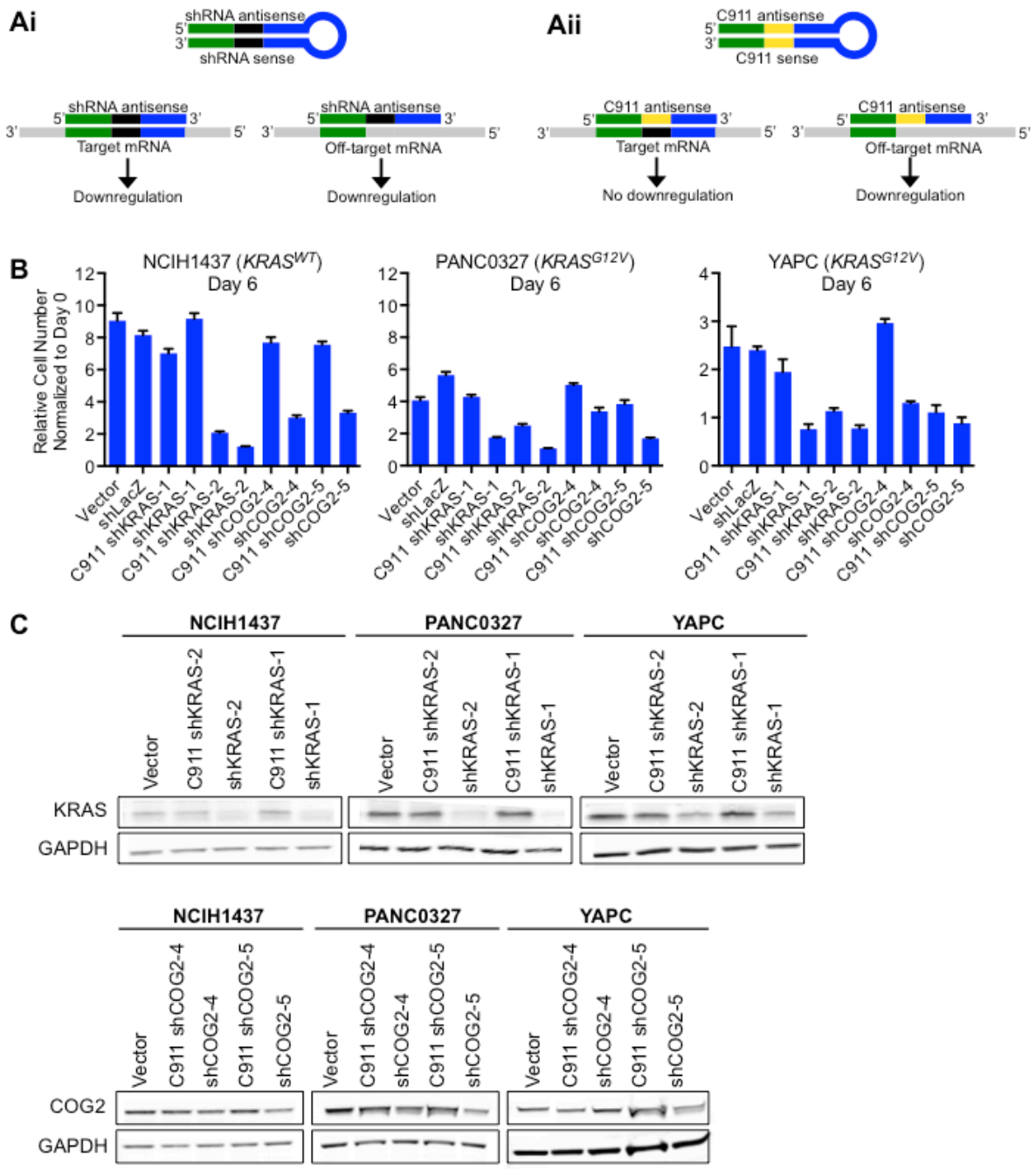

Figure 13. COG2 is not a specific co-dependency of *KRAS*-mutant cell lines. (A) Design of C911 seed-control shRNAs, in which the three nucleotides at position 9 to 11 of the shRNA target sequence (black) are converted to their reverse complement (yellow)[167]. **(B)** Cell proliferation assay to determine seed effects of shRNAs targeting COG2 and KRAS using C911 seed control shRNAs. 4 technical replicates, data represented as mean ± SEM. **(C)** Immunoblot analysis of KRAS and COG2 depletion.

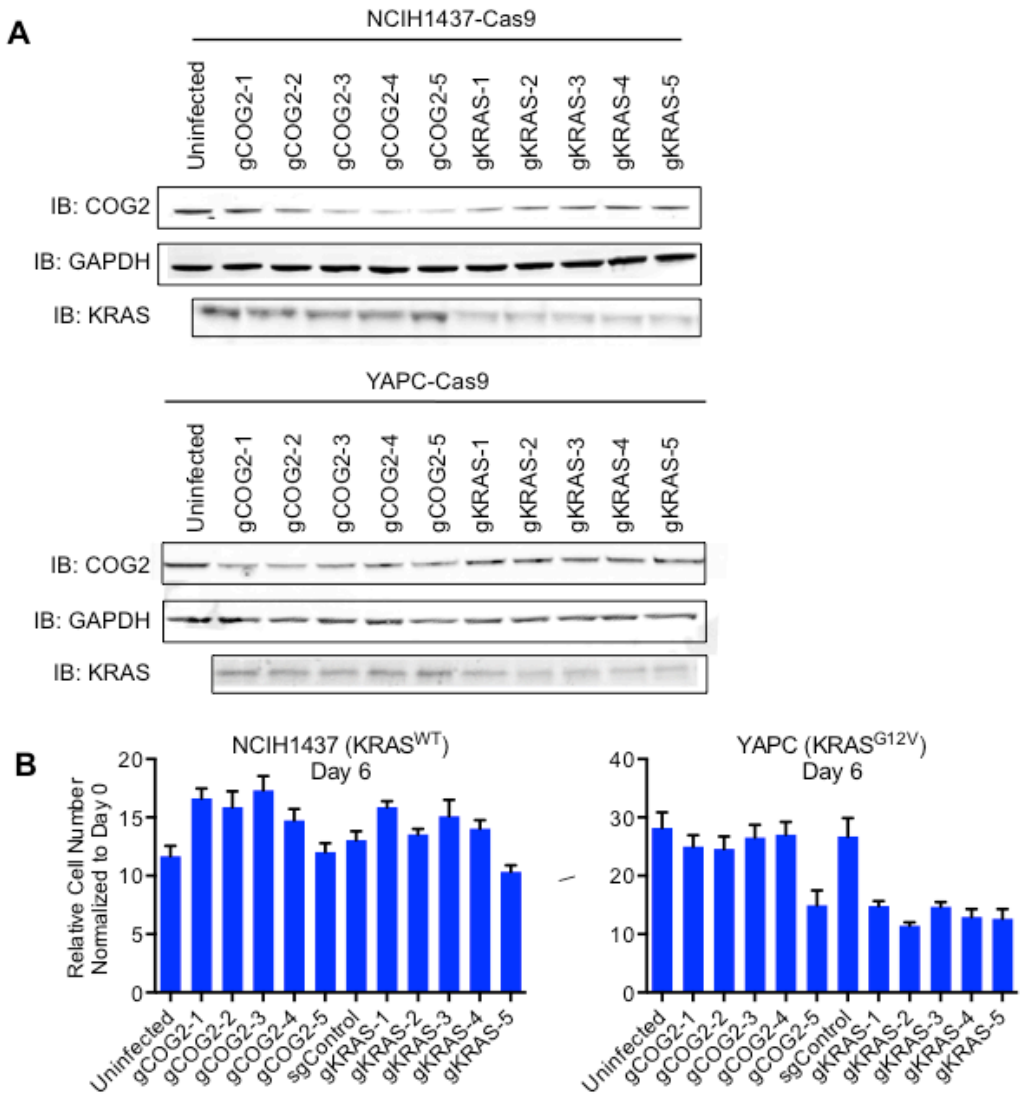

Figure 14. CRISPR/Cas9-mediated COG2 knockout does not affect viability in *KRAS*-mutant cells. (A) Immunoblot analysis of COG2 and KRAS expression in NCIH1437-Cas9 and YAPC-Cas9 cells expressing the indicated gRNAs. Cells were infected with gRNA constructs and selected. Lysates were harvested 7 days post infection. **(B)** Crystal violet proliferation assay to determine effect of COG2 and KRAS knockout on cell viability. 4 technical replicates representative of 2 independent experiments, data represented as mean ± SEM.

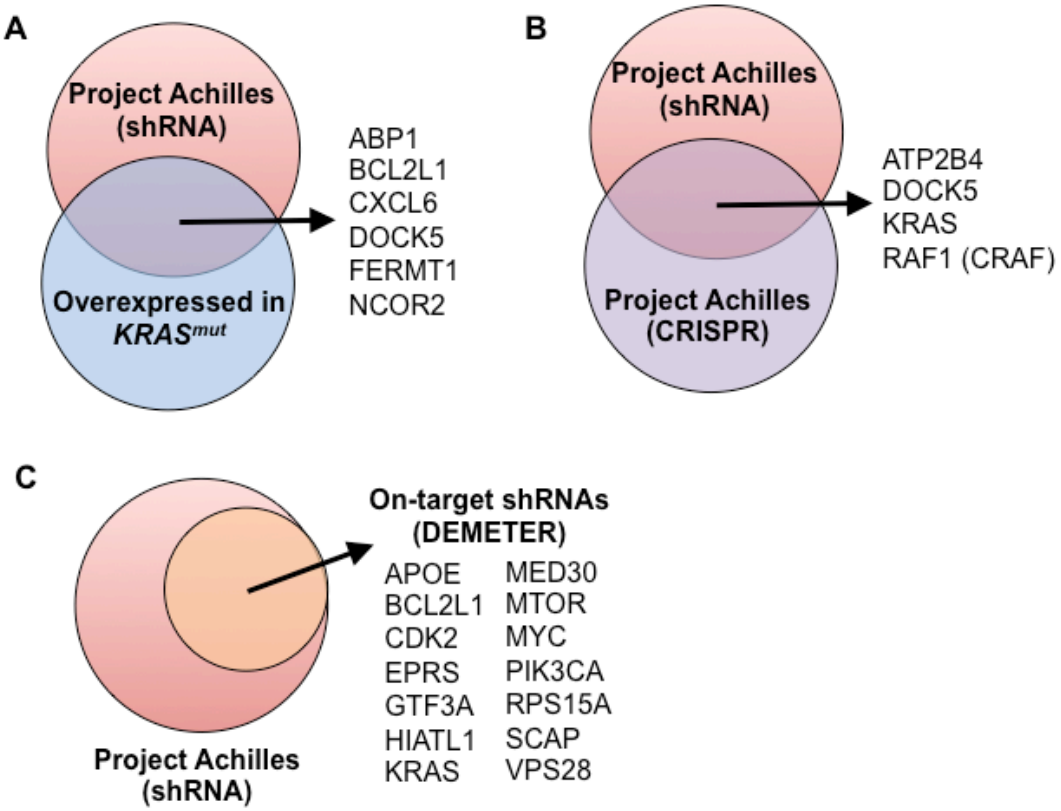

Figure 15. Approaches to prioritize candidate co-dependencies of oncogenic KRAS identified by analyzing Project Achilles shRNA data. (A) Prioritize genes whose expression is upregulated in *KRAS*-mutant cell lines. **(B)** Select genes that are also found to be selectively essential in *KRAS*-mutant cells in Project Achilles CRISPR-Cas9 data. **(C)** Filter for genes for which at least two shRNAs have >50% on-target effect as assessed by DEMETER[11].

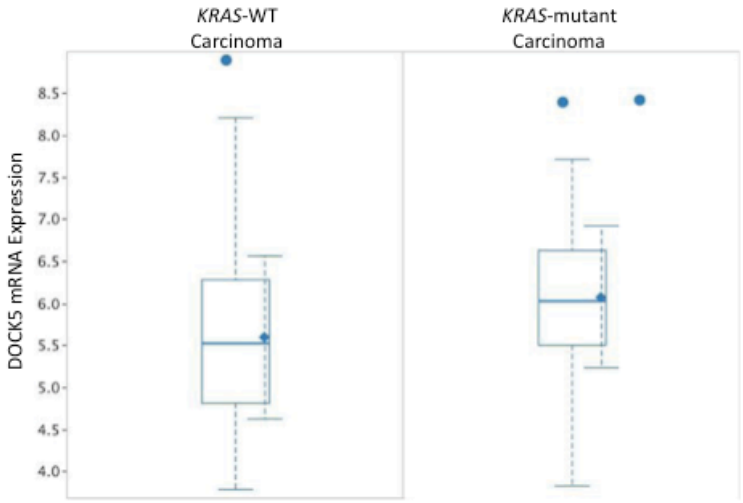

Figure 16. DOCK5 expression is upregulated in KRAS-mutant cell lines. In RNA-sequencing data of cell lines in the Cancer Cell Line Encyclopedia[164], DOCK5 is significantly more highly expressed in the 130 *KRAS*-mutant compared to 769 *KRAS*-WT carcinoma cell lines (t-test, $p < 0.001$).

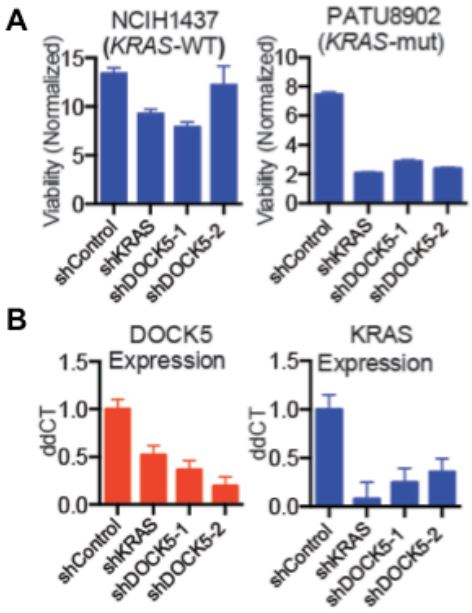

Figure 17. shRNAs targeting DOCK5 also reduce *KRAS* expression. (A) Effect of DOCK5 suppression on cell viability. Cells were infected with the indicated shRNAs, selected, and seeded in 96-well plates in quadruplicate 4 days post infection. Cell viability was measured by CellTiter-Glo 9 days post infection (5 days post seeding) and normalized to the number of cells seeded. Two representative cell lines are depicted. 4 technical replicates, data represented as mean ± SEM. **(B)** Effect of the indicated shRNAs on DOCK5 and KRAS expression (qRT-PCR) in NCIH1437 (*KRAS*-WT) cells. 4 technical replicates, data represented as mean ± SEM.

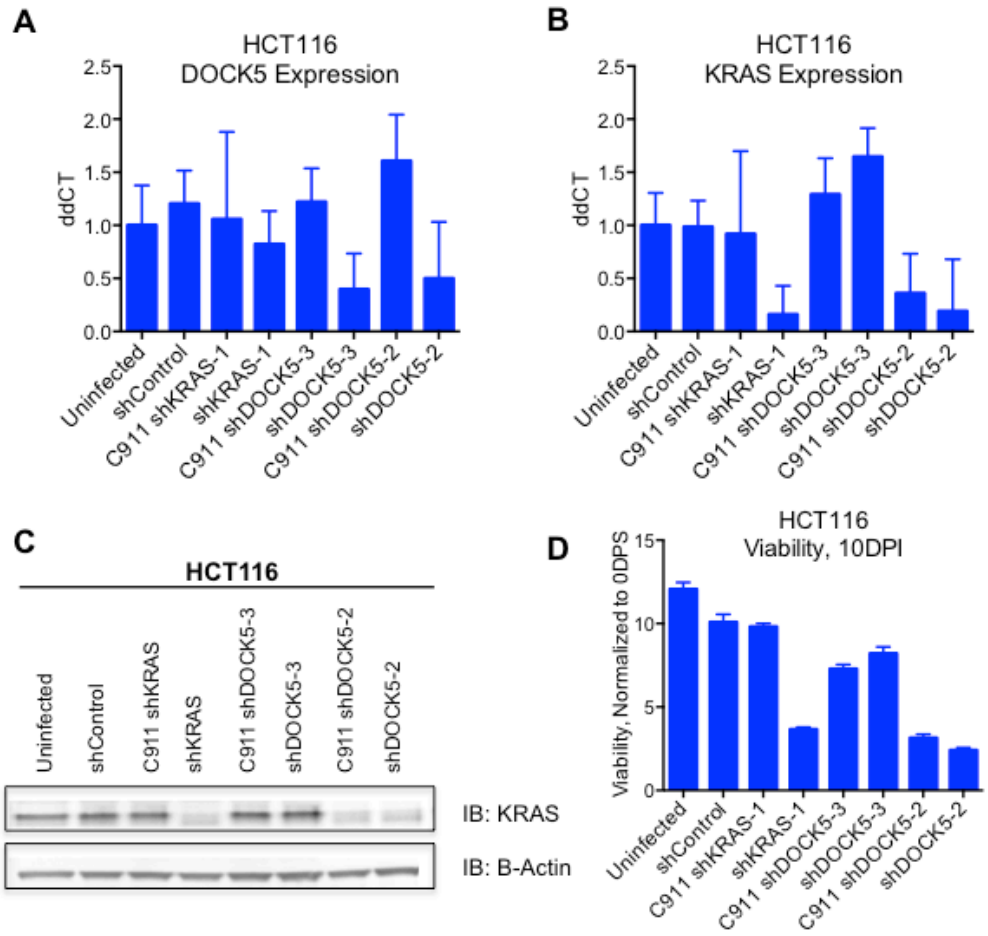

Figure 18. DOCK5 shRNAs decrease KRAS expression via off-target effects. qRT-PCR evaluation of DOCK5 **(A)** and KRAS **(B)** expression in in HCT116 (*KRAS*-mutant, colon) cells expressing the indicated shRNAs. C911 indicates seed-control shRNAs, in which the three nucleotides at position 9 to 11 of the shRNA target sequence are converted to their reverse complement[167], which abrogates 'on-target' depletion of target mRNA while preserving 'off-target' seed effects. 4 technical replicates, data represented as mean ± SEM. **(C)** Immunoblot analysis of KRAS expression in HCT116 cells expressing the indicated shRNAs. **(D)** Effect of DOCK5 suppression on cell viability. Cells were infected with the indicated shRNAs, selected, and seeded in 96-well plates in quadruplicate 4 days post infection. Cell viability was measured by CellTiter-Glo 10 days post infection (6 days post seeding) and normalized to the number of cells seeded. 3 technical replicates, data represented as mean ± SEM.

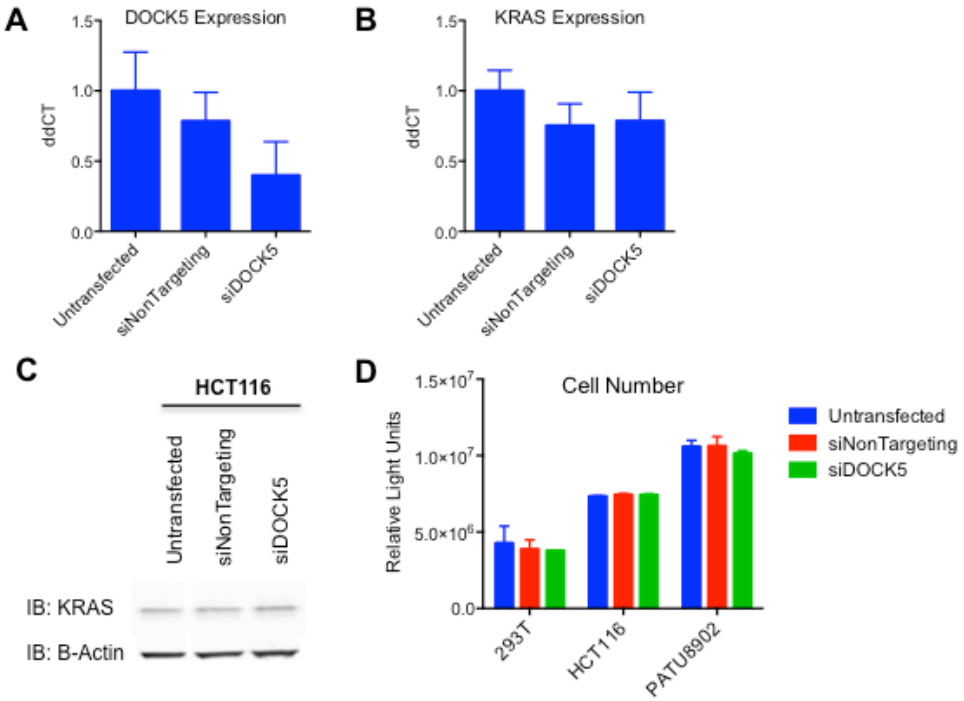

Figure 19. siRNA-mediated DOCK5 depletion does not affect KRAS expression or viability. HCT116 (*KRAS*-mutant, colon) cells were transfected with Dharmacon SMARTpool control (siNonTargeting) or DOCK5-targeting siRNAs. After 48 hours, expression of DOCK5 **(A)** and KRAS **(B)** was determined by qRTPCR. KRAS expression was also assessed by immunoblot **(C)**. **(D)** Cell viability was measured by CellTiter-Glo 6 days post transfection. 3 technical replicates, data represented as mean ± SEM.

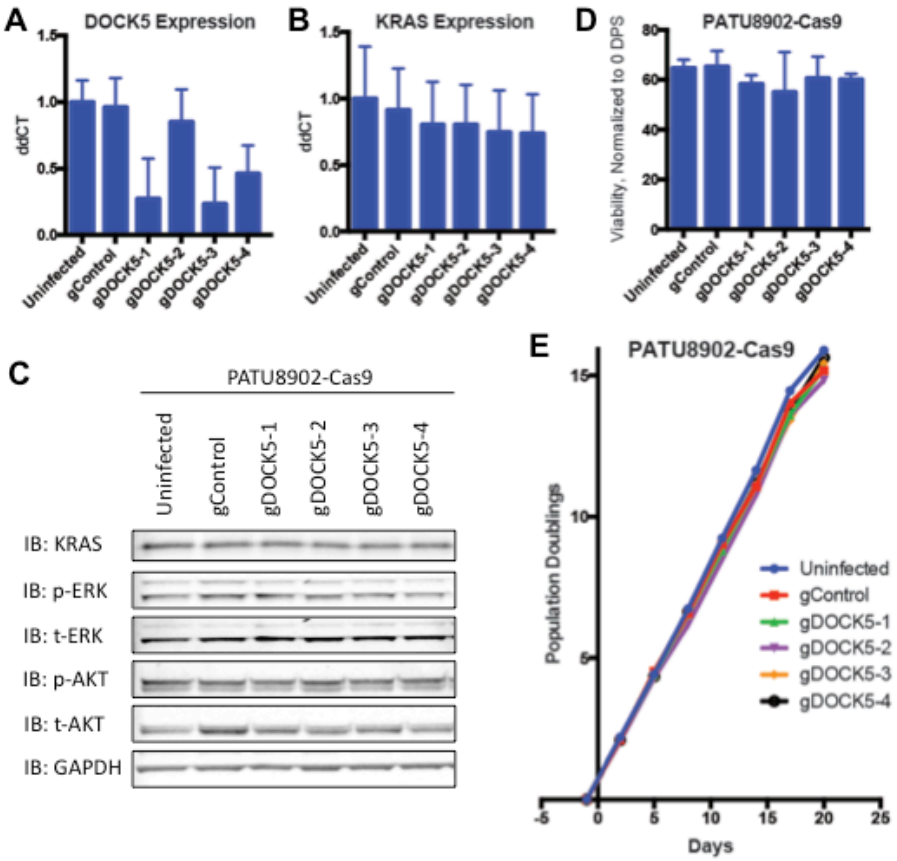

Figure 20. CRISPR-mediated DOCK5 knockout does not affect KRAS expression or cell viability. PATU8902-Cas9 cells were infected with the indicated gRNAs and selected. 8 days post gRNA infection, expression of DOCK5 **(A)** and KRAS **(B)** were assessed using q-RTPCR. 4 technical replicates representative of 2 independent experiments, data represented as mean ± SEM. **(C)** Effect of DOCK5 knockout on KRAS expression and MAPK pathway activity was evaluated by immunoblot. **(D)** Effect of DOCK5 knockout on cell viability was assessed using a crystal violet assay. Cells were seeded in 6 well plates 8 days post gRNA infection. Cells were fixed and stained with crystal violet 8 days post seeding (DPS). 4 technical replicates representative of 2 independent experiments, data represented as mean ± SEM. **(E)** Cell counting assay to determine the effect of DOCK5 knockout on cell proliferation. Cells were seeded in 10cm plates 20 days post gRNA infection. Cells were counted and passaged every 3-4 days. 2 technical replicates representative of 2 independent experiments, data represented as mean ± SEM.

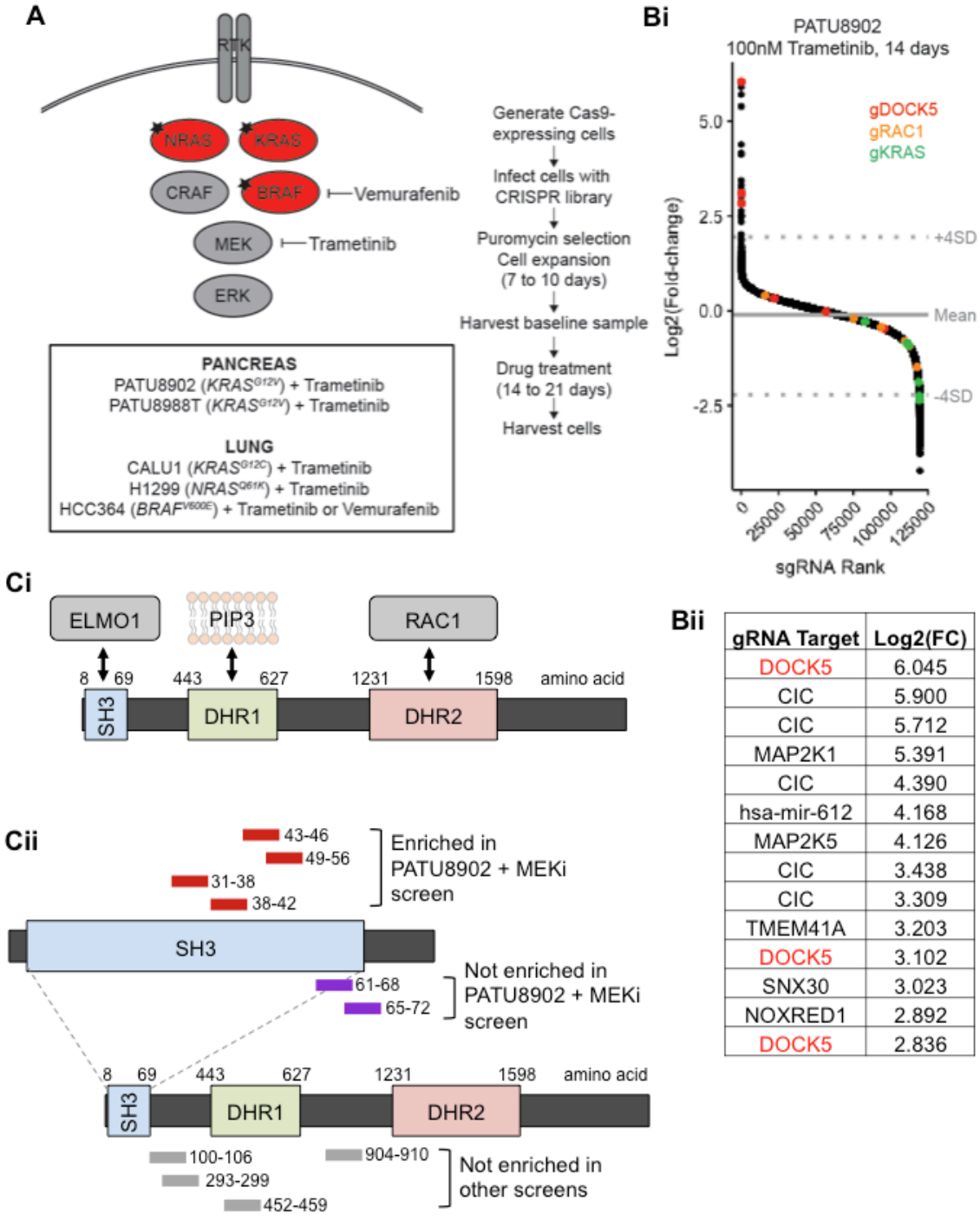

gRNA Target	Log2(FC)
DOCK5	6.045
CIC	5.900
CIC	5.712
MAP2K1	5.391
CIC	4.390
hsa-mir-612	4.168
MAP2K5	4.126
CIC	3.438
CIC	3.309
TMEM41A	3.203
DOCK5	3.102
SNX30	3.023
NOXRED1	2.892
DOCK5	2.836

Figure 21. DOCK5 modulates sensitivity to MAPK pathway inhibition. (A) Outline of strategy for pooled genome-scale CRISPR-Cas9 screens in *RAS*- or *BRAF*-mutant cancer cell lines treated with MAPK pathway inhibitors. **(Bi)** Distribution of $\log_2$ fold-change in gRNA representation on day 14 versus day 0 of PATU8902 cells treated with 100nM trametinib. Average of two biological replicates. Gray lines indicate the average $\log_2$ fold-change (solid) or 4 SD above average $\log_2$ fold-change (dashed) of all screened gRNAs. gRNAs targeting DOCK5 (red), RAC1(orange), and KRAS (green)

are indicated. $\log_2$ fold-change of top 15 most enriched gRNAs are indicated in **(Bii)**. **(Ci)** Schematic of DOCK5 structure. At baseline, the N-terminal SH3 domain of DOCK5 interacts with its C-terminal DHR2 domain, autoinhibiting GEF activity. Interaction between SH3 domain and ELMO1 abrogates autoinhibition. DHR1 domain mediates interactions with lipids (PIP3). DHR2 interacts with RAC1 and promotes the exchange of GDP for GTP. (**Cii)** DOCK5-targeting gRNAs that became strongly enriched in PATU8902 cells treated with the MEK inhibitor trametinib target theDOCK5 N-terminal SH3 domain (red). DOCK5-targeting gRNAs that did not become enriched in the PATU8902 screen (purple) or in other screens of *RAS*-mutant cells treated with MAPK pathway inhibitors (gray) target regions downstream of the SH3 domain.

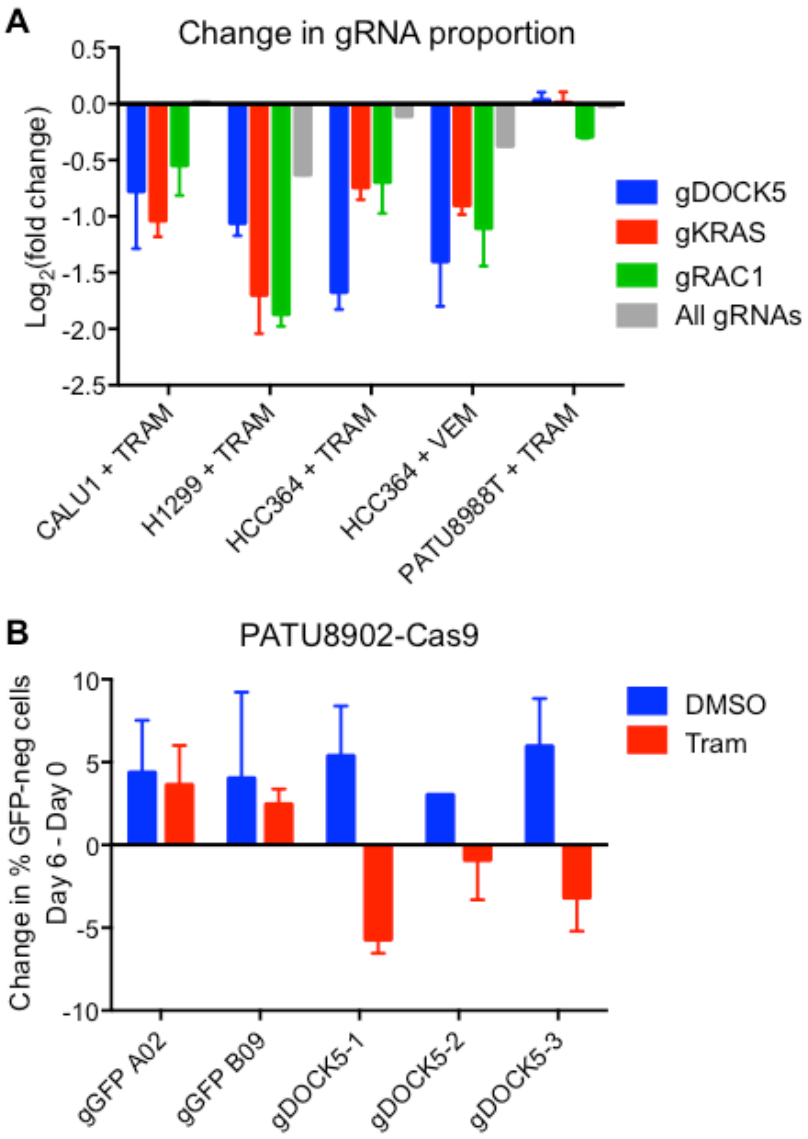

Figure 22. DOCK5 knockout sensitizes cells to MAPK pathway inhibition. (A) gRNAs targeting DOCK5, RAC1, and KRAS are depleted in the majority genome-scale CRISPR-Cas9 screens. Average $\log_2$(fold change) of the 3 most depleted gRNAs targeting DOCK5 (blue), RAC1 (red), or KRAS (green) on Day 14 of the indicated genome-scale CRISPR-Cas9 screen. Gray bars indicate the average $\log_2$(fold change) of all gRNAs in the screen. TRAM = trametinib (MEK inhibitor). VEM = vemurafenib (BRAF inhibitor) . 2 biological replicates, data represented as mean ± SEM. **(B)** Competition assay demonstrates that *DOCK5*-knockout cells have reduced viability/proliferation compared to parental *DOCK5*-WT cells. PATU8902 (*KRAS*-mutant, pancreas) cells expressing GFP were mixed with unlabeled PATU8902-Cas9 cells expressing the indicated gRNA in a 1:1 ratio. Change in percentage GFP-expressing cells was assessed after 6 days. 2 technical replicates representative of 2 independent experiments, data represented as mean ± SEM.

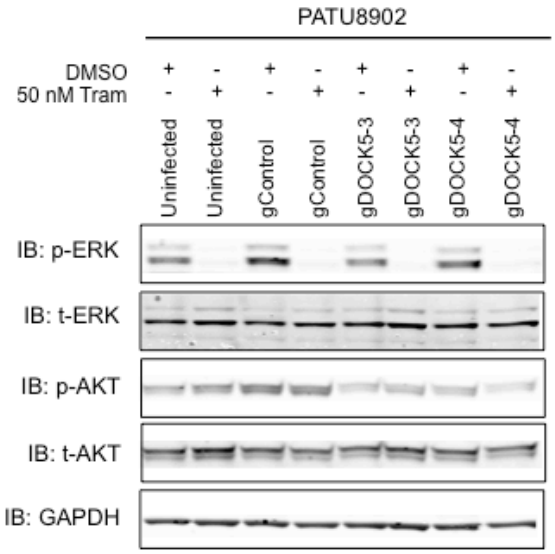

Figure 23. *DOCK5* deletion reduces p-AKT. Immunoblot analysis of expression of the indicated proteins in PATU8902 cells (*KRAS*-mutant, pancreas) treated with DMSO (control) or 50nm Trametinib (MEK inhibitor) for 24 hours.

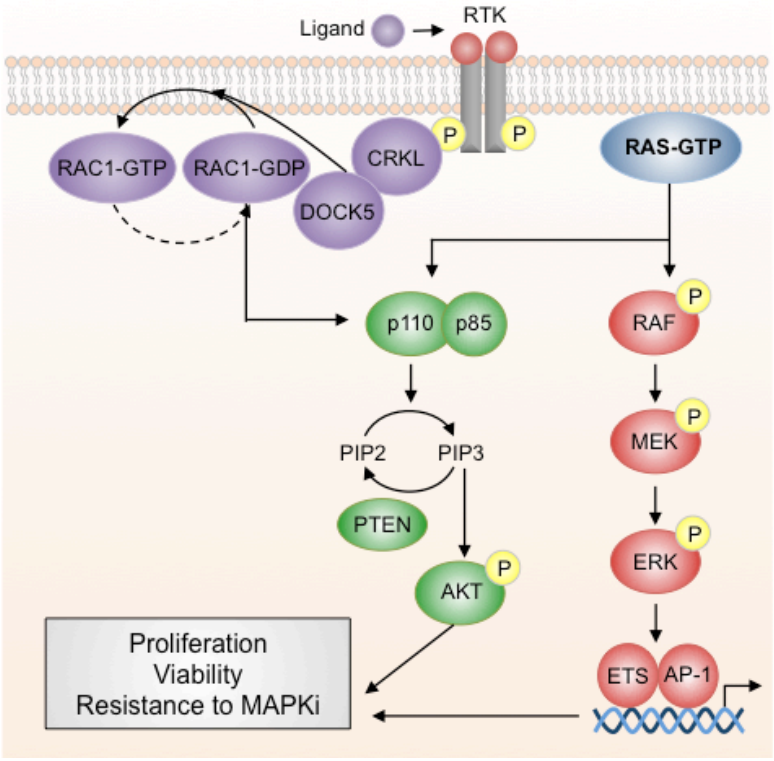

Figure 24. Signal convergence downstream of RAS and DOCK5. Proposed model in which oncogenic RAS and DOCK5-RAC1 converge to activate the PI3K pathway, which promotes cell proliferation and viability. Reduced DOCK5 activity may increase sensitivity to MAPK inhibition in *RAS*-mutant cells by reducing PI3K pathway activity.

References

1. Rehman, F. L., Lord, C. J. & Ashworth, A. Synthetic lethal approaches to breast cancer therapy. *Nat Rev Clin Oncol* **7,** 718–724 (2010).
2. William G Kaelin, J. Synthetic lethality: a framework for the development of wiser cancer therapeutics. **1,** 99 (2009).
3. Barbie, D. A. *et al.* Systematic RNA interference reveals that oncogenicKRAS-driven cancers require TBK1. *Nature* **461,** 108–112 (2009).
4. Luo, J. *et al.* A Genome-wide RNAi Screen Identifies Multiple Synthetic Lethal Interactions with the Ras Oncogene. *Cell* **137,** 835–848 (2009).
5. Vicent, S. *et al.* Wilms tumor 1 (WT1) regulates KRAS-driven oncogenesis and senescence in mouse and human models. *J. Clin. Invest.* **120,** 3940–3952 (2010).
6. Wang, Y. *et al.* Critical role for transcriptional repressor Snail2 in transformation by oncogenic RAS in colorectal carcinoma cells. *Oncogene* **29,** 4658–4670 (2010).
7. Yu, M. *et al.* RNA sequencing of pancreatic circulating tumour cells implicates WNT signalling in metastasis. *Nature* **487,** 510–513 (2013).
8. Scholl, C. *et al.* Synthetic lethal interaction between oncogenic KRAS dependency and STK33 suppression in human cancer cells. *Cell* **137,** 821–834 (2009).
9. Zhu, Z. *et al.* Inhibition of KRAS-driven tumorigenicity by interruption of an autocrine cytokine circuit. *Cancer Discovery* **4,** 452–465 (2014).
10. Cheung, H. W. *et al.* Systematic investigation of genetic vulnerabilities across cancer cell lines reveals lineage-specific dependencies in ovarian cancer. *Proceedings of the National Academy of Sciences* **108,** 12372–12377 (2011).
11. Tsherniak, A. *et al.* Defining a Cancer Dependency Map. *Cell* **170,** 564–576.e16 (2017).
12. Cowley, G. S. *et al.* Parallel genome-scale loss of function screens in 216 cancer cell lines for the identification of context-specific genetic dependencies. *Sci Data* **1,** 140035 (2014).
13. Gilbert, L. A. *et al.* CRISPR-mediated modular RNA-guided regulation of transcription in eukaryotes. *Cell* **154,** 442–451 (2013).
14. Wang, T. *et al.* Gene Essentiality Profiling Reveals Gene Networks and Synthetic Lethal Interactions with Oncogenic Ras. *Cell* **168,** 890–903.e15 (2017).
15. Aguirre, A. J. *et al.* Genomic Copy Number Dictates a Gene-Independent Cell Response to CRISPR/Cas9 Targeting. *Cancer Discovery* **6,** 914–929 (2016).
16. Nijhawan, D. *et al.* Cancer Vulnerabilities Unveiled by Genomic Loss. *Cell* **150,** 842–854 (2012).
17. Rosenbluh, J. *et al.* β-Catenin-driven cancers require a YAP1 transcriptional complex for survival and tumorigenesis. *Cell* **151,** 1457–1473 (2012).
18. Cox, A. D. & Der, C. J. Ras history: The saga continues. *Small GTPases* **1,** 2–27 (2010).
19. Scolnick, E. M., Papageorge, A. G. & Shih, T. Y. Guanine nucleotide-binding activity as an assay for src protein of rat-derived murine sarcoma viruses. *Proc*

Natl Acad Sci USA **76,** 5355–5359 (1979).
20. Shih, T. Y., Papageorge, A. G., Stokes, P. E., Weeks, M. O. & Scolnick, E. M. Guanine nucleotide-binding and autophosphorylating activities associated with the p21src protein of Harvey murine sarcoma virus. *Nature* **287,** 686–691 (1980).
21. Hurley, J. B., Simon, M. I., Teplow, D. B., Robishaw, J. D. & Gilman, A. G. Homologies between signal transducing G proteins and ras gene products. *Science* **226,** 860–862 (1984).
22. Stephen, A. G., Esposito, D., Bagni, R. K. & McCormick, F. Dragging ras back in the ring. *Cancer Cell* **25,** 272–281 (2014).
23. Malumbres, M. & Barbacid, M. RAS oncogenes: the first 30 years. *Nat Rev Cancer* **3,** 459–465 (2003).
24. Karnoub, A. E. & Weinberg, R. A. Ras oncogenes: split personalities. *Nat Rev Mol Cell Biol* **9,** 517–531 (2008).
25. Trahey, M. & McCormick, F. A cytoplasmic protein stimulates normal N-ras p21 GTPase, but does not affect oncogenic mutants. *Science* **238,** 542–545 (1987).
26. Scheffzek, K., Lautwein, A., Kabsch, W., Reza Ahmadian, M. & Wittinghofer, A. Crystal structure of the GTPase-activating domain of human p120GAP and implications for the interaction with Ras. *Nature* **384,** 591–596 (1996).
27. Gupta, S. *et al.* Binding of Ras to Phosphoinositide 3-Kinase p110α Is Required for Ras- Driven Tumorigenesis in Mice. *Cell* **129,** 957–968 (2007).
28. Blasco, R. B. *et al.* c-Raf, but not B-Raf, is essential for development of K-Ras oncogene-driven non-small cell lung carcinoma. *Cancer Cell* **19,** 652–663 (2011).
29. Collisson, E. A. *et al.* A central role for RAF→MEK→ERK signaling in the genesis of pancreatic ductal adenocarcinoma. *Cancer Discovery* **2,** 685–693 (2012).
30. González-García, A. *et al.* RalGDS is required for tumor formation in a model of skin carcinogenesis. *CCELL* **7,** 219–226 (2005).
31. Ehrenreiter, K. *et al.* Raf-1 addiction in Ras-induced skin carcinogenesis. *Cancer Cell* **16,** 149–160 (2009).
32. Hamad, N. M. *et al.* Distinct requirements for Ras oncogenesis in human versus mouse cells. *Genes & Development* **16,** 2045–2057 (2002).
33. Cox, A. D., Fesik, S. W., Kimmelman, A. C., Luo, J. & Der, C. J. Drugging the undruggable RAS: Mission Possible? *Nature Publishing Group* **13,** 828–851 (2014).
34. Kandoth, C. *et al.* Mutational landscape and significance across 12 major cancer types. *Nature* **502,** 333–339 (2013).
35. Liu, P. *et al.* Oncogenic PIK3CA-driven mammary tumors frequently recur via PI3K pathway–dependent and PI3K pathway–independent mechanisms. *Nat Med* **17,** 1116–1120 (2011).
36. Forbes, S. A. *et al.* COSMIC: exploring the world's knowledge of somatic mutations in human cancer. *Nucleic Acids Research* **43,** D805–11 (2015).
37. Prior, I. A., Lewis, P. D. & Mattos, C. A Comprehensive Survey of Ras Mutations in Cancer. *Cancer Research* **72,** 2457–2467 (2012).
38. Weinstein, I. B. Cancer. Addiction to oncogenes--the Achilles heal of cancer.

Science **297,** 63–64 (2002).
39. Weinstein, I. B. Disorders in cell circuitry during multistage carcinogenesis: the role of homeostasis. *Carcinogenesis* **21,** 857–864 (2000).
40. Haber, D. A., Gray, N. S. & Baselga, J. The Evolving War on Cancer. *Cell* **145,** 19–24 (2011).
41. Sharma, S. V. & Settleman, J. Oncogene addiction: setting the stage for molecularly targeted cancer therapy. *Genes & Development* **21,** 3214–3231 (2007).
42. Singh, A. *et al.* A Gene Expression Signature Associated with 'K-Ras Addiction' Reveals Regulators of EMT and Tumor Cell Survival. *Cancer Cell* **15,** 489–500 (2009).
43. Brummelkamp, T. R., Bernards, R. & Agami, R. Stable suppression of tumorigenicity by virus-mediated RNA interference. *Cancer Cell* **2,** 243–247 (2002).
44. Lim, K.-H. *et al.* Activation of RalA is critical for Ras-induced tumorigenesis of human cells. *Cancer Cell* **7,** 533–545 (2005).
45. Chin, L. *et al.* Essential role for oncogenic Ras in tumour maintenance. *Nature Publishing Group* **400,** 468–472 (1999).
46. Fisher, G. H. *et al.* Induction and apoptotic regression of lung adenocarcinomas by regulation of a K-Ras transgene in the presence and absence of tumor suppressor genes. *Genes & Development* **15,** 3249–3262 (2001).
47. Hingorani, S. R. *et al.* Preinvasive and invasive ductal pancreatic cancer and its early detection in the mouse. *Cancer Cell* **4,** 437–450 (2003).
48. Ying, H. *et al.* Oncogenic Kras Maintains Pancreatic Tumors through Regulation of Anabolic Glucose Metabolism. *Cell* **149,** 656–670 (2012).
49. Collins, M. A. & Pasca di Magliano, M. Kras as a key oncogene and therapeutic target in pancreatic cancer. *Front. Physiol.* **4,** 407 (2013).
50. Collins, M. A. *et al.* Metastatic Pancreatic Cancer Is Dependent on Oncogenic Kras in Mice. *PLoS ONE* **7,** e49707 (2012).
51. Kwong, L. N. *et al.* Oncogenic NRAS signaling differentially regulates survival and proliferation in melanoma. *Nat Med* **18,** 1503–1510 (2012).
52. Luo, J., Solimini, N. L. & Elledge, S. J. Principles of cancer therapy: oncogene and non-oncogene addiction. *Cell* (2009).
53. Normanno, N., Bianco, C., De Luca, A. & Salomon, D. S. The role of EGF-related peptides in tumor growth. *Front. Biosci.* **6,** D685–707 (2001).
54. Sibilia, M. *et al.* The EGF receptor provides an essential survival signal for SOS-dependent skin tumor development. *Cell* **102,** 211–220 (2000).
55. Allegra, C. J. *et al.* American Society of Clinical Oncology Provisional Clinical Opinion: Testing for KRAS Gene Mutations in Patients With Metastatic Colorectal Carcinoma to Predict Response to Anti-Epidermal Growth Factor Receptor Monoclonal Antibody Therapy. *Journal of Clinical Oncology* **27,** 2091–2096 (2009).
56. Allegra, C. J. *et al.* Extended RAS Gene Mutation Testing in Metastatic Colorectal Carcinoma to Predict Response to Anti-Epidermal Growth Factor Receptor Monoclonal Antibody Therapy: American Society of Clinical Oncology Provisional Clinical Opinion Update 2015. *Journal of Clinical Oncology* (2015).

doi:10.1200/JCO.2015.63.9674
57. Pao, W. *et al.* KRAS mutations and primary resistance of lung adenocarcinomas to gefitinib or erlotinib. *PLoS Med.* **2,** e17 (2005).
58. Eberhard, D. A. *et al.* Mutations in the Epidermal Growth Factor Receptor and in KRAS Are Predictive and Prognostic Indicators in Patients With Non–Small-Cell Lung Cancer Treated With Chemotherapy Alone and in Combination With Erlotinib. *jco.ascopubs.org*
59. Zhu, C. Q. *et al.* Role of KRAS and EGFR as biomarkers of response to erlotinib in National Cancer Institute of Canada Clinical Trials Group Study BR.21. *Journal of Clinical Oncology* **26,** 4268–4275 (2008).
60. Mao, C. *et al.* KRAS mutations and resistance to EGFR-TKIs treatment in patients with non-small cell lung cancer: a meta-analysis of 22 studies. *Lung Cancer* **69,** 272–278 (2010).
61. Karachaliou, N. *et al.* KRAS mutations in lung cancer. *Clin Lung Cancer* **14,** 205–214 (2013).
62. Goody, R. S., Frech, M. & Wittinghofer, A. Affinity of guanine nucleotide binding proteins for their ligands: facts and artefacts. *Trends Biochem. Sci.* **16,** 327–328 (1991).
63. Arkin, M. R. & Wells, J. A. Small-molecule inhibitors of protein-protein interactions: progressing towards the dream. *Nat Rev Drug Discov* **3,** 301–317 (2004).
64. Herrmann, C. *et al.* Sulindac sulfide inhibits Ras signaling. *Oncogene* **17,** 1769–1776 (1998).
65. Waldmann, H. *et al.* Sulindac-derived Ras pathway inhibitors target the Ras-Raf interaction and downstream effectors in the Ras pathway. *Angew. Chem. Int. Ed. Engl.* **43,** 454–458 (2004).
66. Karaguni, I.-M. *et al.* New indene-derivatives with anti-proliferative properties. *Bioorganic & Medicinal Chemistry Letters* **12,** 709–713 (2002).
67. Kato-Stankiewicz, J. *et al.* Inhibitors of Ras/Raf-1 interaction identified by two-hybrid screening revert Ras-dependent transformation phenotypes in human cancer cells. *Proc Natl Acad Sci USA* **99,** 14398–14403 (2002).
68. Rosnizeck, I. C. *et al.* Stabilizing a Weak Binding State for Effectors in the Human Ras Protein by Cyclen Complexes. *Angew. Chem. Int. Ed.* **49,** 3830–3833
69. Shima, F. *et al.* In silico discovery of small-molecule Ras inhibitors that display antitumor activity by blocking the Ras-effector interaction. *Proceedings of the National Academy of Sciences* **110,** 8182–8187 (2013).
70. Hocker, H. J. *et al.* Andrographolide derivatives inhibit guanine nucleotide exchange and abrogate oncogenic Ras function. *Proceedings of the National Academy of Sciences* **110,** 10201–10206 (2013).
71. Maurer, T. *et al.* Small-molecule ligands bind to a distinct pocket in Ras and inhibit SOS-mediated nucleotide exchange activity. *Proceedings of the National Academy of Sciences* **109,** 5299–5304 (2012).
72. Patgiri, A., Yadav, K. K., Arora, P. S. & Bar-Sagi, D. An orthosteric inhibitor of the Ras-Sos interaction. *Nature Chemical Biology* **7,** 585–587 (2011).
73. Sacco, E. *et al.* Binding properties and biological characterization of new sugar-

derived Ras ligands. *Med. Chem. Commun.* **2,** 396–401 (2011).
74. Sun, Q. *et al.* Discovery of small molecules that bind to K-Ras and inhibit Sos-mediated activation. *Angew. Chem. Int. Ed. Engl.* **51,** 6140–6143 (2012).
75. Taveras, A. G. *et al.* Ras oncoprotein inhibitors: the discovery of potent, ras nucleotide exchange inhibitors and the structural determination of a drug-protein complex. *Bioorganic & Medicinal Chemistry* **5,** 125–133 (1997).
76. Ostrem, J. M., Peters, U., Sos, M. L., Wells, J. A. & Shokat, K. M. K-Ras(G12C) inhibitors allosterically control GTP affinity and effector interactions. *Nature* – (2013). doi:10.1038/nature12796
77. Lim, S. M. *et al.* Therapeutic targeting of oncogenic K-Ras by a covalent catalytic site inhibitor. *Angew. Chem. Int. Ed. Engl.* **53,** 199–204 (2014).
78. Cancer Genome Atlas Research Network. Comprehensive molecular profiling of lung adenocarcinoma. *Nature* **511,** 543–550 (2014).
79. Appels, N. M. G. M., Beijnen, J. H. & Schellens, J. H. M. Development of farnesyl transferase inhibitors: a review. *The Oncologist* **10,** 565–578 (2005).
80. Rowell, C. A., Kowalczyk, J. J., Lewis, M. D. & Garcia, A. M. Direct demonstration of geranylgeranylation and farnesylation of Ki-Ras in vivo. *J. Biol. Chem.* **272,** 14093–14097 (1997).
81. Whyte, D. B. *et al.* K- and N-Ras Are Geranylgeranylated in Cells Treated with Farnesyl Protein Transferase Inhibitors. *Journal of Biological Chemistry* **272,** 14459–14464 (1997).
82. Lerner, E. C. *et al.* Inhibition of the prenylation of K-Ras, but not H- or N-Ras, is highly resistant to CAAX peptidomimetics and requires both a farnesyltransferase and a geranylgeranyltransferase I inhibitor in human tumor cell lines. *Oncogene* **15,** 1283–1288 (1997).
83. Goldstein, J. L. Polylysine and CVIM Sequences of K-RasB Dictate Specificity of Prenylation and Confer Resistance to Benzodiazepine Peptidomimetic in Vitro. *Journal of Biological Chemistry* **270,** 6221–6226 (1995).
84. Caunt, C. J., Sale, M. J., Smith, P. D. & Cook, S. J. MEK1 and MEK2 inhibitors and cancer therapy: the long and winding road. *Nat Rev Cancer* **15,** 577–592 (2015).
85. Lito, P., Rosen, N. & Solit, D. B. Tumor adaptation and resistance to RAF inhibitors. *Nat Med* **19,** 1401–1409 (2013).
86. Chapman, P. B. *et al.* Improved Survival with Vemurafenib in Melanoma with BRAF V600E Mutation. *N. Engl. J. Med.* **364,** 2507–2516 (2011).
87. Hauschild, A. *et al.* Dabrafenib in BRAF-mutated metastatic melanoma: a multicentre, open-label, phase 3 randomised controlled trial. *Lancet* **380,** 358–365 (2012).
88. Heidorn, S. J. *et al.* Kinase-dead BRAF and oncogenic RAS cooperate to drive tumor progression through CRAF. *Cell* **140,** 209–221 (2010).
89. Hatzivassiliou, G. *et al.* RAF inhibitors prime wild-type RAF to activate the MAPK pathway and enhance growth. *Nature* **464,** 431–435 (2010).
90. Poulikakos, P. I., Zhang, C., Bollag, G., Shokat, K. M. & Rosen, N. RAF inhibitors transactivate RAF dimers and ERK signalling in cells with wild-type BRAF. *Nature* **464,** 427–430 (2010).
91. Hall-Jackson, C. A. *et al.* Paradoxical activation of Raf by a novel Raf inhibitor.

Chem. Biol. **6,** 559–568 (1999).
92. Zhang, C. *et al.* RAF inhibitors that evade paradoxical MAPK pathway activation. *Nature* **526,** 583–586 (2015).
93. Girotti, M. R. *et al.* Paradox-breaking RAF inhibitors that also target SRC are effective in drug-resistant BRAF mutant melanoma. *Cancer Cell* **27,** 85–96 (2015).
94. Flaherty, K. T. *et al.* Improved survival with MEK inhibition in BRAF-mutated melanoma. *N. Engl. J. Med.* **367,** 107–114 (2012).
95. Jänne, P. A. *et al.* Selumetinib plus docetaxel for KRAS-mutant advanced non-small-cell lung cancer: a randomised, multicentre, placebo-controlled, phase 2 study. *Lancet Oncol.* **14,** 38–47 (2013).
96. Infante, J. R. *et al.* Safety, pharmacokinetic, pharmacodynamic, and efficacy data for the oral MEK inhibitor trametinib: a phase 1 dose-escalation trial. *Lancet Oncol.* **13,** 773–781 (2012).
97. Blumenschein, G. *et al.* A randomized phase 2 study of the MEK1/MEK2 inhibitor trametinib (GSK1120212) compared with docetaxel in KRAS-mutant advanced non-small cell lung cancer (NSCLC). *Ann. Oncol.* (2015). doi:10.1093/annonc/mdv072
98. Ascierto, P. A. *et al.* MEK162 for patients with advanced melanoma harbouring NRAS or Val600 BRAF mutations: a non-randomised, open-label phase 2 study. *Lancet Oncol.* **14,** 249–256 (2013).
99. Carlino, M. S. *et al.* Differential activity of MEK and ERK inhibitors in BRAF inhibitor resistant melanoma. *Molecular Oncology* **8,** 544–554 (2014).
100. Eser, S. *et al.* Selective Requirement of PI3K/PDK1 Signaling for Kras Oncogene-Driven Pancreatic Cell Plasticity and Cancer. *Cancer Cell* **23,** 406–420 (2013).
101. Castellano, E. *et al.* Requirement for Interaction of PI3-Kinase p110α with RAS in Lung Tumor Maintenance. *Cancer Cell* **24,** 617–630 (2013).
102. Lim, K.-H. & Counter, C. M. Reduction in the requirement of oncogenic Ras signaling to activation of PI3K/AKT pathway during tumor maintenance. *CCELL* **8,** 381–392 (2005).
103. Engelman, J. A. *et al.* Effective use of PI3K and MEK inhibitors to treat mutant Kras G12D and PIK3CA H1047R murine lung cancers. *Nat Med* **14,** 1351–1356 (2008).
104. Ihle, N. T. *et al.* Mutations in the phosphatidylinositol-3-kinase pathway predict for antitumor activity of the inhibitor PX-866 whereas oncogenic Ras is a dominant predictor for resistance. *Cancer Research* **69,** 143–150 (2009).
105. Molina-Arcas, M., Hancock, D. C., Sheridan, C., Kumar, M. S. & Downward, J. Coordinate direct input of both KRAS and IGF1 receptor to activation of PI3 kinase in KRAS-mutant lung cancer. *Cancer Discovery* **3,** 548–563 (2013).
106. Shimizu, T. *et al.* The clinical effect of the dual-targeting strategy involving PI3K/AKT/mTOR and RAS/MEK/ERK pathways in patients with advanced cancer. *Clin. Cancer Res.* **18,** 2316–2325 (2012).
107. Do, K., Speranza, G., Bishop, R. & Khin, S. Biomarker-driven phase 2 study of MK-2206 and selumetinib (AZD6244, ARRY-142886) in patients with colorectal cancer. *Investigational new …* (2015).

108. Kaelin, W. G. The Concept of Synthetic Lethality in the Context of Anticancer Therapy. *Nat Rev Cancer* **5,** 689–698 (2005).
109. Bender, A. & Pringle, J. R. Use of a screen for synthetic lethal and multicopy suppressee mutants to identify two new genes involved in morphogenesis in Saccharomyces cerevisiae. *Molecular and Cellular Biology* **11,** 1295–1305 (1991).
110. Lucchesi, J. C. Synthetic lethality and semi-lethality among functionally related mutants of Drosophila melanfgaster. *Genetics* **59,** 37–44 (1968).
111. Hartwell, L. H., Szankasi, P., Roberts, C. J., Murray, A. W. & Friend, S. H. Integrating genetic approaches into the discovery of anticancer drugs. *Science* **278,** 1064–1068 (1997).
112. Bryant, H. E. *et al.* Specific killing of BRCA2-deficient tumours with inhibitors of poly(ADP-ribose) polymerase. *Nature* **434,** 913–917 (2005).
113. Farmer, H. *et al.* Farmer et al. - 2005 - Targeting the DNA repair defect in BRCA mutant cells as a therapeutic strategy. *Oncogene* **434,** 917–921 (2005).
114. Fong, P. C. *et al.* Inhibition of poly(ADP-ribose) polymerase in tumors from BRCA mutation carriers. *N. Engl. J. Med.* **361,** 123–134 (2009).
115. O'Neil, N. J., Bailey, M. L. & Hieter, P. Synthetic lethality and cancer. *Nat. Rev. Genet.* **18,** 613–623 (2017).
116. Downward, J. RAS Synthetic Lethal Screens Revisited: Still Seeking the Elusive Prize? *Clinical Cancer Research* **21,** 1802–1809 (2015).
117. Fire, A. *et al.* Potent and specific genetic interference by double-stranded RNA in Caenorhabditis elegans. *Nature* **391,** 806–811 (1998).
118. Wilson, R. C. & Doudna, J. A. Molecular mechanisms of RNA interference. *Annu Rev Biophys* **42,** 217–239 (2013).
119. Mohr, S. E., Smith, J. A., Shamu, C. E., Neumüller, R. A. & Perrimon, N. RNAi screening comes of age: improved techniques and complementary approaches. *Nat Rev Mol Cell Biol* **15,** 591–600 (2014).
120. Cong, L. *et al.* Multiplex Genome Engineering Using CRISPR/Cas Systems. *Science* **339,** 819–823 (2013).
121. Mali, P. *et al.* RNA-Guided Human Genome Engineering via Cas9. *Science* **339,** 823–826 (2013).
122. Beijersbergen, R. L., Wessels, L. F. A. & Bernards, R. Synthetic Lethality in Cancer Therapeutics. *Annu. Rev. Cancer Biol.* **1,** 141–161 (2017).
123. Berns, K. *et al.* A large-scale RNAi screen in human cells identifies new components of the p53 pathway. *Oncogene* **428,** 431–437 (2004).
124. Paddison, P. J. *et al.* A resource for large-scale RNA-interference-based screens in mammals. *Oncogene* **428,** 427–431 (2004).
125. Vizeacoumar, F. J. *et al.* A negative genetic interaction map in isogenic cancer cell lines reveals cancer cell vulnerabilities. *Molecular Systems Biology* **9,** (2013).
126. Boettcher, M. & McManus, M. T. Choosing the Right Tool for the Job: RNAi, TALEN, or CRISPR. *Molecular Cell* **58,** 575–585 (2015).
127. Wang, T., Wei, J. J., Sabatini, D. M. & Lander, E. S. Genetic Screens in Human Cells Using the CRISPR-Cas9 System. *Science* **343,** 80–84 (2014).
128. Zhou, Y. *et al.* High-throughput screening of a CRISPR/Cas9 library for

functional genomics in human cells. *Nature* **509,** 487–491 (2014).
129. Shalem, O., Sanjana, N. E. & Zhang, F. High-throughput functional genomics using CRISPR-Cas9. *Nat. Rev. Genet.* **16,** 299–311 (2015).
130. Birmingham, A. *et al.* 3' UTR seed matches, but not overall identity, are associated with RNAi off-targets. *Nat Meth* **3,** 199–204 (2006).
131. Jackson, A. L. *et al.* Expression profiling reveals off-target gene regulation by RNAi. *Nature Biotechnology* **21,** 635–637 (2003).
132. Fellmann, C. *et al.* Functional identification of optimized RNAi triggers using a massively parallel sensor assay. *Molecular Cell* **41,** 733–746 (2011).
133. Bhinder, B. & Djaballah, H. Systematic analysis of RNAi reports identifies dismal commonality at gene-level and reveals an unprecedented enrichment in pooled shRNA screens. *Comb. Chem. High Throughput Screen.* **16,** 665–681 (2013).
134. Munoz, D. M. *et al.* CRISPR Screens Provide a Comprehensive Assessment of Cancer Vulnerabilities but Generate False-Positive Hits for Highly Amplified Genomic Regions. *Cancer Discovery* **6,** 900–913 (2016).
135. Reynolds, A. *et al.* Rational siRNA design for RNA interference. *Nature Biotechnology* **22,** 326–330 (2004).
136. Jackson, A. L. & Linsley, P. S. Recognizing and avoiding siRNA off-target effects for target identification and therapeutic application. *Nature Publishing Group* **9,** 57–67 (2010).
137. Sigoillot, F. D. *et al.* A bioinformatics method identifies prominent off-targeted transcripts in RNAi screens. *Nat Meth* **9,** 363–366 (2012).
138. Buehler, E. *et al.* siRNA off-target effects in genome-wide screens identify signaling pathway members. *Sci. Rep.* **2,** 428 (2012).
139. Shao, D. D. *et al.* ATARiS: Computational quantification of gene suppression phenotypes from multisample RNAi screens. *Genome Res.* **23,** 665–678 (2013).
140. Cho, S. W. *et al.* Analysis of off-target effects of CRISPR/Cas-derived RNA-guided endonucleases and nickases. *Genome Res.* **24,** 132–141 (2014).
141. Doench, J. G. *et al.* Optimized sgRNA design to maximize activity and minimize off-target effects of CRISPR-Cas9. *Nature Biotechnology* (2016). doi:10.1038/nbt.3437
142. Doench, J. G. *et al.* Rational design of highly active sgRNAs for CRISPR-Cas9-mediated gene inactivation. *Nature Biotechnology* **32,** 1262–1267 (2014).
143. Wang, T. *et al.* Identification and characterization of essential genes in the human genome. *Science* **350,** 1096–1101 (2015).
144. Haber, J. E. *et al.* Systematic triple-mutant analysis uncovers functional connectivity between pathways involved in chromosome regulation. *Cell Rep* **3,** 2168–2178 (2013).
145. McCormick, F. KRAS as a Therapeutic Target. *Clin. Cancer Res.* **21,** 1797–1801 (2015).
146. Kumar, M. S. *et al.* The GATA2 Transcriptional Network Is Requisite for RAS Oncogene-Driven Non-Small Cell Lung Cancer. *Cell* **149,** 642–655 (2012).
147. Steckel, M. *et al.* Determination of synthetic lethal interactions in. *Cell Res* **22,** 1227–1245 (2012).
148. Gao, B. & Roux, P. P. Translational control by oncogenic signaling pathways. *Biochimica et Biophysica Acta (BBA) - Gene Regulatory Mechanisms* **1849,**

753–765 (2015).
149. Smith, D. *et al.* RAS mutation status and bortezomib therapy for relapsed multiple myeloma. *Br. J. Haematol.* **169,** 905–908 (2015).
150. Druker, B. J. *et al.* Efficacy and safety of a specific inhibitor of the BCR-ABL tyrosine kinase in chronic myeloid leukemia. *N. Engl. J. Med.* **344,** 1031–1037 (2001).
151. Lynch, T. J. *et al.* Activating mutations in the epidermal growth factor receptor underlying responsiveness of non-small-cell lung cancer to gefitinib. *N. Engl. J. Med.* **350,** 2129–2139 (2004).
152. Baselga, J. *et al.* Phase II Trial of Pertuzumab and Trastuzumab in Patients With Human Epidermal Growth Factor Receptor 2-Positive Metastatic Breast Cancer That Progressed During Prior Trastuzumab Therapy. *Journal of Clinical Oncology* **28,** 1138–1144 (2010).
153. Vogel, C. L. *et al.* Efficacy and safety of trastuzumab as a single agent in first-line treatment of HER2-overexpressing metastatic breast cancer. *J. Clin. Oncol.* **20,** 719–726 (2002).
154. Kwak, E. L. *et al.* Anaplastic lymphoma kinase inhibition in non-small-cell lung cancer. *N. Engl. J. Med.* **363,** 1693–1703 (2010).
155. Berns, K. & Bernards, R. Understanding resistance to targeted cancer drugs through loss of function genetic screens. *Drug Resist. Updat.* **15,** 268–275 (2012).
156. Garraway, L. A. & Janne, P. A. Circumventing Cancer Drug Resistance in the Era of Personalized Medicine. *Cancer Discovery* **2,** 214–226 (2012).
157. Van Allen, E. M. *et al.* The genetic landscape of clinical resistance to RAF inhibition in metastatic melanoma. *Cancer Discovery* **4,** 94–109 (2014).
158. Holohan, C., Van Schaeybroeck, S., Longley, D. B. & Johnston, P. G. Cancer drug resistance: an evolving paradigm. *Nat Rev Cancer* **13,** 714–726 (2013).
159. Prahallad, A. *et al.* Unresponsiveness of colon cancer to BRAF(V600E) inhibition through feedback activation of EGFR. *Oncogene* **483,** 100–103 (2012).
160. Corcoran, R. B. *et al.* EGFR-mediated re-activation of MAPK signaling contributes to insensitivity of BRAF mutant colorectal cancers to RAF inhibition with vemurafenib. *Cancer Discovery* **2,** 227–235 (2012).
161. van Geel, R. M. J. M. *et al.* A Phase Ib Dose-Escalation Study of Encorafenib and Cetuximab with or without Alpelisib in Metastatic BRAF-Mutant Colorectal Cancer. *Cancer Discovery* **7,** 610–619 (2017).
162. Corcoran, R. B. *et al.* Synthetic lethal interaction of combined BCL-XL and MEK inhibition promotes tumor regressions in KRAS mutant cancer models. *Cancer Cell* **23,** 121–128 (2013).
163. Sun, C. *et al.* Intrinsic Resistance to MEK Inhibition in KRAS Mutant Lung and Colon Cancer through Transcriptional Induction of ERBB3. *Cell Rep* **7,** 86–93 (2014).
164. Barretina, J. *et al.* The Cancer Cell Line Encyclopedia enables predictive modelling of anticancer drug sensitivity. *Nature* **483,** 603–307 (2012).
165. Puyol, M. *et al.* A Synthetic Lethal Interaction between K-Ras Oncogenes and Cdk4 Unveils a Therapeutic Strategy for Non-small Cell Lung Carcinoma. *Cell* **18,** 63–73 (2010).

166. Marcotte, R. *et al.* Essential Gene Profiles in Breast, Pancreatic, and Ovarian Cancer Cells. *Cancer Discovery* **2,** 172–189 (2012).
167. Buehler, E., Chen, Y.-C. & Martin, S. C911: A bench-level control for sequence specific siRNA off-target effects. *PLoS ONE* **7,** e51942 (2012).
168. Shalem, O. *et al.* Genome-scale CRISPR-Cas9 knockout screening in human cells. *Science* **343,** 84–87 (2014).
169. Côté, J.-F. & Vuori, K. Identification of an evolutionarily conserved superfamily of DOCK180-related proteins with guanine nucleotide exchange activity. *J. Cell. Sci.* **115,** 4901–4913 (2002).
170. Root, D. E., Hacohen, N., Hahn, W. C., Lander, E. S. & Sabatini, D. M. Genome-scale loss-of-function screening with a lentiviral RNAi library. *Nat Meth* **3,** 715–719 (2006).
171. Konermann, S. *et al.* Genome-scale transcriptional activation by an engineered CRISPR-Cas9 complex. *Nature* **517,** 583–588 (2014).
172. Wang, B. *et al.* ATXN1L, CIC, and ETS Transcription Factors Modulate Sensitivity to MAPK Pathway Inhibition. *Cell Rep* **18,** 1543–1557 (2017).
173. Krall, E. B. *et al.* KEAP1 loss modulates sensitivity to kinase targeted therapy in lung cancer. *Elife* **6,** e18970 (2017).
174. Sanders, M. A., Ampasala, D. & Basson, M. D. DOCK5 and DOCK1 regulate Caco-2 intestinal epithelial cell spreading and migration on collagen IV. *J. Biol. Chem.* **284,** 27–35 (2009).
175. Gadea, G. & Blangy, A. Dock-family exchange factors in cell migration and disease. *European Journal of Cell Biology* (2014). doi:10.1016/j.ejcb.2014.06.003
176. Lu, M. *et al.* A Steric-inhibition model for regulation of nucleotide exchange via the Dock180 family of GEFs. *Curr. Biol.* **15,** 371–377 (2005).
177. Hsu, P. D., Lander, E. S. & Zhang, F. Development and applications of CRISPR-Cas9 for genome engineering. *Cell* **157,** 1262–1278 (2014).
178. Ma, Y. *et al.* Targeted AID-mediated mutagenesis (TAM) enables efficient genomic diversification in mammalian cells. *Nat Meth* **13,** 1029–1035 (2016).
179. Hess, G. T. *et al.* Directed evolution using dCas9-targeted somatic hypermutation in mammalian cells. *Nat Meth* **13,** 1036–1042 (2016).
180. Gilbert, L. A. *et al.* Genome-Scale CRISPR-Mediated Control of Gene Repression and Activation. *Cell* **159,** 647–661 (2014).
181. Rothstein, R. J. One-step gene disruption in yeast. *Meth. Enzymol.* **101,** 202–211 (1983).
182. Boone, C., Bussey, H. & Andrews, B. J. Exploring genetic interactions and networks with yeast. *Nat. Rev. Genet.* **8,** 437–449 (2007).
183. Costanzo, M. *et al.* The Genetic Landscape of a Cell. *Science* **327,** 425–431 (2010).
184. Costanzo, M. *et al.* A global genetic interaction network maps a wiring diagram of cellular function. *Science* **353,** (2016).
185. Measday, V. *et al.* Systematic yeast synthetic lethal and synthetic dosage lethal screens identify genes required for chromosome segregation. *Proceedings of the National Academy of Sciences* **102,** 13956–13961 (2005).
186. Nijhawan, D. *et al.* Cancer Vulnerabilities Unveiled by Genomic Loss. *Cell* **150,**

842–854 (2012).
187. Nishikimi, A., Kukimoto-Niino, M., Yokoyama, S. & Fukui, Y. Immune regulatory functions of DOCK family proteins in health and disease. *Exp. Cell Res.* **319,** 2343–2349 (2013).
188. Cook, D. R., Rossman, K. L. & Der, C. J. Rho guanine nucleotide exchange factors: regulators of Rho GTPase activity in development and disease. *Oncogene* **33,** 4021–4035 (2014).
189. Marei, H. & Malliri, A. GEFs: Dual regulation of Rac1 signaling. *Small GTPases* **8,** 90–99 (2017).
190. Campa, C. C., Ciraolo, E., Ghigo, A., Germena, G. & Hirsch, E. Crossroads of PI3K and Rac pathways. *Small GTPases* **6,** 71–80 (2015).
191. Welch, H. C. E., Coadwell, W. J., Stephens, L. R. & Hawkins, P. T. Phosphoinositide 3-kinase-dependent activation of Rac. *FEBS Lett* **546,** 93–97 (2003).
192. Bar-Sagi, D. A Ras by any other name. *Molecular and Cellular Biology* **21,** 1441–1443 (2001).
193. Engelman, J. A. & Settleman, J. Acquired resistance to tyrosine kinase inhibitors during cancer therapy. *Curr. Opin. Genet. Dev.* **18,** 73–79 (2008).
194. Vives, V. *et al.* The Rac1 exchange factor Dock5 is essential for bone resorption by osteoclasts. *J. Bone Miner. Res.* **26,** 1099–1110 (2011).
195. Omi, N. *et al.* Mutation of Dock5, a member of the guanine exchange factor Dock180 superfamily, in the rupture of lens cataract mouse. *Exp. Eye Res.* **86,** 828–834 (2008).
196. Laurin, M. *et al.* The atypical Rac activator Dock180 (Dock1) regulates myoblast fusion in vivo. *Proceedings of the National Academy of Sciences* **105,** 15446–15451 (2008).
197. Lin, Y. & Zheng, Y. Approaches of targeting Rho GTPases in cancer drug discovery. *Expert Opin Drug Discov* **10,** 991–1010 (2015).
198. Sun, C. *et al.* Reversible and adaptive resistance to BRAF(V600E) inhibition in melanoma. *Nature* **508,** 118–122 (2014).
199. Manchado, E. *et al.* A combinatorial strategy for treating KRAS-mutant lung cancer. *Nature Publishing Group* **534,** 647–651 (2016).
200. Zhu, Z. *et al.* Inhibition of KRAS-driven tumorigenicity by interruption of an autocrine cytokine circuit. *Cancer Discovery* **4,** 452–465 (2014).
201. Cerami, E. *et al.* The cBio Cancer Genomics Portal: An Open Platform for Exploring Multidimensional Cancer Genomics Data. *Cancer Discovery* **2,** 401–404 (2012).
202. Gao, J. *et al.* Integrative analysis of complex cancer genomics and clinical profiles using the cBioPortal. *Science Signaling* **6,** pl1 (2013).
203. Morgan-Lappe, S. E. *et al.* Identification of Ras-related nuclear protein, targeting protein for xenopus kinesin-like protein 2, and stearoyl-CoA desaturase 1 as promising cancer targets from an RNAi-based screen. *Cancer Research* **67,** 4390–4398 (2007).
204. Sarthy, A. V. *et al.* Survivin depletion preferentially reduces the survival of activated K-Ras-transformed cells. *Molecular Cancer Therapeutics* **6,** 269–276 (2007).

205. Fröhling, S. & Scholl, C. STK33 kinase is not essential in KRAS-dependent cells--letter. *Cancer Research* **71,** 7716–author reply 7717 (2011).
206. Babij, C. *et al.* STK33 Kinase Activity Is Nonessential in KRAS-Dependent Cancer Cells. *Cancer Research* **71,** 5818–5826 (2011).
207. Weïwer, M. *et al.* A Potent and Selective Quinoxalinone-Based STK33 Inhibitor Does Not Show Synthetic Lethality in KRAS-Dependent Cells. *ACS Med. Chem. Lett.* **3,** 1034–1038 (2012).
208. Singh, A. *et al.* TAK1 Inhibition Promotes Apoptosis in KRAS-Dependent Colon Cancers. *Cell* **148,** 639–650 (2012).
209. Beronja, S. *et al.* RNAi screens in mice identify physiological regulators of oncogenic growth. *Nature* **501,** 185–190 (2013).
210. Kim, H. S. *et al.* Systematic Identification of Molecular Subtype-Selective Vulnerabilities in Non-Small-Cell Lung Cancer. *Cell* **155,** 552–566 (2013).
211. Cullis, J. *et al.* The RhoGEF GEF-H1 Is Required for Oncogenic RAS Signaling via KSR-1. *Cancer Cell* **25,** 181–195 (2014).
212. Costa-Cabral, S. *et al.* CDK1 Is a Synthetic Lethal Target for KRAS Mutant Tumours. *PLoS ONE* **11,** e0149099 (2016).
213. Wang, B. *Mechanisms of Resistance to MAPK Pathway Inhibition in RAS-mutant Cancers*. Doctoral thesis: http://nrs.harvard.edu/urn-3:HUL.InstRepos:33493475 (2016).